The Industrial Application of Digital Signal Processing

Stephen John Roome BSc MSc ARCS

Thesis submitted for the award of the degree of Doctor of Philosophy

The City University

London EC1V 0HB

Department of Electrical, Electronic and Information Engineering

July 1989

Contents

List of Tables

List of Figures

Acknowledgements

I should like to thank Professor Finkelstein and Dr. W.J.Hill for supervising this research programme and for their encouragement and support. I should also like to thank the director of THORN EMI Central Research Laboratories for permission to submit this thesis and THORN EMI Computer Systems Division, EMI Music and EMI Records (UK) for their co-operation.

The investigation of the application of digital signal processing to the automatic detection and assessment of gramophone record pressing faults was carried out under the leadership of Mr J.W.Richards, now with Sony Broadcast UK Ltd. He also carried out the initial computer simulations and designed the digital signal processing hardware. I should like to thank him for his direction, help, and encouragement.

Finally I should like to thank all those friends and colleagues who have contributed by fruitful discussion and friendly criticism including Mr D.R. Bream, now with Software Sciences and Dr P.A. Jefford, now with STC .

Declaration

I grant powers of discretion to the University Librarian to allow this thesis to be copied in whole or in part without further reference to me. This permission covers only single copies made for study purposes, subject to normal conditions of acknowledgement.

Abstract

This thesis describes an investigation into the application of digital signal processing techniques to the solution of industrial signal processing problems. The investigation took the form of three case studies chosen to illustrate the variety of possible applications.

The first was the computer simulation of a digital microwave communications link which utilised narrowband FM modulation and partial response techniques. In order to ensure that the behaviour of the simulation reliably matched that of the modelled system it was found necessary to have a sound theoretical background, implementation using good software engineering methodology together with methodical testing and validation.

The second case study was a comprehensive investigation of adaptive noise cancelling systems concentrating on issues important for practical implementation of the technique: stability and convergence of the adaptation algorithm; misadjustment noise and effects due to realizability constraints. It was found that theoretical predictions of the systems behaviour were in good agreement with the results of computer simulation except for the level of output misadjustment noise. In order to make the mathematics of the LMS algorithm tractable it was assumed that the input data formed a series of uncorrelated vectors. It was found that this assumption is only appropriate for the prediction of misadjustment noise when the reference input is uncorrelated.

The final case study concerned the automatic detection and assessment of pressing faults on gramophone records for quality assurance purposes. A pattern recognition technique for identifying the signals due to gramophone record defects and a numerical method for assessing the perceived severity of the defects were developed empirically. Prototype equipment was designed, built and tested in extended field trials. The equipment was shown to be superior to previous equipment developed using analogue signal processing techniques.

These case studies demonstrate that digital signal processing is a powerful and widely applicable technique for the solution of industrial signal processing problems. Solutions may be theoretical or obtained by experiment or simulation. The strengths and weaknesses of each approach are illustrated.

Chapter 1

The Industrial Application of Digital Signal Processing

1.1 Digital signal Processing

Signal processing is concerned with the manipulation and extraction of information from signals. Traditionally this processing has been carried out using analogue electrical systems. Recent advances in digital circuit technology, in particular the development of Large Scale Integration (LSI) and Very Large Scale Integration (VLSI) integrated circuits, now mean that it is practicable to carry out many complex signal processing tasks using digital devices.

Digital signal processing (DSP) has many inherent advantages compared to analogue signal processing. These include:

- When a digital signal is processed the only degradation that takes place is due to rounding errors within arithmetic devices. This can be designed to be as small as desired. By contrast the signals within an analogue system are inevitably degraded by thermal noise.
- As each processing operation does not degrade the signal there is no inherent upper limit to the complexity of a digital signal processing system as there is for an analogue one.
- Digital signals can be stored without degradation for an unlimited time.

- A digital signal processing system can be implemented using general purpose programmable devices. This often enables a digital signal processing system to be cheaper than its analogue counterpart.

Since digital devices operate in discrete time steps the signals in a digital signal processing system consist of a sequence of numbers. In order to process an analogue signal using a digital system it is therefore necessary to sample the signal, usually at equal time intervals. The numbers within a digital signal processing system can only be represented to a finite precision so that signals in digital signal processing systems are inherently quantized. If the digital signal is obtained by the A/D conversion of an analogue signal then quantization will represent the addition of an error component to the signal which is denoted quantization noise. Discrete time and quantization are characteristic of digital signal processing systems.

1.2 Research Programme

This thesis describes an investigation into the application of digital signal processing to the solution of industrial signal processing problems. The investigation took the form of three case studies into real engineering problems. The application areas are diverse in order to reflect the wide variety of possible applications.

A signal processing problem may be addressed in a number of ways. Theoretical investigation is very powerful and can lead to a deep understanding of the problem and its solutions. Experimental investigation avoids the problems of idealization and approximation which often accompany theoretical models but the design and construction of hardware can be expensive and time consuming. A third alternative, simulation on a general purpose digital computer, is becoming increasingly attractive.

In a computer simulation of a signal processing system a mathematical model of the system is implemented by programming a general purpose digital computer. Experimentation is then carried out by applying suitable input signals to the model and observing outputs of interest. The computer simulation is therefore a digital signal processing system implemented using general purpose hardware. It differs from applied digital signal processing systems in that the input signals are created mathematically rather than by the A/D conversion of an analogue signal and and that the outputs are not converted back into analogue form.

All three methods of investigation were used during the case studies and the the advantages and disadvantages of each method when applied to industrial signal processing problems are illustrated.

1.2.1 First case study

The first case study is concerned with the design of a computer simulation of a state-of the-art microwave communications link. The link was difficult to investigate theoretically and experimentation at microwave frequencies is very expensive so computer simulation was an essential part of the design process. The theory and implementation of the simulation are discussed and examples of the results given.

1.2.2 Second case study

One of the most frequent signal processing tasks is the estimation of a signal corrupted by interference or noise. The traditional method of dealing with this problem is to filter the corrupted signal, retaining those frequency components dominated by the wanted signal, and discarding those where the signal is mainly due to interference. This approach, known as optimal filtering, can be implemented using either analogue or digital techniques.

An alternative technique is to estimate the interfering signal using a second sensor. The signal from the sensor is suitably filtered and then subtracted from the corrupted signal. Such systems are known as noise cancelling systems. In order to create practical noise cancelling systems it is necessary that the system be adaptive so that it can learn the statistics of the correlation of the signals from the two sensors and track them as they vary slowly with time. It is theoretically possible to construct an analogue adaptive noise cancelling system, but in practice such systems are only implemented in digital form.

The second case study is a comprehensive investigation of adaptive noise cancelling systems. It consists of a theoretical investigation, concentrating on issues which will be important for industrial application of the technique: stability and convergence of the adaptive algorithm; the effect of gradient estimation noise and effects due to realizability constraints. The theoretical predictions are then compared with extensive computer simulations.

1.2.3 Third case study

The third case study is concerned with the design of equipment to automatically detect and assess pressing faults on gramophone records. Essentially this involves determining whether any segment of the replayed signal is due to a manufacturing defect or is recorded programme. If a signal segment is considered to be due to a manufacturing defect then the perceived severity of the resulting noise must be estimated. This must be achieved for a variety of possible manufacturing defects and in the presence of a wide variety of recorded programme.

An earlier programme of research carried out by THORN EMI has resulted in an analogue signal processing system which is moderately successful in performing these tasks. In this case study digital signal processing techniques are applied to the problem. A prototype system was constructed and extensive field trials carried out at a gramophone record manufacturing plant.

Chapter 2

Computer Simulation of a Signal Processing System

2.1 Introduction

Many electrical engineers now have ready access to a substantial amount of computer power, either in the form of personal computers, engineering workstations or a terminal on a time sharing computer system. One of the most effective ways in which this computer power may be employed is in the simulation of engineering systems, which allows ideas to be explored with far less time and expense than would be required for construction and experimentation with hardware prototypes.

Computer simulation offers many advantages when designing a signal processing system.

- It enables the effects of various design decisions to be examined cheaply and rapidly.
- Internal variables not accessible in the real world may be examined, and real world constraints such as causality may be removed [4]. Although such esoteric operations may seem to be of little practical use, in fact removing these constraints often gives valuable insight into the operation of a system.
- Computer simulations are usually totally repeatable.

A computer simulation of a signal processing system is a digital signal processing system which uses the hardware of a general purpose computer to carry out its operations. The essential difference between the simulation and an applied digital signal processing system is that the input signals are mathematically created from models of the sources rather than by A/D converting signals from sensors. The simulation will probably also operate at a much lower processing speed than an applied system.

For the simulation to be useful its behaviour must reliably match that of the system being simulated. If the system to be simulated is itself digital, this is relatively easy to achieve as the simulation is essentially a second implementation of the same system. This investigation is intended to use a systems view of the simulation of analogue signal processing systems in order to develop an appropriate methodology. The subject of this chapter has been published in a paper entitled 'Computer simulation of a digital radio system', by the author, in the June 1988 issue of the Journal of the IERE.

2.2 The Radio System

The signal processing system which has been simulated during this investigation was a state-of-the-art microwave communication link under development by THORN EMI, Computer Systems Division. This radio system used a combination of narrowband FM modulation and partial response techniques in order to achieve high spectral efficiency. This proved to be very difficult to deal with theoretically. It is very expensive and time consuming to carry out hardware experiments at microwave frequencies and so simulation was regarded as being essential to the design process. Although the purpose of the radio link is to transmit digital information, and hence it is referred to as a digital radio, it is an analogue signal processing system which is relatively difficult to simulate.

The digital radio system was designed to be an 8 Mbit point-to-point communications link operating at a frequency of 13 GHz, and apart from using partial response techniques was conventional in design. A block diagram of the radio is shown in Figure 2.1.

2.2.1 Partial Response Systems

Partial response techniques are methods of obtaining greater information transmission capacity within a given bandwidth than is implied by the

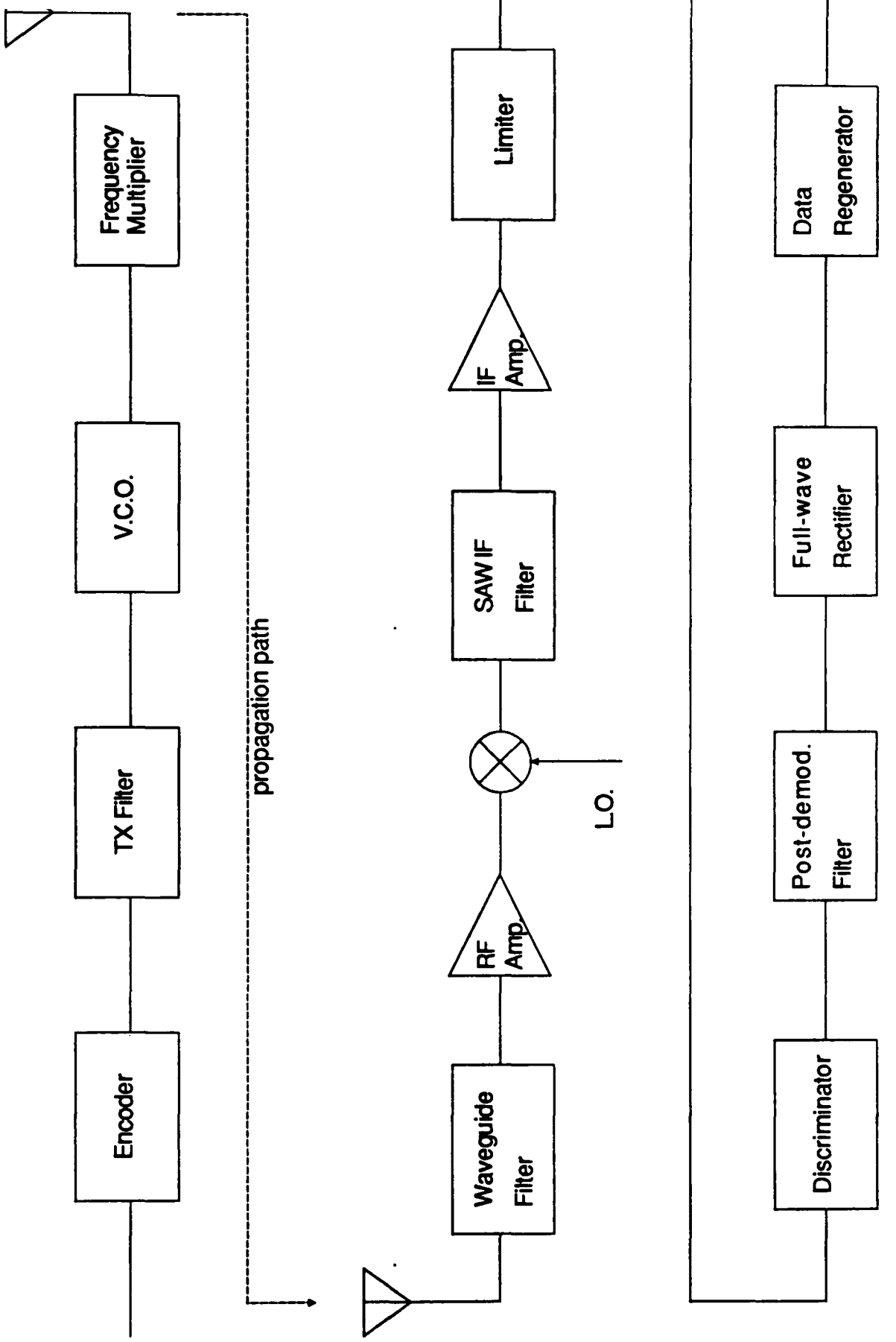

Figure 2.1: Block diagram of the digital microwave radio

Nyquist theorems. The principle is to allow the narrow-band filtering of the channel to distort the transmitted signal, but in a controlled manner. The signal is coded before transmission in an equal and opposite manner, which is then cancelled by the response of the channel [1].

If we consider convenient forms of distortion which we could choose for a channel transmitting digital symbols with a period T one option is for the output signal to be equal to the input plus an echo of the previous input.

We thus require the impulse response of the channel to be

$$h(t) = \delta(t) + \delta(t - T) \tag{2.1}$$

The frequency response of the channel is

$$H(\omega) = 2e^{\frac{-j\omega T}{2}} \cos \frac{\omega T}{2} \tag{2.2}$$

This represents a transmission channel which is not band-limited. However if we multiply by an ideal low pass filter at the Nyquist frequency $\omega_n = \frac{\pi}{T}$ we obtain the channel

$$\begin{aligned} H(\omega) &= 2e^{\frac{-j\omega T}{2}} \cos \frac{\omega T}{2} \qquad & \frac{-\pi}{T} < \omega < \frac{\pi}{T} \\ &= 0 \qquad & otherwise \end{aligned} \tag{2.3}$$

This channel has an impulse response

$$h(t) = \frac{1}{T} \left\{ \frac{sin(\frac{\pi t}{T})}{(\frac{\pi t}{T})} + \frac{sin(\frac{\pi(t-T)}{T})}{\frac{\pi(t-T)}{T}} \right\} \tag{2.4}$$

unlike the ideal low pass filter, a good approximation to this channel can be achieved in practice. This channel has twice the information capacity of a binary transmission of the same bandwidth and is hence known as a duobinary partial response channel [2].

If we consider an input signal with binary '1' represented by an impulse $+\delta(t)$ and '0' represented by a negative impulse $-\delta(t)$ then the output signal from the duobinary channel can take on *three* values at the sampling instant. These values may usefully be interpreted as representing '0', '1' and '2' as shown in the truth table below

x_{n-1}	x_n	$y(nT)$	y_n
0	0	$-2/T$	0
0	1	0	1
1	0	0	1
1	1	$2/T$	2

(2.5)

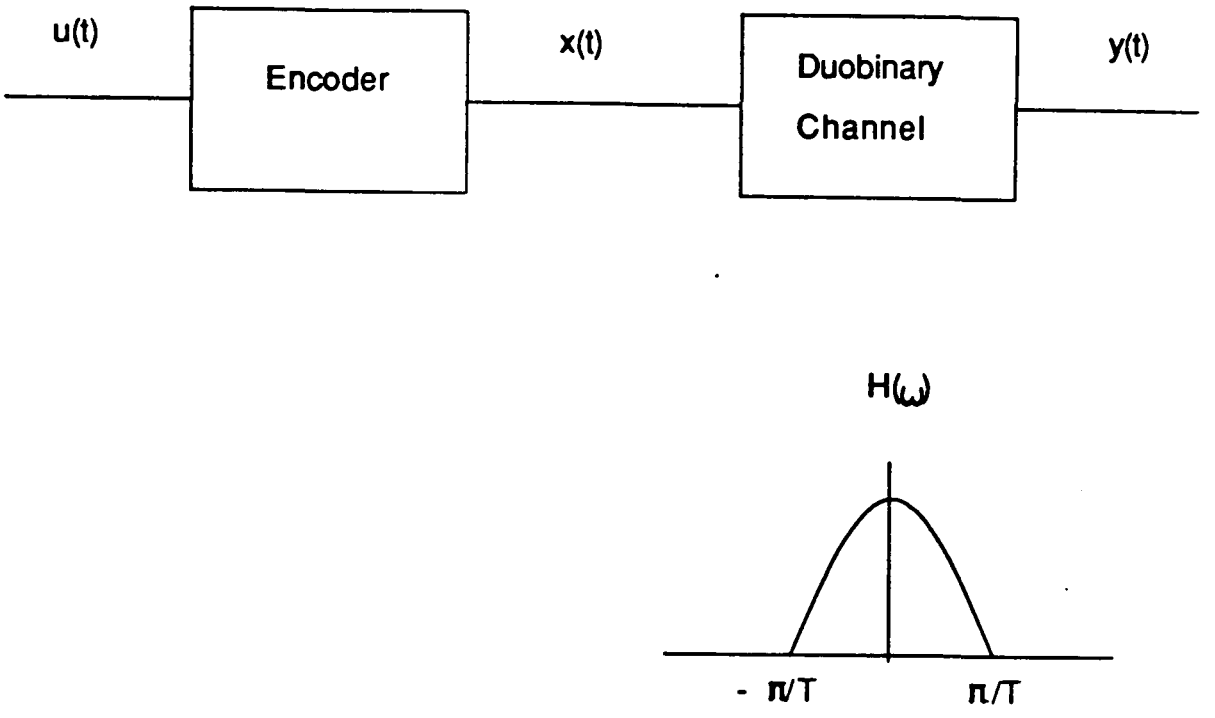

Figure 2.2: Block diagram of duobinary partial response system

The output signal from the channel could be interpreted to determine the input data using appropriate logic. Once an error occurred it would tend to propagate causing subsequent bits to be decoded in error. However, by precoding the binary data the decoding of the transmitted bit can be simplified and error propagation prevented.

If we consider the encoding process and channel in series, as shown in figure 2.2, then we have

$$y_n = x_n + x_{n-1} \tag{2.6}$$

Thus to invert this relationship we require

$$u_n = x_n + x_{n-1} \tag{2.7}$$

$$ie \quad x_n = u_n - x_{n-1} \tag{2.8}$$

This relationship describes a simple recursive filter which may be easily implemented. The only obstacle to equations (6) and (8) representing inverse operations on the transmitted data is that the input values u_n are binary data whereas the output values y_n are three valued.

This difficulty is readily overcome by interpreting equations (6) and (8) as operations in modulo 2 arithmetic. In physical terms this means that the binary input data stream is encoded, transmitted over the duobinary channel which creates an output signal which may take on three values at

the sampling instant. The outer two levels $-2/T$ and $+2/T$ are interpreted as binary '0' whilst the centre level 0 is interpreted as binary '1'.

The duobinary partial response technique outlined above formed the basis for the digital communications link design. However a whole family of partial response systems exist based on different choices for the relationship equation (1) [1],[3].

2.3 Theoretical Background

2.3.1 Equivalent Baseband Representation

For a direct computer simulation of the signal processing operations carried out by the radio it would be necessary to represent the signals by sampled versions with a sampling rate high enough to avoid aliasing. For the 13 GHz 8 Mbit radio we are considering, this would imply a sampling rate of at least 26 GHz. To simulate just one data symbol passing through the system would then require over 3000 samples. This would clearly involve unacceptable processing time for a realistic number of bits. Fortunately, the behaviour of the system can be accurately predicted by simulating a system in which the carrier frequency (and the intermediate frequency) are translated to dc.

This method may be illustrated by considering a carrier wave at frequency ω_c submitted to a generalised modulation scheme. This gives a signal of the form

$$x(t) = r(t)\cos\{\omega_c t + \phi(t)\} \tag{2.9}$$

Now we may rewrite this in the form

$$x(t) = Re.\left\{\tilde{x}(t)e^{j\omega_c t}\right\} = \frac{\tilde{x}(t)}{2}e^{j\omega_c t} + \frac{\tilde{x}^*(t)}{2}e^{-j\omega_c t} \tag{2.10}$$

where $\tilde{x}(t) = r(t)e^{\phi(t)}$ is known as the *complex envelope* of the signal $x(t)$, and $\tilde{x}^*(t)$ denotes its complex conjugate. Note that $\tilde{x}(t)$ is a complex signal, and that it contains all the information concerning the modulation contained in signal $x(t)$.

The frequency domain relationship between the signal $x(t)$ and its complex envelope $\tilde{x}(t)$ may be obtained by fourier transformation of equation (10) to yield

$$X(\omega) = \frac{1}{2}\tilde{X}(\omega - \omega_c) + \frac{1}{2}\tilde{X}^*(-\omega - \omega_c) \tag{2.11}$$

In general, carrier based communication systems are narrowband, that is their transfer functions can be written in the form

$$H(\omega) = \tilde{H}(\omega - \omega_c) + \tilde{H}^*(-\omega - \omega_c) \tag{2.12}$$

Where $\tilde{H}(\omega)$ is a band-limited function with bandwidth $B << \omega_c$, known as the equivalent baseband transfer function.

For a narrowband, linear, time-invariant system with input signal $x(t)$, transfer function $H(\omega)$ and output signal $y(t)$ it can be shown [5] that

$$y(t) = Re.\left\{\tilde{y}(t)e^{j\omega_c t}\right\} \tag{2.13}$$

$$\text{with} \quad \tilde{Y}(\omega) = \tilde{H}(\omega)\tilde{X}(\omega) \tag{2.14}$$

where $\tilde{Y}(\omega)$ and $\tilde{X}(\omega)$ are the fourier transforms of the complex envelope representations of $y(t)$ and $x(t)$ respectively.

This convenient result enables us to analyse and simulate carrier based communication systems entirely in terms of the complex envelope representations of the signals. The resulting model of the system is known as the baseband equivalent system.

The simulation of the 8 MBit 13 GHz radio was based on its block diagram shown in figure 2.1. Converting this into a form suitable for efficient implementation using baseband equivalent representation and making certain simplifications, gave the system model shown in figure 2.3.

2.3.2 Discretization

Due to the discrete nature of digital computers it is necessary to convert the continuous signals and processes present in the baseband equivalent model to their discrete equivalents. This 'discretization' process is easier to achieve accurately if the sampling rate is chosen to be rather higher than the minimum value implied by the sampling theorem. The sampling rate chosen for the digital radio simulation was $512M$ sample s^{-1} which is 64 times the symbol rate.

Figure 2.3: Simplified system model used as basis of simulation

The processes present in the baseband equivalent model will generally be described either in terms of transfer functions or in terms of differential equations. In the first case it will be most convenient to implement them in the frequency domain, whilst integral and differential equations are most readily implemented in the time domain. Conversion between the two domains is readily and efficiently achieved by using one of the family of Fast Fourier Transform (FFT) algorithms.

Implementation of filters in the frequency domain is straight forward. Two convenient methods are the use of piece-wise linear approximations [6], and pole/zero descriptions of filter transfer functions. Alternatively it is possible to simulate filters in the time domain either by implementing the convolution of the signal with the impulse response of the filter or by approximating the desired response by a suitable digital filter [7], however both these approaches will tend to be more difficult to apply and to require more computation.

The implementation of discrete time approximations to integral and differential equations is more difficult. To obtain accurate modelling when a low sampling rate has been chosen requires the use of specialised techniques and the reader is referred to [8] and [9] for more details. However by using a sampling rate that is several times that of the minimum specified by the sampling theorem the discretization problem is considerably eased. This process is illustrated by the implementation of the narrowband FM modulation operation within the radio simulation.

The input signal to the modulator $x(t)$ is the result of smoothing the data signal in which $+1$ volt represents binary "1" and -1v represents binary

"0".

Modulation by a continuous phase frequency shift keying (CPFSK) modulator results in the output signal $y(t)$ given by:

$$y(t) = Re.\{Ae^{j(\omega_c t + \phi(t))}\} \tag{2.15}$$

$$where \quad \phi(t) \;=\; \omega_{pk} \int_0^t x(\tau) d\tau$$

The equivalent baseband representation of this operation is given by:

$$\tilde{y}(t) = Ae^{j\phi(t)} \tag{2.16}$$

$$with \quad \phi(t) \quad as\ above$$

These equations are then readily discretized by using the trapezium method to implement the integration, and taking $A = 1$ for convenience. If a lower sampling rate had been chosen to implement the simulation a more sophisticated numerical integration method would be required.

2.3.3 The Discrete Fourier Transform

If we consider a continuous signal $x(t)$ in the system to be simulated, it is represented within the simulation by a finite segment of the signal which we will denote $x'(t)$. $x'(t)$ may be considered to have been formed from $x(t)$ by multiplying it by a *window function* $w(t)$.

$$\begin{array}{lllll} x'(t) & = & x(t)w(t) & & \\ where \quad w(t) & = & 1 & 0 \le t \le T_w & \\ & = & 0 & otherwise & \end{array} \tag{2.17}$$

This has the effect of modifying the spectrum of $x(t)$ according to

$$X'(\omega) = X(\omega) \star W(\omega) \tag{2.18}$$

where $\star$ denotes the convolution operation.

The signal segment is actually manipulated within the computer as an array, created by sampling $x'(t)$. Representing the sampling operation as multiplication by a Dirac comb [12] we obtain

$$x_s(t) = x'(t).\sum_n \delta(t - nt_s) \tag{2.19}$$

Where t_s is the sampling interval of the simulation. The spectrum of the sampled signal $X_s(\omega)$ obtained by Fourier transformation of the above is given by

$$\begin{aligned} X_s(\omega) &= X'(\omega) \star \omega_s \sum_n \delta(\omega - n\omega_s) \qquad (2.20) \\ with \quad \omega_s &= \frac{2\pi}{t_s} \end{aligned}$$

Evaluation of the convolution integral then gives

$$X_s(\omega) = \frac{1}{t_s}\sum_n X'(\omega - n\omega_s) \tag{2.21}$$

This equation expresses the familiar relationship between the spectrum of a signal, and that of its sampled version.

When the DFT is used to transform between the time and frequency domains within a computer simulation, the frequency domain representation is also a sampled version of a windowed function. The effect of the truncation of the frequency scale is unimportant since any signals within the simulation will be aliased into the Nyquist bandwidth anyway.

After DFT the frequency domain representation of the signals $x(t)$ again consists of an array, which may be regarded as having been obtained by sampling the spectrum $X_s(\omega)$. Representing as before the sampling operation by multiplication by a Dirac comb, we obtain

$$\begin{aligned} X_p(\omega) &= X_s(\omega).\sum_m \delta(\omega - m\omega_o) \qquad (2.22) \\ where \quad \omega_o &= \frac{2\pi}{T_w} \end{aligned}$$

Taking the inverse Fourier transform of the above yields

$$x_p(t) = x_s(t) \star \frac{T_w}{2\pi} \sum_m \delta(t - mT_w) \tag{2.23}$$

Evaluation of the convolution integral then gives

$$x_p(t) = \frac{T_w}{2\pi} \sum_m x_s(t - mT_w) \tag{2.24}$$

This equation expresses a complementary relationship to that of the sampling theorem, sometimes known as the frequency sampling theorem. The signal $x_p(t)$ whose spectrum has been obtained is periodic with period T_w. It consists of an infinite repetition of the sampled segment $x_s(t)$.

This inherent periodicity causes problems whenever the signal $x(t)$ is not itself periodic with period T_w. The most familiar instance of this phenomenon occurs during spectral analysis using the DFT, and is known as spectral leakage. If a sinusoidal signal of frequency ω is analysed, a spike will be obtained only if ω is an integer number of times ω_o. At all other frequencies energy will 'leak' away from the single spectral line. One way of regarding the cause of the leakage, is that it is due to the discontinuities present where the signal segments $x'(t)$ are joined to create the periodic signal $x_p(t)$. Two methods for dealing with these problems are:

1. Ensure that the signals within the system model are periodic with period T_w.
2. Use a window function other than the rectangular window to smooth the discontinuity.

In the digital radio simulation the length of the simulation was chosen to be exactly 512 symbol periods so that it was expected that no window problems would arise, however this turned out not to be true as explained later.

2.4 Software Engineering

In the last few years the term software engineering has become common to denote an academic discipline concerned with the effective creation and

maintenance of computer software. Although the term is relatively new, academic study has been directed toward this area for at least 20 years and major advances have been made [13]. In order to create a simulation program that reliably models the behavior of the real system it is necessary to use a sound software engineering methodology.

2.4.1 Top-down Development

Top-down development, sometimes called development by successive refinement is the preferred method for designing any complex engineering system. Top-down development recognises that the human brain can only handle a certain level of complexity. It controls complexity by hiding most of the detail of a system in *black boxes*. In a physical system black boxes are subsystems whose inputs,outputs and the relationship between them are known but whose internal structure is invisible; in a software system the concept is almost identical except that the black box is a software component.

Software systems are thus designed by configuring software components. Once a suitable system has been designed, each black box itself becomes a software system to design using lower level software components, and so on. As a rigorous formal method this approach starts from a statement of the software specification, and proceeds until all the software components are so simple that their implementation is trivial. Taken this far the method is rather inflexible, and requires that the full software specification be known at the start of software development.

Most engineering software, including simulations, must be developed in the face of uncertain and changing requirements. To cope with this uncertainty the rigorous approach which leads to *building* software is amended so that software is organically *evolved* [13]. Essentially the method is the same except that the software specification is made far simpler than will be finally required. Once working software is achieved, the specification (at various levels of abstraction) is successively refined, so that the software evolves passing through working software of steadily increasing complexity.

2.4.2 Modular Programming

Modular programming is a natural adjunct of top-down development. At a certain level of development the black boxes are chosen to be *modules*. A module is a piece of software which will be developed in isolation. It will be

designed, written, compiled and tested as far as possible in isolation from the rest of the software. The advantages of modular development are

- The modular structure reflects the top-down design of the software
- Software development can be readily split between members of a team
- Libraries of useful modules can be created and reused
- Interaction between changes in different parts of the software is minimised
- Documentation is aided
- Compilation time is greatly reduced, since only a small part of the software is re-compiled after a change.

There are currently two problems with modular programming

- Modular programming is not supported by all languages and operating systems
- The checking of the interface between communicating modules provided by many linking programs is poor.

Nevertheless modular programming is so useful that it was considered essential for the development of the radio simulation.

2.4.3 Structured Programming

Structured programming is concerned with the control structures that occur within a program. Programs are constructed by using a small number of well understood primitive control structures rather than the undisciplined logical tangles which can be created using GOTO statements.

It has been shown that any program can be written using only three primitive control structures, namely

- Sequential
- Selection (IF-THEN-ELSE)

- Iteration (WHILE-DO)

However although these structures are theoretically sufficient, in practice they are often supplemented. PASCAL for example has a second selection structure (CASE-OF) and two other iteration structures (REPEAT-UNTIL, FOR -DO). Whatever the actual set of control structures used there is no doubt that structured programs are easier to understand,test,debug and modify [14].

In order to implement certain flow-charts using structured programming techniques it is necessary to create additional boolean variables purely to control the flow of execution. This is a small price to pay for the benefits that structured programming brings.

2.4.4 Implementation

When implementing simulation software it is advantageous to employ a good programming style, i.e. such aspects as adequate commenting; indentation of the source text to reflect its control structure and appropriate typing and naming of variables. These points are dealt with in many programming texts and will not be discussed here [15], [16], [17] .

The digital radio simulation was written in FORTRAN 77 to run on a DEC VAX under the VMS operating system. This language was chosen because it supports modular development and structured programming, and has inbuilt complex arithmetic. Other popular choices for writing simulation programs are PASCAL and C.

2.5 Testing and Validation

Testing of the simulation to ensure its correct operation is an essential part of the simulation process. Testing is carried out by comparing the simulation outputs against theoretical expectations and against experimental results. It is also necessary to ensure that the model of the communication system, which will generally embody many assumptions and approximations, accurately reflects the real world system. This *validation* process can only be carried out by comparison of the simulation outputs with experimental results.

At the current state of software engineering it is not possible to test a piece of software, of the complexity of the digital radio simulation, so that it can be proven to be error free. If the testing process is tackled in a methodical manner however, a high degree of confidence can be obtained.

Ensuring the correctness of the implementation of the system model is greatly eased by writing the software in modules which reflect the functional blocks in the system model. Each module may then be tested separately, and in simple combinations, before attempting to determine correct operation of the entire simulation. For example the FM modulator module, briefly described in section 4.2, was tested by examining the output signals first for dc inputs, and then for random binary signals. In both cases the correct output signals are well known from theory.

The IF frequency filtering of the radio was intended to be carried out by SAW filters with a centre frequency of 70 MHz. The filters were modelled by low order pole/zero approximations to their frequency responses, with phase compensation. To ensure that these were sufficiently accurate models they were compared with experimental measurements from the candidate SAW filters.

As the performance of the complete radio system could not be well predicted by theory, the complete simulation was validated by comparing signals and spectra from the simulation with outputs from a bench mock up of the radio constructed by THORN EMI Electronics, Computer Systems Division. The very close agreement between the experimental results and the outputs from the simulation (when its parameters were chosen to match those of the mock up) gave a high degree of confidence in the performance of the simulation.

2.6 Problems

Two problems encountered during the validation process will now be described, both because they are illustrative, and because they are likely to be encountered by others attempting to simulate communication systems.

During the testing process the complete radio simulation was tested with all '0' and all '1' data inputs. For these cases the theoretical complications caused by the combination of filtered FM modulation, and partial response techniques are bypassed and the resulting signals and spectra may be readily predicted.

For these cases the output from the discriminator should be constant. In practice it was found to have a transient component extending over the

first few symbols. However the transient was not present if the modules implementing the RF and IF filtering were removed, and it was in this area that the problem was originally thought to reside. It transpired that the transient was actually an example of the problems caused by windowing phenomena.

It will be recalled that it was expected that there would be no windowing problems within the simulation since the data sequence was chosen so that an integer number of symbols was present in the transform window. The input signal created by concatenating these segments would then be periodic. However it has been overlooked that once the signal had been FM modulated the periodicity was destroyed, causing a phase discontinuity at the joins of the signal segments. This had no observable effects until the frequency domain representation was changed by multiplication by the RF and IF filter characteristics. The discontinuity then caused the observed transient.

For the data sequences all '0' and all '1', the discontinuity can be eliminated by choosing an appropriate frequency deviation. To prove that this was actually the cause of the transient the simulation was run again with the deviation changed from 1.5 MHz to 1.496 MHz, calculated to restored periodicity, and the transient as expected was eliminated. For the 512 bit data sequence used during the simulation no elegant method of eliminating the phase discontinuity was found. The effects of the transient on the simulation outputs were eliminated by discarding a portion of signal at each end of the segment.

The second problem was the choice of an appropriate 512 bit sequence for the simulation. In the digital radio system being simulated the data to be transmitted was scrambled so that the spectrum of the data, and hence the transmitted spectrum, was well controlled. During development of the simulation it was thought that a bit sequence selected by a pseudo-random number generator would be suitable for all simulation purposes, particularly because of its long length (512 symbols). In practice the random data sequence gave very good results when investigating the time domain performance of the system, but caused problems in the frequency domain.

The first lobe of the power spectrum of the random sequence is shown in figure 2.4. It will be seen that although it has the expected $\sin x/x$ shape, it is rather noisy and in particular has large negative going spikes. It was known that periodic sequences constructed from m sequences have optimum autocorrelation properties [5]. This implied that their spectral properties were also most nearly like that of a truly random sequence. A 512 bit sequence was constructed by using a 511 bit m sequence appended with a '0', and this proved to have rather better spectral properties. Fig. 5 shows

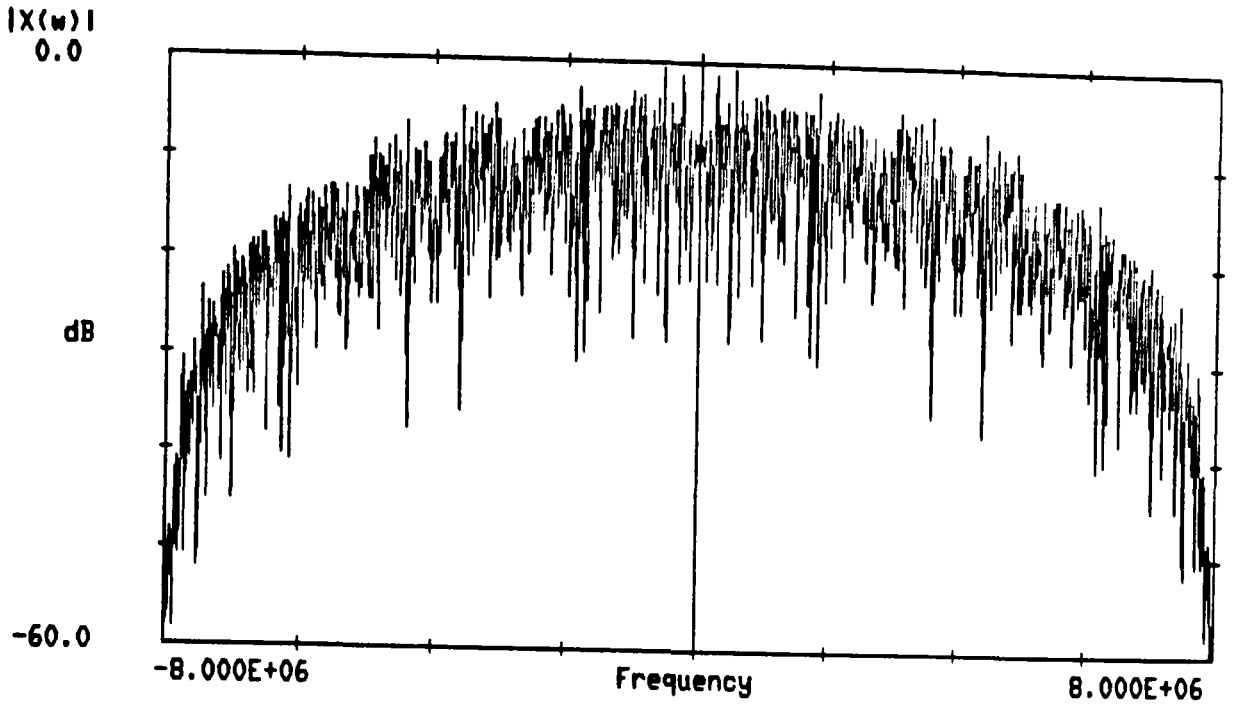

Figure 2.4: Power spectrum of 512 bit random sequence

the first lobe of the power spectrum of the new sequence, and it will be noted that it is much less noisy. This sequence was found to be satisfactory, and was used for all further simulations where a random sequence was required.

2.7 Results

The completed and validated digital radio simulation was used to finalize the design, and carry out a number of investigations on the performance of the radio. Only a few results will be shown here, to demonstrate the capability of the simulation.

The array of numbers representing the time or frequency domain description of the signal at any part of the system could be stored. This array could then be read by separate display programs and the graphics output could be experimented with until it was in a visually satisfactory form.

Figure 2.6 shows the eye diagram of the ideal duobinary channel described in section 2.1. As expected the diagram has three levels at the decision instant. No noise has been introduced during the simulation, and the finite width of the levels at the decision instant is due to the presence of a small amount of intersymbol interference. This is because the ideal duobinary channel described in section 2.1 was derived for the transmission of impulses. The

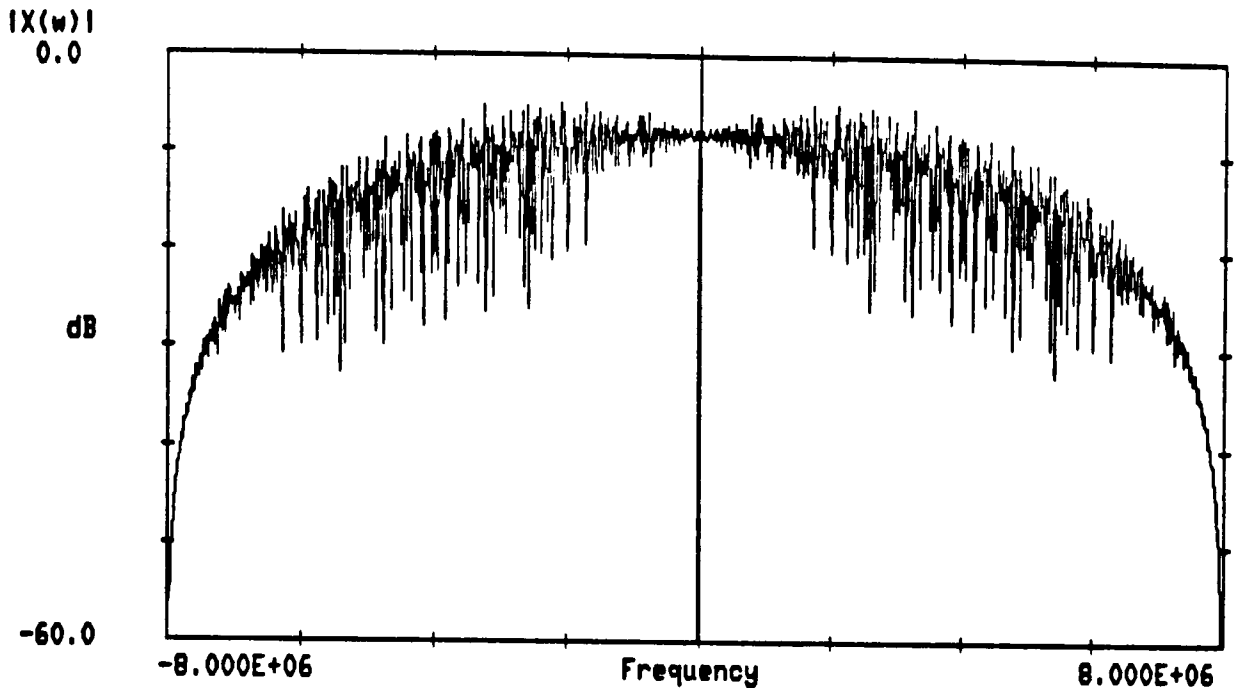

Figure 2.5: Power spectrum of m-based sequence

symbols were actually transmitted in the form of uniform pulses of length T, and this modifies the ideal channel by a factor $\frac{(\omega T/2)}{sin(\omega T/2)}$.

The eye diagram for this 'compensated' channel is shown in figure 2.7 It will be seen that the intersymbol interference is now eliminated at the decision instants, but that this has been accompanied by increased timing variation (jitter) of the transitions.

The eye diagram for the final radio design is shown in figure 2.8. It will be noted that there is intersymbol interference present, due to non-ideal system filtering. This is caused by the need to meet stringent transmitted signal spectra criteria, and tradeoffs between filter complexity and performance. This predicted eye diagram is extremely close to that measured on the final equipment. The transmitted power spectrum of the radio predicted by the simulation is shown in figure 2.9. A smoothed version of this spectrum is compared to experimental results from the final equipment in figure 2.10. It will be seen that the agreement is very good.

Many investigations on possible design improvements to the radio were carried out, and results were obtained much more quickly than would have been possible by hardware experimentation. As examples investigations were carried out

- to examine a design based on an alternative form of partial response system denoted modified duobinary [1].

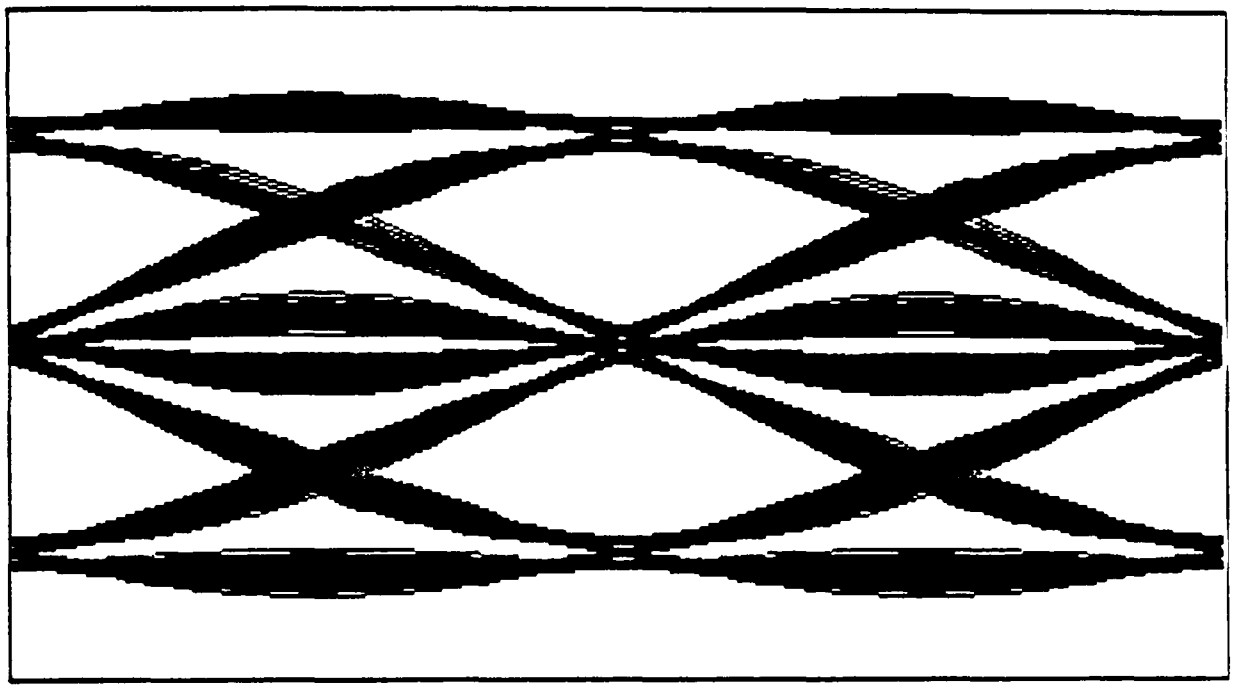

Figure 2.6: Eye diagram for ideal duobinary channel

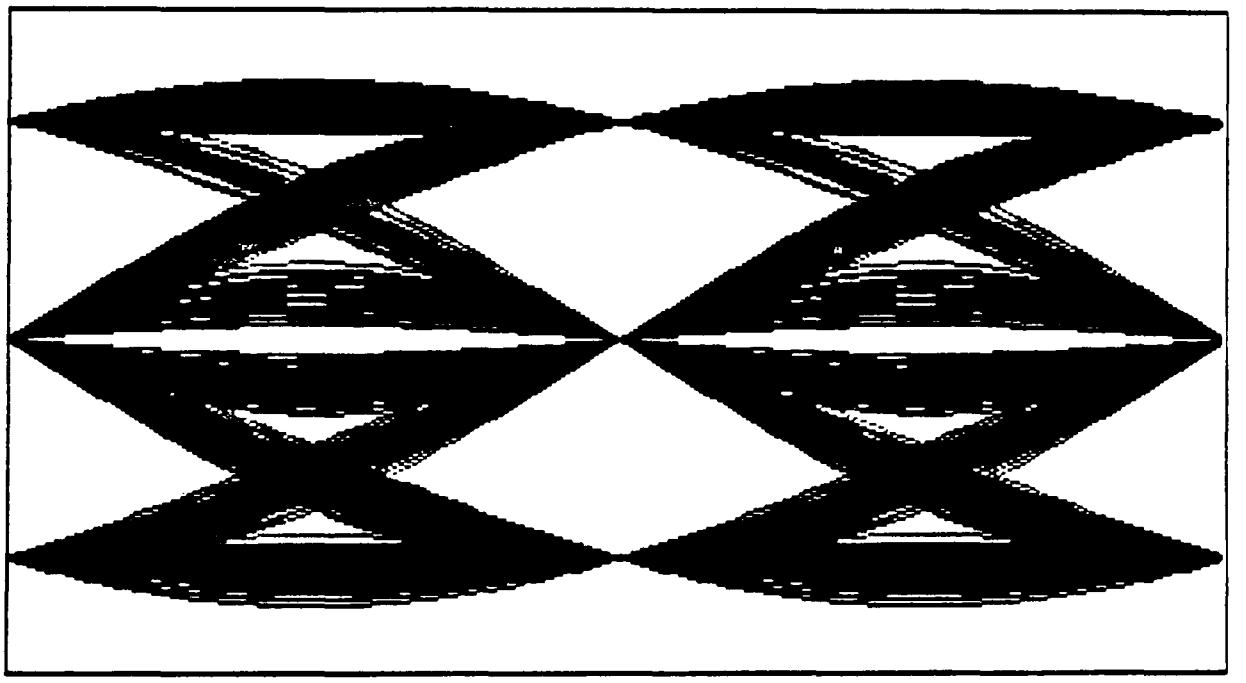

Figure 2.7: Eye diagram of compensated duobinary channel

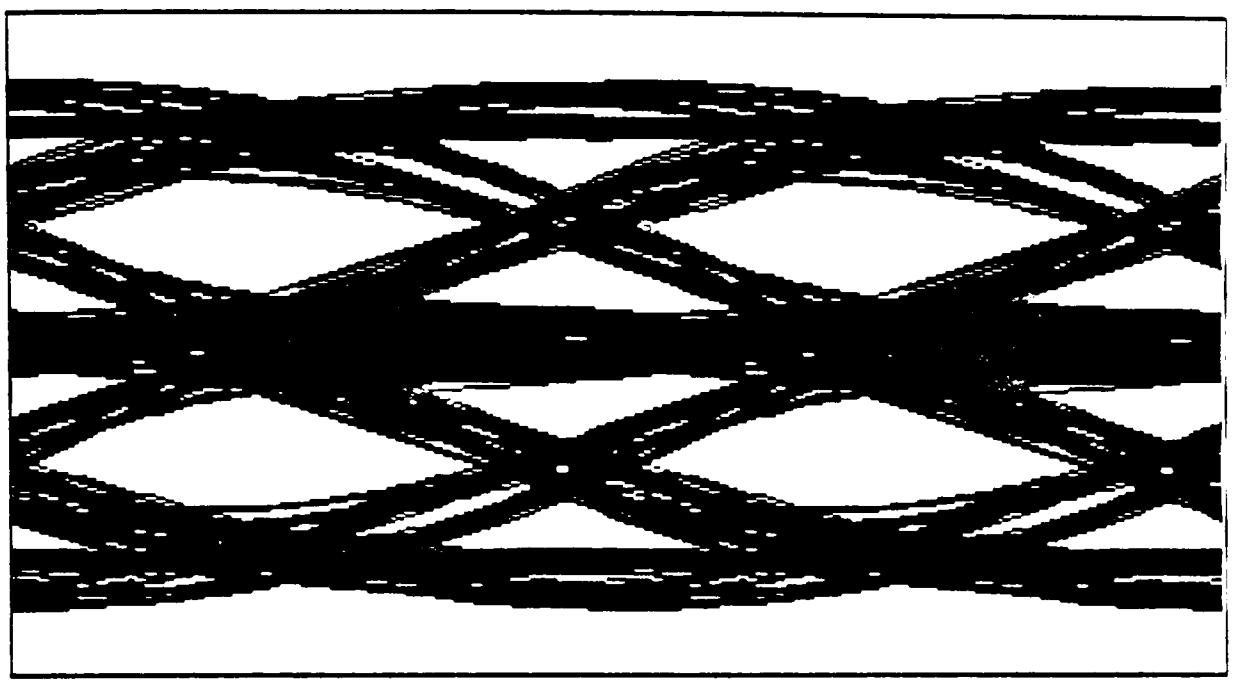

Figure 2.8: Eye diagram of digital radio system

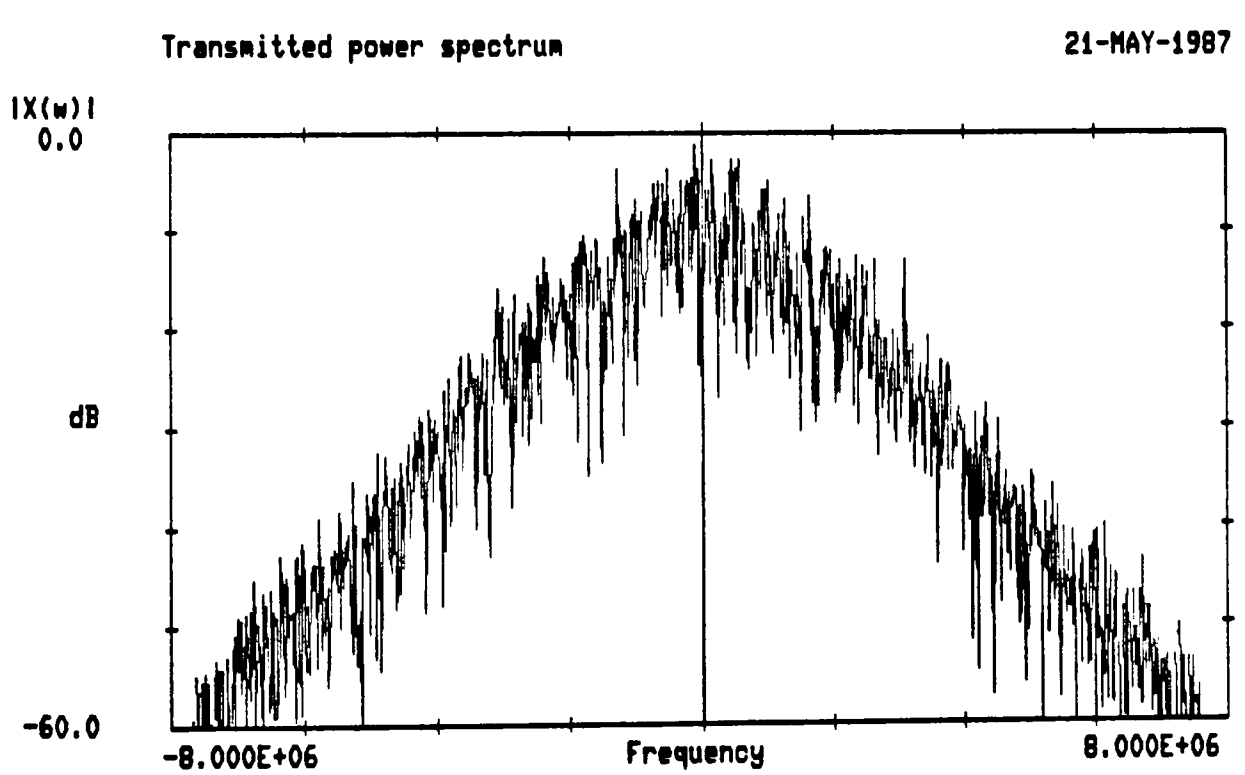

Figure 2.9: Transmitted power spectrum of the digital radio

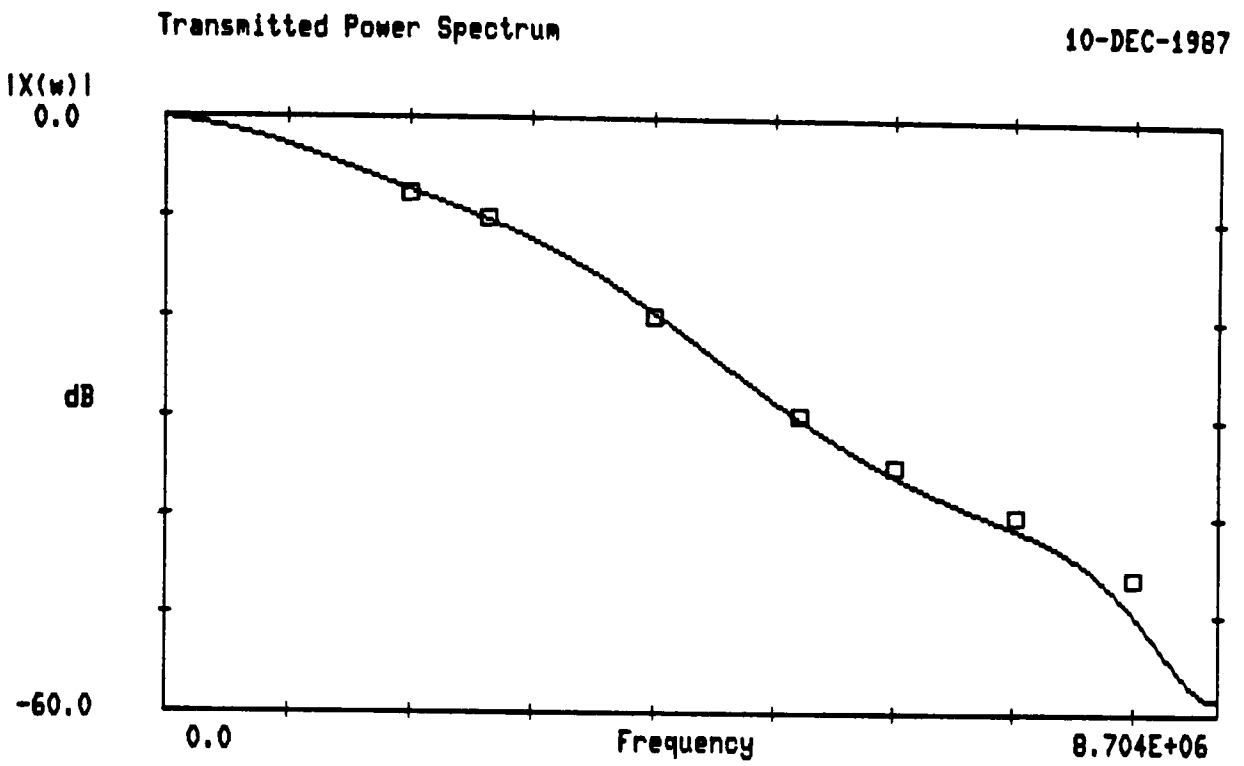

Figure 2.10: Comparison of smoothed power spectrum with experimental results

- to examine designs based on SAW IF filters from alternative manufacturers
- to examine the effect of propagation channel impairments on the system [18]

2.8 Conclusions

A systems approach has been used to design a dedicated simulation of a state-of-the-art radio system, and the resulting programme has been shown to closely model the behaviour of the equivalent real-world system. The simulation described did not include noise sources. This is because the very low bit error rates (BER) of interest when designing modern digital communication systems ($< 10^{-6}$) mean that it is impractical to simulate BER performance directly. A range of techniques for indirectly estimating BER within simulations have been developed [19].

The radio was used as an example of a complex analogue signal processing system and the lessons learnt during the development of the simulation are believed to be generally applicable to the simulation of any signal processing system. For the simulation to be of any use its behaviour must reliably match

that of the real world system it is designed to model. Confidence that the behaviour of the simulation accurately models that of the real system comes from the following sources.

- Sound theoretical background. In particular an understanding of sampling, the discrete Fourier transform, window effects and the baseband equivalent model of a carrier system.
- Implementation of the simulation using good software engineering practice: top-down development, successive refinement, modular and structured programming.
- Methodical testing of the simulation against theoretical expectations. A modular programme structure greatly assists this process since it allows functional blocks to be tested in isolation and then in simple combinations.
- Validation of the simulation against experiment.

The use of programme modules to implement functional blocks in the model of the signal processing system has the additional advantage of creating a pool of reliable modules. These are then available for future simulation activity.

Chapter 3

Adaptive Noise Cancelling

3.1 Introduction

A common signal processing requirement is to estimate a wanted signal from data that has been corrupted by interference or the addition of noise. The best method of doing this depends on the information that is available regarding the wanted and noise signals. The most common approach is to filter the signal so as to attenuate frequencies where the noise component is dominant. This approach is known as optimum filtering and there is a large body of literature on the subject [22]. The design of the filter requires that the signal and noise statistics be known or estimated. Optimum filters may be implemented in either analogue or digital form.

If it is possible to obtain a second signal that is predominantly or completely due to the noise or interference, then the unwanted component of the primary signal may be estimated from this second input and subtracted from the primary signal. In order for this approach to be effective it is necessary that the system be adaptive so that it can learn the statistics of the correlation between the unwanted signal and that provided by this reference input. This alternative approach is known as Adaptive Noise Cancelling, and does not require detailed knowledge of the signal or noise statistics. The complexity of the signal processing required is only a practical proposition using digital signal processing.

Adaptive Noise Cancelling was originally proposed by Widrow *et al* in 1975 [23]. Since then a number of papers have appeared proposing applications of, or improvements to the concept.This chapter presents a theoretical treatment of Adaptive Noise Cancelling systems, concentrating on issues important in practical applications of the technique:

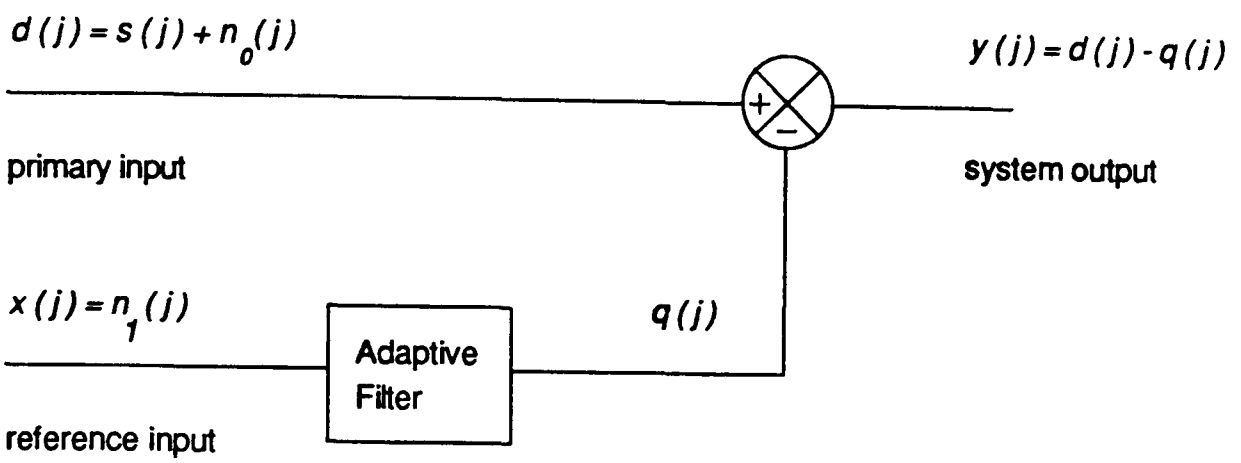

Figure 3.1: The adaptive noise cancelling system

- stability and convergence of the adaptive algorithm
- the effects of gradient estimation noise
- effects due to causality and truncation

The theoretical predictions are then compared with the results of computer simulations.

3.2 Adaptive Noise Cancelling

An adaptive noise cancelling system is shown schematically in figure 3.1. The primary input to the system consists of the discrete time signal $d(j)$ which consists of the wanted signal $s(j)$ plus additive noise $n_0(j)$. The second input, known as the reference input, consists of noise $n_1(j)$ which is correlated in some unknown way with $n_0(j)$. This is adaptively filtered to produce an optimal estimate of $n_0(j)$ and then subtracted from the primary input to produce the system output.

The error signal used to drive the adaptive algorithm is the system output $y(j)$. The adaptive algorithm adjusts the adaptive filter so as to minimise the output power $E\{(j)^2\}$. Now

$$y(j) = s(j) + n_0(j) - q(j) \tag{3.25}$$

Squaring and taking expectation values yields

$$E\{y(j)^2\} = E\{s(j)^2\} + E\{(n_0(j) - q(j))^2\} + 2E\{s(j)(n_0(j) - q(j))\} \quad (3.26)$$

If we assume that $s(j)$, $n_0(j)$ and $n_1(j)$ are statistically stationary and have zero means, and that $s(j)$ is uncorrelated with both $n_0(j)$ and $n_1(j)$ then

$$E\{y(j)^2\} = E\{s(j)^2\} + E\{(n_0(j) - q(j))^2\} \quad (3.27)$$

The signal power $E\{s(j)^2\}$ will be unaffected as the filter is adjusted, thus minimizing $E\{y(j)^2\}$ will result in the minimization of $E\{(n_0(j) - q(j))^2\}$. Hence the optimal filter output $q(j)$ is an l.m.s. estimate of the additive noise $n_0(j)$. Also from equation 1 $y(j)$ will then be an l.m.s. estimate of $s(j)$.

3.3 Idealised solutions to noise cancelling problems

3.3.1 Introduction

In this section solutions to noise cancellation problems are derived in order to establish the potential performance of the adaptive noise cancellation technique. The solutions are idealised in that they do not take into account the causality and finite order of practical adaptive filters. The statistics of the signal and noise are assumed stationary, and the filter is optimal in the l.m.s. sense-and hence fixed. The treatment is based on that in [23], but is more general.

3.3.2 The Wiener filter

A Wiener filter is a linear estimator designed to yield an optimal estimate of a signal $d(j)$, the desired response, from data samples $x(j)$ [24]. The output of the filter is given by

$$q(j) = \sum_{l=-\infty}^{\infty} w(l)x(j-l) \quad (3.28)$$

Where $w(l)$ is the impulse response of the filter, which extends over both positive and negative time. The error signal is given by

$$e(j) = d(j) - q(j) \tag{3.29}$$

The values of $w(l)$ which minimise the mean square error signal may be obtained by invoking the orthogonality principle [25], which states that, for the optimum filter, the error signal $e(j)$ is orthogonal to the data $x(j)$ i.e. $E\{x(i)e(j)\} = 0$ .This gives

$$E\left\{x(i)[d(j) - \sum_{l=-\infty}^{\infty} w(l)x(j-l)]\right\} = 0 \tag{3.30}$$

After some rearrangement we obtain

$$R_{dx}(k) = \sum_{l=-\infty}^{\infty} w^*(l)R_{xx}(k-l) \tag{3.31}$$

where $R_{dx}(k)$ is the cross correlation between $x(j)$ and $d(j)$ and $R_{xx}(k)$ is the autocorrelation of $x(j)$ given by

$$R_{dx}(k) = E\{d(j+k)x(j)\} \tag{3.32}$$

$$R_{xx}(k) = E\{x(j)x(j+k)\} \tag{3.33}$$

Equation 3.31 may be conveniently solved by Z transforming it to yield

$$W^*(z) = \frac{S_{dx}(z)}{S_{xx}(z)} \tag{3.34}$$

Where $W^*(z)$ is the Wiener transfer function, $S_{dx}(z)$ is the cross-power spectral density between $x(j)$ and $d(j)$ and $S_{xx}(z)$ is the power spectral density of $x(j)$.

This result is useful because in an adaptive noise cancelling system the adaptive filter is adjusted so as to minimise the mean square value of the output signal $y(j) = d(j) - q(j)$. It is thus attempting to filter the reference input $x(j)$ to form an l.m.s. estimate of the primary input $d(j)$. If the input signals are stationary, the ideal solution is given by the Wiener theory.

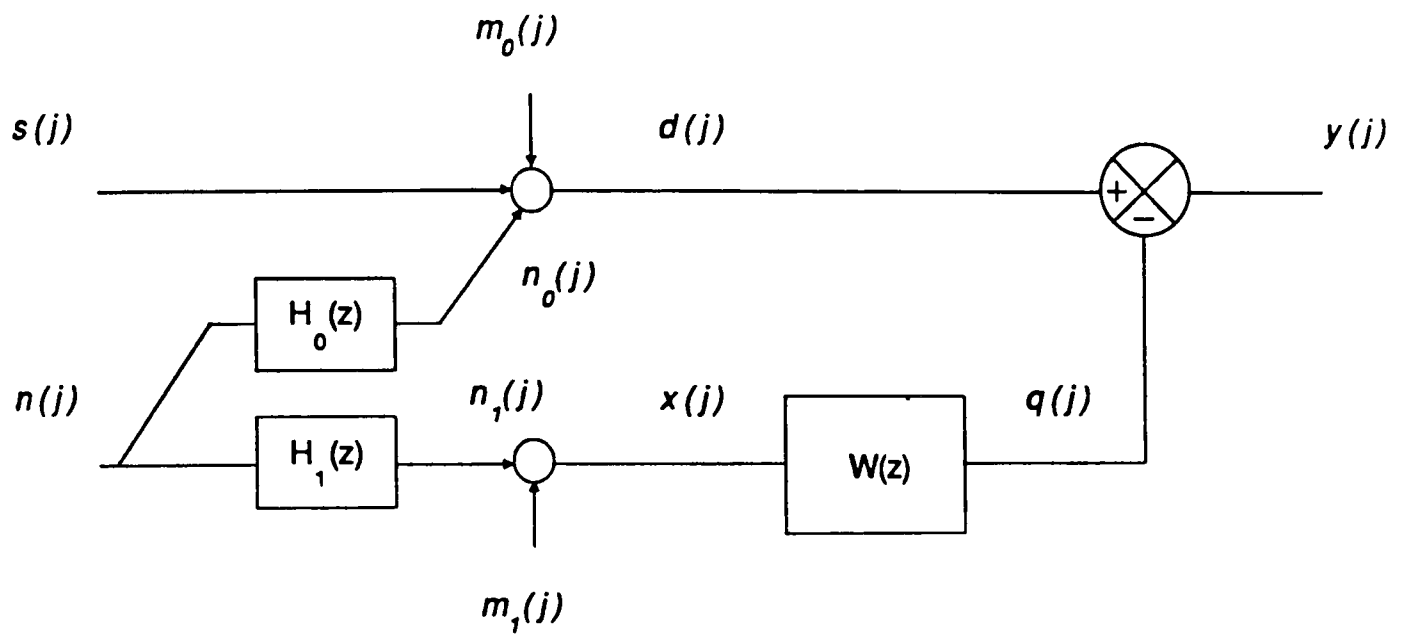

Figure 3.2: Adaptive noise cancelling system with typical input signals

3.3.3 Typical noise cancelling situation

Figure 3.2 shows an adaptive noise cancellation with a typical set of input signals, as follows:

The primary input is given by

$$d(j) = s(j) + n_0(j) + m_0(j) \tag{3.35}$$

where $s(j)$ is the wanted signal

$n_0(j)$ is an interfering signal (noise) to be removed, due to propagation of noise source $n(j)$ via channel $H_0(z)$

$m_0(j)$ is an additional noise, present only at this input

and the reference input is given by

$$x(j) = n_1(j) + m_1(j) \tag{3.36}$$

where $n_1(j)$ is a noise signal correlated with $n_0(j)$,due to propagation of noise source $n(j)$ via channel $H_1(z)$

$m_1(j)$ is an additional noise, present only at this input

$s(j), n(j), m_0(j), m_1(j)$ are all assumed to be stationary, zero mean and uncorrelated with each other. Now it may easily be shown that

$$S_{xx}(z) = S_{n_1 n_1}(z) + S_{m_1 m_1}(z) \tag{3.37}$$

$$\text{and} \quad S_{dx}(z) \;=\; S_{n_0 n_1}(z) \tag{3.38}$$

thus from eqn 3.34 the ideal (Wiener) transfer function is

$$W^*(z) = \frac{S_{n_0 n_1}(z)}{S_{n_1 n_1}(z) + S_{m_1 m_1}(z)} = \frac{S_{nn}(z) H_0(z) H_1(\frac{1}{z})}{S_{nn}(z) H_1(z) H_1(\frac{1}{z}) + S_{m_1 m_1}(z)} \tag{3.39}$$

if the additive noise in the reference input $m_1(j)$ is zero this simplifies to

$$W^*(z) = \frac{H_0(z)}{H_1(z)} \tag{3.40}$$

This is the result that we would expect, since it means that the noise in the reference input n_1 is filtered to recreate n_0 and noise cancellation is complete.

The output signal consists of the wanted signal $s(j)$ together with the following three noise components

- $m_0(j)$ propagating directly to the system output
- $m_1(j)$ propagating via the transfer function $-W^*(z)$
- $n(j)$ propagating via two paths, resulting in the transfer function $H_0(z) - H_1(z)W^*(z)$

The output noise power is thus given by

$$\begin{aligned} S_{\epsilon\epsilon}(z) \;=\;& S_{m_0 m_0}(z) \\ &+ S_{m_1 m_1}(z) W^*(z) W^*(\tfrac{1}{z}) \\ &+ S_{nn}(z)[H_0(z) - H_1(z)W^*(z)][H_0(\tfrac{1}{z}) - H_1(\tfrac{1}{z})W^*(\tfrac{1}{z})] \end{aligned} \tag{3.41}$$

These results can be simplified by defining $A(z)$ and $B(z)$ as the ratio of the power spectra of the uncorrelated to the correlated noise signals at the primary and reference inputs respectively

$$A(z) = \frac{S_{m_0 m_0}(z)}{S_{n_0 n_0}(z)} = \frac{S_{m_0 m_0}(z)}{S_{nn}(z) H_0(z) H_0(\frac{1}{z})} \tag{3.42}$$

$$B(z) = \frac{S_{m_1 m_1}(z)}{S_{n_1 n_1}(z)} = \frac{S_{m_1 m_1}(z)}{S_{nn}(z) H_1(z) H_1(\frac{1}{z})} \tag{3.43}$$

then $W^*(z)$ and $S_{\epsilon\epsilon}(z)$ can be written

$$W^*(z) = \frac{H_0(z)}{H_1(z)[B(z)+1]} \tag{3.44}$$

$$S_{\epsilon\epsilon}(z) = S_{nn}(z) H_0(z) H_0(\frac{1}{z}) \left[A(z) + \frac{B(z)}{B(z)+1} \right] \tag{3.45}$$

The effectiveness of noise cancellation may be expressed by the improvement in the ratio of the signal power spectrum to the noise power spectrum between the primary input and the system output. The ratio at the primary input is given by

$$\sigma_{pri}(z) = \frac{S_{ss}(z)}{S_{n_0 n_0}(z) + S_{m_0 m_0}(z)} \tag{3.46}$$

and at the system output by

$$\sigma_{out}(z) = \frac{S_{ss}(z)}{S_{\epsilon\epsilon}(z)} \tag{3.47}$$

The improvement ratio $\frac{\sigma_{out}(z)}{\sigma_{pri}(z)}$ may then be shown to be

$$\frac{\sigma_{out}(z)}{\sigma_{pri}(z)} = \frac{[1+A(z)][1+B(z)]}{[A(z)+A(z)B(z)+B(z)]} \tag{3.48}$$

It is evident that to achieve a large improvement in the signal to noise ratio of a corrupted signal both $A(z)$ and $B(z)$ should be small i.e. the level of uncorrelated additive noise in both inputs should be small. For $A(z) \ll 1$ and $B \ll 1$ the above becomes

$$\frac{\sigma_{out}(z)}{\sigma_{pri}(z)} = \frac{1}{A(z)+B(z)} \tag{3.49}$$

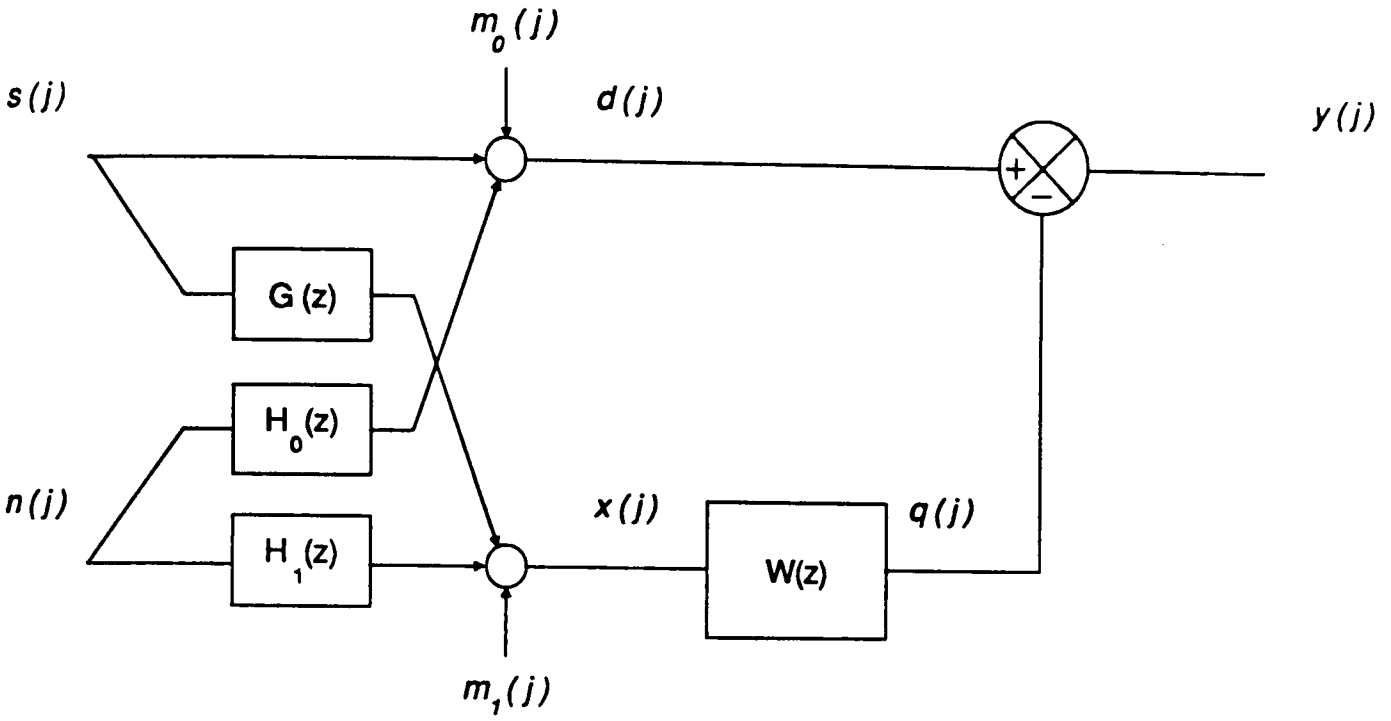

Figure 3.3: Example of leakage of wanted signal into reference input

3.3.4 Effect of signal components in the reference input

One of the problems in obtaining a reference input signal for an Adaptive Noise Cancelling system is ensuring that it does not contain components of the wanted signal. If present these will be subtracted from the wanted signal causing signal distortion and impaired noise cancellation.

Figure 3.3 shows an adaptive noise cancelling system with a set of input signals in which there is a transmission channel for wanted signal components into the reference input. The primary input, as before, is given by

$$d(j) = s(j) + n_0(j) + m_0(j) \tag{3.50}$$

and the reference input is now given by

$$x(j) = s_1(j) + n_1(j) + m_1(j) \tag{3.51}$$

where $s_1(j)$ is due to propagation of the wanted signal via channel $G(z)$ and $n_1(j)$ and $m_1(j)$ are as previously defined. $s(j), n(j), m_0(j), m_1(j)$ are again assumed to be stationary, zero mean and uncorrelated with each other.

Then we have

$$S_{xx}(z) = S_{s_1 s_1}(z) + S_{n_1 n_1}(z) + S_{m_1 m_1}(z) \tag{3.52}$$

$$\text{and} \quad S_{dx}(z) = S_{ss_1}(z) + S_{n_1 n_0}(z) \tag{3.53}$$

thus the ideal (Wiener) transfer function is now

$$W^*(z) = \frac{S_{ss_1}(z) + S_{n_1 n_0}(z)}{S_{s_1 s_1}(z) + S_{n_1 n_1}(z) + S_{m_1 m_1}(z)} \tag{3.54}$$

$$= \frac{S_{ss}(z)G(\frac{1}{z}) + S_{nn}(z)H_0(z)H_1(\frac{1}{z})}{S_{ss}(z)G(z)G(\frac{1}{z}) + S_{nn}H_1(z)H_1(\frac{1}{z}) + S_{m_1 m_1}(z)} \tag{3.55}$$

If we define $A(z)$ and $B(z)$ as before and define $\sigma_{ref}(z)$ as the ratio of signal power spectral density to noise power spectral density at the reference input

$$\sigma_{ref}(z) = \frac{S_{ss}(z)G(z)G(\frac{1}{z})}{S_{n_1 n_1}(z) + S_{m_1 m_1}(z)} \tag{3.56}$$

then after some algebra $W^*(z)$ can be shown to be

$$W^*(z) = \frac{\sigma_{ref}(z)}{[\sigma_{ref}(z)+1]G(z)} + \frac{H_0(z)}{H_1(z)[B(z)+1][\sigma_{ref}(z)+1]} \tag{3.57}$$

The form of the optimal transfer function is made clearer by assuming that the level of uncorrelated noise in the reference input is small, i.e. $B(z) \ll 1$. Then

$$W^*(z) \simeq \frac{1}{\sigma_{ref}(z)+1}\left[\frac{\sigma_{ref}(z)}{G(z)} + \frac{H_0(z)}{H_1(z)}\right] \tag{3.58}$$

The Wiener transfer function is thus a linear combination of the transfer function which causes cancellation of the noise and of that which causes cancellation of the signal; whose proportions are dependent on the value of the signal to noise ratio $\sigma_{ref}(z)$. Comparing the above two equations it can be seen that the effect of uncorrelated noise components in the reference input is to attenuate the transfer function component causing noise cancellation.

If there is no signal component in the reference input, the wanted signal propagates to the system output unaltered i.e. the transfer function of the

system is unity. With signal components present the transfer function of the system becomes

$$T(z) = 1 - G(z)W^*(z) \tag{3.59}$$

$$\tag{3.60}$$

$$= \frac{1}{[\sigma_{ref}(z)+1]}\left(1 - \frac{H_0(z)G(z)}{H_1(z)[B(z)+1]}\right) \tag{3.61}$$

To characterize the effect on the wanted signal it is useful to examine the quantity $D(z) = G(z)G(1/z)W^*(z)W^*(1/z)$.

$$D(z) = \frac{\left\{[B(z)+1]\sigma_{ref}(z) + \frac{H_0(z)G(z)}{H_1(z)}\right\}\left\{[B(\frac{1}{z})+1]\sigma_{ref}(z) + \frac{H_0(\frac{1}{z})G(\frac{1}{z})}{H_1(\frac{1}{z})}\right\}}{[B(z)+1]^2[\sigma_{ref}(z)+1]^2} \tag{3.62}$$

If $\sigma_{ref}(z) \ll 1$ this becomes

$$D(z) \simeq \frac{H_0(z)H_0(\frac{1}{z})G(z)G(\frac{1}{z})}{H_1(z)H_1(\frac{1}{z})[B(z)+1]^2} = \frac{\sigma_{ref}(z)}{\sigma_{pri}(z)[B(z)+1][A(z)+1]} \tag{3.63}$$

It is evident that the amplitude response of the system to sinusoidal input signals is bounded by

$$1 - |G(\omega)W^*(\omega)| \leq |T(\omega)| \leq 1 + |G(\omega)W^*(\omega)| \tag{3.64}$$

Thus the ripple in the amplitude response of the system is bounded by $\sqrt{D}(\omega)$. Similarly (provided $D(\omega) < 1$) the phase response of the system is bounded by $sin^{-1}\sqrt{D}(\omega)$

The general expressions for the output noise power, and for the output signal to noise density ratio are now rather complex. However if the level of the uncorrelated noise components in the primary and reference inputs are sufficiently low to be neglected, then the output power due to the wanted signal is given by

$$S_{ss}(z)(1 - G(z)W^*(z))(1 - G(\frac{1}{z})W^*(\frac{1}{z})) \tag{3.65}$$

and the output noise power is given by

$$S_{nn}(z)(H_0(z) - H_1(z)W^*(z))(H_0(\frac{1}{z}) - H_1(\frac{1}{z})W^*(\frac{1}{z})) \tag{3.66}$$

The signal to noise density ratio at the output may then be shown to be given by the remarkably simple result

$$\sigma_{out}(z) = \frac{1}{\sigma_{ref}(z)} \tag{3.67}$$

3.4 The Adaptation Algorithm

3.4.1 Choice of adaptation algorithm

The purpose of an adaptation algorithm is to adjust the characteristics of an adaptive system so as to minimise some error criterion, in this case the mean square output signal. There are many possible choices, but the use of the LMS algorithm is almost universal for adaptive noise cancelling systems. The reason for this is probably historical, but it also appears to be a good choice for this application.

The LMS algorithm has the following advantages

- simplicity and hence ease of implementation
- numerical ruggedness
- its properties are well characterized

The principal disadvantage of the LMS algorithm is that its rate of convergence is proportional to the ratio between the maximum and minimum eigenvalues of the autocorrelation matrix[28]. Thus its rate of convergence may be poor when the input signals are highly coloured.

Cowan has carried out a comparison of the properties of adaptation algorithms for FIR filters and concluded that under high noise conditions the LMS algorithm was probably superior [26]. In an adaptive noise cancellation system the adaptation algorithm is attempting to estimate the noise component of the signal at the primary input. The wanted signal component is (hopefully) uncorrelated with this component and thus represents a disturbance signal to the algorithm. The adaptation algorithm of an adaptive noise cancelling system is therefore effectively operating under high noise conditions and the LMS algorithm is a sensible choice.

3.4.2 Adaptive transversal filter

The LMS algorithm is generally used to adapt the weights of an adaptive transversal filter, which is of finite impulse response (FIR) type. The use of an adaptive infinite impulse response (IIR) filter could well lead to improved system characteristics for the same number of adaptive elements. It is possible to modify the LMS algorithm so as to adapt the coefficients of a recursive filter. However the use of recursive filters with all adaptive algorithms is subject to two problems which have severely restricted their application:

- The filter will become unstable if its z-plane poles move outside the unit circle during the adaptation process.
- The error surface will generally be non-quadratic, and may have local minima.

Overcoming these problems is currently an active area of adaptive systems research, however this investigation was restricted to the adaptive transversal filter.

The output signal from an adaptive transversal filter is given by

$$q(j) = \mathbf{W}(j)^T \mathbf{X}(j) = \mathbf{X}(j)^T \mathbf{W}(j) \tag{3.68}$$

where the input vector $\mathbf{X}(j)$ is given by

$$\mathbf{X}(j)^T = \{\, x(j)\ x(j-1)\ \ldots\ x(j-n+1)\,\} \tag{3.69}$$

and the weight vector $\mathbf{W}(j)$ is given by

$$\mathbf{W}(j)^T = \{w_0\ w_1\ \ldots\ w_{n-1}\,\} \tag{3.70}$$

Now if $x(j)$ and $d(j)$ are stationary processes, it is easily shown that the mean square error signal is given by:

$$E[e(j)^2] = E[d(j)^2] + \mathbf{W}(j)^T \mathbf{\Phi}_{xx} \mathbf{W}(j) - 2\mathbf{\Phi}_{dx}^T \mathbf{W}(j) \tag{3.71}$$

where the $\mathbf{\Phi}_{xx}$, the input correlation matrix, is given by

$$\mathbf{\Phi}_{xx} = E\{\mathbf{X}(j)\mathbf{X}(j)^T\} = \begin{Bmatrix} R_{xx}(0) & R_{xx}(1) & \ldots & R_{xx}(n-1) \\ R_{xx}(1) & R_{xx}(0) & \ldots & \cdot \\ \cdot & \cdot & \cdot & \cdot \\ \cdot & \cdot & R_{xx}(0) & R_{xx}(1) \\ R_{xx}(n-1) & \ldots & R_{xx}(1) & R_{xx}(0) \end{Bmatrix} \tag{3.72}$$

and $\mathbf{\Phi}_{dx}$ is given by

$$\mathbf{\Phi}_{dx} = E\{d(j)\mathbf{X}(j)\} = \left\{ \begin{array}{c} R_{dx}(0) \\ R_{dx}(1) \\ . \\ . \\ R_{dx}(n-1) \end{array} \right\} \tag{3.73}$$

The weight vector that minimises this error is given by

$$\mathbf{W}_{\text{opt}} = \mathbf{\Phi}_{xx}^{-1}\mathbf{\Phi}_{dx} \tag{3.74}$$

and the mean square error ξ_{opt} is then given by

$$\xi_{\text{opt}} = E[d(j)^2] - \mathbf{\Phi}_{dx}^T\mathbf{W}_{\text{opt}} \tag{3.75}$$

3.4.3 The LMS Algorithm

Since the quantities $\mathbf{\Phi}_{xx}$ and $\mathbf{\Phi}_{dx}$ are statistical expectation values, in general they can only be estimated. The LMS algorithm is an iterative procedure, due to Widrow and Hoff [27], for finding approximate solutions to this equation in real time.

The algorithm is a gradient descent algorithm, whereby the weight vector at iteration j+1 is given by:

$$\mathbf{W}(j+1) = \mathbf{W}(j) - \mu\nabla(j) \tag{3.76}$$

The parameter μ controls the rate of convergence, and the stability of the adaptive process. $\nabla(j)$ is the gradient of the error surface with respect to the coefficients of the weight vector.

$$\nabla(j) = \frac{\partial\{E[e(j)^2]\}}{\partial\mathbf{W}(j)} = 2\mathbf{\Phi}_{xx}\mathbf{W}(j) - 2\mathbf{\Phi}_{dx} \tag{3.77}$$

The LMS algorithm estimates the gradient, in a crude but effective manner by assuming that $e(j)^2$ is an estimate of the mean square error $E[e(j)^2]$.Thus

$$\hat{\nabla}(j) = \frac{\partial\{e(j)^2\}}{\partial\mathbf{W}(j)} = 2e(j)\frac{\partial\{e(j)^2\}}{\partial\mathbf{W}(j)} = -2e(j)\mathbf{X}(j) \tag{3.78}$$

giving the LMS algorithm

$$\mathbf{W}(j+1) = \mathbf{W}(j) + 2\mu e(j)\mathbf{X}(j) \tag{3.79}$$

3.4.4 Convergence

A great deal of effort has been directed toward analysis of the properties of the LMS Algorithm. In order to make the mathematics tractable it is generally assumed that the input data forms a sequence of uncorrelated vectors. It has been shown that the resulting analysis of convergence will be accurate provided that the adaptation rate is sufficiently small [31].

Taking expectation values of equation 3.79, and substituting for $e(j)$ gives

$$E\{\mathbf{W}(j+1)\} = E\{\mathbf{W}(j)\} + 2\mu E\{[d(j) - \mathbf{W}(j)^T\mathbf{X}(j)]\,\mathbf{X}(j)\} \quad (3.80)$$

$$= E\{\mathbf{W}(j)\} + 2\mu\mathbf{\Phi}_{dx} - 2\mu E\{[\mathbf{X}(j)\mathbf{X}(j)^T]\,\mathbf{W}(j)\} \quad (3.81)$$

making the independent vectors assumption this becomes

$$E\{\mathbf{W}(j+1)\} = [\mathbf{I} - 2\mu\mathbf{\Phi}_{xx}]E\{\mathbf{W}(j)\} + 2\mu\mathbf{\Phi}_{dx} \quad (3.82)$$

Thus from an initial weight vector $\mathbf{W}(0)$ we have

$$E\{\mathbf{W}(j+1)\} = [\mathbf{I} - 2\mu\mathbf{\Phi}_{xx}]^{j+1}\mathbf{W}(0) + 2\mu\mathbf{\Phi}_{dx}\sum_{i=0}^{j}[\mathbf{I} - 2\mu\mathbf{\Phi}_{xx}]^i \quad (3.83)$$

Since the autocorrelation matrix $\mathbf{\Phi}_{xx}$ is symmetric, we can carry out the similarity transformation

$$\mathbf{\Phi}_{xx} = \mathbf{M}^{-1}\mathbf{\Lambda}\mathbf{M} \quad (3.84)$$

where $\mathbf{M}$ is the orthonormal modal matrix of Φ_{xx} , and $\mathbf{\Lambda}$ is its eigenvalue matrix [30], to obtain

$$E\{\mathbf{W}(j+1)\} = \mathbf{M}^{-1}\,[\mathbf{I} - 2\mu\mathbf{\Lambda}]^{j+1}\,\mathbf{M}\mathbf{W}(0) + 2\mu\mathbf{M}^{-1}\sum_{i=0}^{j}[\mathbf{I} - 2\mu\mathbf{\Lambda}]^i\,\mathbf{M}\mathbf{\Phi}_{dx} \quad (3.85)$$

We wish to examine the behaviour of the above as $j \to \infty$. The diagonal matrix $[\mathbf{I} - 2\mu\mathbf{\Lambda}]^{j+1}$ will tend to zero provided all the elements of $[\mathbf{I} - 2\mu\mathbf{\Lambda}]$ have magnitude less than unity. The first term will thus tend to zero, subject to a stability constraint on the value of μ.

$\sum_{i=0}^{j}[\mathbf{I}-2\mu\mathbf{\Lambda}]^i$ is a diagonal matrix whose p^{th} component is $[1-2\mu\lambda_p]$, and since

$$\lim_{j\to\infty}\sum_{i=0}^{j}[1-2\mu\lambda_p]^i = \frac{1}{2\mu\lambda_p} \tag{3.86}$$

$$\text{then} \quad \lim_{j\to\infty}\sum_{i=0}^{j}[\mathbf{I}-2\mu\mathbf{\Lambda}]^i = \frac{\mathbf{\Lambda}^{-1}}{2\mu} \tag{3.87}$$

The second term will thus tend toward $\mathbf{M}^{-1}\mathbf{\Lambda}^{-1}\mathbf{M}\mathbf{\Phi}_{dx}$. We therefore obtain

$$\lim_{j\to\infty} E\{\mathbf{W}(j)\} = \mathbf{M}^{-1}\mathbf{\Lambda}^{-1}\mathbf{M}\mathbf{\Phi}_{dx} = \mathbf{\Phi}_{xx}^{-1}\mathbf{\Phi}_{dx} = \mathbf{W}_{\text{opt}} \tag{3.88}$$

The mean weight vector will therefore converge to the optimal weight vector, provided that μ is sufficiently small.

3.4.5 Stability

For the first term in equation 3.85 to tend to zero, the elements of the diagonal matrix $[\mathbf{I}-2\mu\mathbf{\Lambda}]$ must all have a magnitude of less than unity. That is

$$|1-2\mu\lambda_p| < 1 \quad p = 0,1,2...n-1 \tag{3.89}$$

Since the autocorrelation matrix $\mathbf{\Phi}_{xx}$ is real, symmetric and positive definite its eigenvalues λ_p are positive real. Thus the above stability condition becomes

$$0 < \mu < \frac{1}{\lambda_{\max}} \tag{3.90}$$

where $\lambda_{\max}$ is the largest eigenvalue of $\mathbf{\Phi}_{xx}$. In practice this stability criterion is difficult to apply since the eigenvalues are not known. Since $\mathbf{\Phi}_{xx}$ is square we have

$$Tr.\mathbf{\Phi}_{xx} = \lambda_0+\lambda_1+...\lambda_{n-1} \tag{3.91}$$

$$\text{therefore} \quad Tr.\mathbf{\Phi}_{xx} > \lambda_{\max} \tag{3.92}$$

Now $Tr.\mathbf{\Phi}_{xx} = nE\{x^2(j)\}$ thus a rather conservative, but easy to apply stability criterion is

$$0 < \mu < \frac{1}{nE\{x^2(j)\}} \tag{3.93}$$

The conditions given above ensure that the mean weight vector converges to the optimal solution. This does not ensure however that the variance of the filter weight vector, or the mean square error signal, are finite. For uncorrelated Gaussian noise signals, Feuer and Weinstein [32] derived the following necessary conditions for finite weight vector variance, and hence mean square error

$$\begin{array}{ccccc} 0 & < & \mu & < & \frac{1}{2\lambda_{max}} \\ \text{and} & & \sum_p \frac{\mu\lambda_p}{1-2\mu\lambda_p} & < & 1 \end{array} \tag{3.94}$$

They also give a more conservative condition, similar to 3.93 above, as

$$0 < \mu < \frac{1}{3nE\{x^2(j)\}} \tag{3.95}$$

In the convergence and stability analyses given above it was assumed that the input signal formed a sequence of uncorrelated input vectors. That is

$$E\{\mathbf{X}(j)\mathbf{X}(j+k)\} = 0, \text{ for } k \neq 0 \tag{3.96}$$

This assumption is made so that the filter weight vector $\mathbf{W}(j)$ can be treated as being independent of the data vector $\mathbf{X}(j)$. It is only strictly true when the reference input $x(j)$ is uncorrelated, but analyses based on this assumption have been found to agree with experimental results under a wide variety of conditions [31].

One condition under which this assumption is violated is when an adaptive noise cancelling system has a sinusoidal signal as its reference input. The system forms a notch filter with a Q determined by the value of μ [33]. If the primary input is a sinewave at a slightly different frequency, the filter weights oscillate at the difference frequency, causing cancellation to occur [29]. It is interesting to note however that the mean weight vector is still equal to the optimum solution [34].

3.4.6 Adaptation rate

We will now consider the manner in which the LMS algorithm approaches its steady state from an arbitrary initial state. The error signal $e(j)$ is defined by

$$e(j) = d(j) - q(j) \tag{3.97}$$

and if the input signals $x(j)$ and $d(j)$ are stationary processes then the mean square error signal is given by

$$E[e(j)^2] = E[d(j)^2] + \mathbf{W}(j)^T \mathbf{\Phi}_{xx} \mathbf{W}(j) - 2\mathbf{\Phi}_{dx}^T \mathbf{W}(j) \tag{3.98}$$

We have already noted that the minimum value of this error is given by

$$\xi_{\text{opt}} = E\{d^2(j)\} - \mathbf{\Phi}_{dx}^T \mathbf{W}_{\text{opt}} \tag{3.99}$$

when the weight vector has its optimum value $\mathbf{W}_{\text{opt}} = \mathbf{\Phi}_{xx}^{-1} \mathbf{\Phi}_{dx}$. Using these values we can simplify the general expression for mean square error, which we will denote $\xi(j)$ to obtain

$$\xi(j) = \xi_{\text{opt}} + [\mathbf{W}(j) - \mathbf{W}_{\text{opt}}(j)]^T \mathbf{\Phi}_{xx} [\mathbf{W}(j) - \mathbf{W}_{\text{opt}}(j)] \tag{3.100}$$

$$= \xi_{\text{opt}} + \mathbf{V}(j)^T \mathbf{\Phi}_{xx} \mathbf{V}(j) \tag{3.101}$$

where $\mathbf{V}(j)$ denotes the difference between the instantaneous weight vector and its optimum value. It is convenient to transform this equation into a new co-ordinate system defined by

$$\mathbf{V}'(j) = \mathbf{M}^{-1} \mathbf{V}(j) \tag{3.102}$$

where, as before, $\mathbf{M}$ is the orthonormal modal matrix of $\mathbf{\Phi}_{xx}$ to obtain

$$\xi(j) = \xi_{\text{opt}} + (\mathbf{V}'(j))^T \mathbf{\Lambda} \mathbf{V}'(j) \tag{3.103}$$

The LMS algorithm is an approximation to a gradient descent algorithm, thus we would expect its mean dynamic behaviour to be that of a true gradient descent algorithm, at least for small values of μ. As before, the gradient descent algorithm is

$$\mathbf{W}(j+1) = \mathbf{W}(j) - \mu \nabla(j) \tag{3.104}$$

Differentiating eqn 3.101 yields an expression for the gradient

$$\nabla(j) = 2\mathbf{\Phi}_{xx} \mathbf{V}(j) \tag{3.105}$$

Substituting this in the above yields after some simplification

$$\mathbf{V}(j+1) = [\mathbf{I} - 2\mu \mathbf{\Phi}_{xx}] \mathbf{V}(j) \tag{3.106}$$

In the transformed (normal) co-ordinate system this becomes

$$\mathbf{V}'(j+1) = [\mathbf{I} - 2\mu\mathbf{\Lambda}]\mathbf{V}'(j) \tag{3.107}$$

Since $\mathbf{\Lambda}$ is diagonal, the effect of the transformation is to reduce the vector equation to a set of uncoupled difference equations. That for the p^{th} component of $\mathbf{V}$ is

$$v'_p(j+1) = [1 - 2\mu\lambda_p]v'_p(j) \tag{3.108}$$

If we assume some arbitrary initial value $v_p(0)$, the solution is given by the simple geometric decay

$$v'_p(j) = [1 - 2\mu\lambda_p]^j v'_p(0) \tag{3.109}$$

Since each component of the vector $\mathbf{V}(j)$ will decay in this way we obtain the solution

$$\mathbf{V}'(j) = [\mathbf{I} - 2\mathbf{\Lambda}]^j \mathbf{V}'(0) \tag{3.110}$$

We can obtain a time-constant for the decay of each component by fitting an exponential to the geometric sequence. We have

$$\frac{v'_p(j+1)}{v'_p(j)} = (1 - 2\mu\lambda_p) \tag{3.111}$$

whereas for an exponential decay with time constant τ_p

$$\frac{v'_p(j+1)}{v'_p(j)} = e^{-\frac{T}{\tau_p}} = 1 - \frac{T}{\tau_p} + \frac{T^2}{2\tau_p^2} \tag{3.112}$$

where T is the sample period. For time constants much greater than one sample period this gives

$$\tau_p = \frac{T}{2\mu\lambda_p} \tag{3.113}$$

The expectation value of the power in the error signal as the algorithm adapts is given by substituting the solution of equation 3.110 into equation 3.103 to reveal

$$\xi(j) = \xi_{\text{opt}} + [\mathbf{V}'(0)^T[\mathbf{I} - 2\mu\mathbf{\Lambda}]^j \mathbf{\Lambda}[\mathbf{I} - 2\mu\mathbf{\Lambda}]^j \mathbf{V}'(0) \tag{3.114}$$

Transforming back to the standard co-ordinate system this becomes

$$\xi(j) = \xi_{\text{opt}} + \mathbf{V}(0)^T[\mathbf{I} - 2\mu\mathbf{\Phi}_{xx}]^j\mathbf{\Phi}_{xx}[\mathbf{I} - 2\mu\mathbf{\Phi}_{xx}]^j\mathbf{V}(0) \tag{3.115}$$

Provided that the adaptive process is convergent, the mean square error will tend toward ξ_{opt}. The total error power is the sum of n modes each of which decays geometrically. The geometric ratio for the p_{th} mode is $(1 - 2\mu\lambda_p)^2$, with a corresponding time constant $T/4\mu\lambda_p$.

The result of plotting mean square error $\xi(j)$ against iteration number j for an adaptive process is known as its learning curve. The learning curve consists of a sum of exponentials, however if the eigenvalues of $\mathbf{\Phi}_{xx}$ are sufficently similar it can be adequately approximated by a single exponential with a time constant τ_{mse} given by equation 3.113 using the average of their values.

$$\lambda_{\text{av}} = \frac{\lambda_0+\lambda_1+\ldots+\lambda_{n-1}}{n} = \frac{Tr.\mathbf{\Phi}_{xx}}{n} \tag{3.116}$$

$$\text{therefore} \qquad \tau_{\text{mse}} = \frac{T}{4\mu E\{x^2(j)\}} \tag{3.117}$$

The learning behaviour discussed in this section is that of a true gradient descent algorithm, where the gradient $\nabla(j)$ is known at each iteration. The LMS algorithm uses a gradient estimate which must inevitably be noisy. Because of the noise in the gradient estimate the LMS algorithm will converge in a more erratic manner than a gradient descent algorithm. Actual learning curves will be noisy and will tend to have longer time constants than predicted by equation 3.113 above [29].

3.4.7 Gradient estimation noise

We noted in the previous section that the imperfect nature of the gradient estimate used in the LMS algorithm will cause the learning curve of the ANC system to appear noisy and will slow convergence compared to the performance of a true gradient descent algorithm. In this section we will examine its effect on the steady state performance of the system.

The gradient estimate used in the LMS algorithm is

$$\hat{\nabla}(j) = -2e(j)\mathbf{X}(j) \tag{3.118}$$

$$= -2[d(j) - \mathbf{W}(j)^T\mathbf{X}(j)]\mathbf{X}(j) \tag{3.119}$$

taking expectation values, for constant $\mathbf{W}(j)$ gives

$$E\{\hat{\nabla}(j)\} = -2E\{d(j)\mathbf{X}(j)\} + 2E\left\{\mathbf{X}(j)\mathbf{X}^T(j)\right\}\mathbf{W}(j) \quad (3.120)$$

$$= -2\mathbf{\Phi}_{dx} + 2\mathbf{\Phi}_{xx}\mathbf{W}(j) \quad (3.121)$$

$$= \nabla(j) \quad (3.122)$$

The gradient estimate is therefore unbiassed, so we can write it in the form

$$\hat{\nabla}(j) = \nabla(j) + \mathbf{N}(j) \quad (3.123)$$

where $\mathbf{N}(j)$ is a gradient estimate noise vector with zero mean. When the adaptive system has reached the steady state, the weight vector will be close to $\mathbf{W}_{\text{opt}}$ and the true gradient will be close to zero. Thus

$$\mathbf{N}(j) = -2e(j)\mathbf{X}(j) \quad (3.124)$$

From the orthogonality principle [25], when $\mathbf{W}(j) = \mathbf{W}_{\text{opt}}$, $e(j)$ and $\mathbf{X}(j)$ are uncorrelated, and if we assume that they have zero mean, then they are statistically independent. The covariance of $\mathbf{N}(j)$ is therefore given by

$$Cov.\{\mathbf{N}(j)\} = E\{\mathbf{N}(j)\mathbf{N}(j)^T\} \quad (3.125)$$

$$= 4E\{e^2(j)\}E\{\mathbf{X}(j)\mathbf{X}(j)^T\} \quad (3.126)$$

$$= 4\xi_{\text{opt}}\mathbf{\Phi}_{xx} \quad (3.127)$$

In the transformed co-ordinate system this becomes

$$Cov.\{N'(j)\} = 4\xi_{\text{opt}}\mathbf{\Lambda} \quad (3.128)$$

We are interested in the effect of the gradient estimation noise on the weight vector. Now the LMS algorithm can be written

$$\mathbf{W}(j+1) = \mathbf{W}(j) - \mu\hat{\nabla}(j) \quad (3.129)$$

$$= \mathbf{W}(j) - \mu[\nabla(j) + \mathbf{N}(j)] \quad (3.130)$$

$$\mathbf{V}(j+1) = \mathbf{V}(j) - \mu[\nabla(j) + \mathbf{N}(j)] \quad (3.131)$$

$$= \mathbf{V}(j) - \mu[2\mathbf{\Phi}_{xx}\mathbf{V}(j) + \mathbf{N}(j)] \quad (3.132)$$

In the transformed co-ordinate system this becomes

$$\mathbf{V}'(j+1) = [\mathbf{I} - 2\mu\mathbf{\Lambda}]\mathbf{V}'(j) - \mu\mathbf{N}'(j) \tag{3.133}$$

In the transformed co-ordinates the components of $\mathbf{N}'(j)$ are uncorrelated as $Cov.\{\mathbf{N}'(j)\}$ is diagonal. The noise components of $\mathbf{V}'(j)$ will therefore be similarly uncorrelated. In the steady state the mean of $\mathbf{V}'(j)$ is zero. Now from equation 3.133 we obtain

$$(\mathbf{V}'(j+1))^T = \mathbf{V}'(j)^T[\mathbf{I} - 2\mu\mathbf{\Lambda}] - \mu\mathbf{N}'(j)^T \tag{3.134}$$

$$\begin{aligned} E\{\mathbf{V}(j+1)\,(\mathbf{V}'(j+1))^T\} \;=\; & \left\{[\mathbf{I} - 2\mu\mathbf{\Lambda}]\mathbf{V}'(j)\mathbf{V}'(j)^T[\mathbf{I} - 2\mu\mathbf{\Lambda}]\right\} \\ & +\mu^2 E\left\{\mathbf{N}'(j)\mathbf{N}'(j)^T\right\} \\ & -E\left\{\mathbf{N}'(j)\mathbf{V}'(j)^T[\mathbf{I} - 2\mu\mathbf{\Lambda}]\right\} \\ & -\mu E\left\{[\mathbf{I} - 2\mu\mathbf{\Lambda}]\mathbf{V}'(j)\mathbf{N}'(j)^T\right\} \end{aligned} \tag{3.135}$$

If we again assume that $\mathbf{X}(j)$ forms a sequence of uncorrelated vectors (see section 3.4.4) then $\mathbf{N}(j)$ will be uncorrelated with $\mathbf{W}(j)$, and thus $\mathbf{N}'(j)$ is uncorrelated with $\mathbf{V}'(j)$. The above therefore simplifies to

$$\begin{aligned} Cov.\{\mathbf{V}'(j+1)\} \;=\; & [\mathbf{I} - 2\mu\mathbf{\Lambda}]Cov.\{\mathbf{V}'(j)\}[\mathbf{I} - 2\mu\mathbf{\Lambda}] \\ & +\mu^2 Cov.\{\mathbf{N}'(j)\} \end{aligned} \tag{3.136}$$

Since we are assuming steady state conditions $Cov\{\mathbf{V}'(j+1)\} = Cov\{\mathbf{V}'(j)\}$. $Cov\{\mathbf{V}'(j)\}$ is diagonal, thus the above becomes

$$Cov\{\mathbf{V}'(j)\} = [\mathbf{I} - 2\mu\mathbf{\Lambda}]^2 Cov\{\mathbf{V}'(j)\} + \mu^2 Cov\{\mathbf{N}'(j)\} \tag{3.137}$$

Substituting for $Cov\{\mathbf{N}(j)\}$ from equation 3.128 gives, after some re-arrangement

$$[\mathbf{I} - \mu\mathbf{\Lambda}]Cov.\{\mathbf{V}'(j)\} = \mu\xi_{\text{opt}}\mathbf{I} \tag{3.138}$$

In practical situations the elements of $\mu\mathbf{\Lambda}$ are considerably less than unity [29] thus we obtain

$$Cov.\{\mathbf{V}'(j)\} = \mu\xi_{\text{opt}}\mathbf{I} \tag{3.139}$$

Transforming back to standard co-ordinates gives

$$Cov.\{\mathbf{V}(j)\} = \mathbf{M}\mu\xi_{\text{opt}}\mathbf{I}\mathbf{M}^{-1} = \mu\xi_{\text{opt}}\mathbf{I} \tag{3.140}$$

The noise components in the weight vector are thus of equal power, and uncorrelated with each other. In this treatment it was assumed that $\mathbf{X}(j)$ formed a series of independent vectors, and that $\mathbf{W}(j)$ was close to $\mathbf{W}_{\text{opt}}$. However Widrow [28] reports that equation 3.140 closely approximates measured weight vector variances under a considerably wider range of conditions than these assumptions imply.

3.4.8 Misadjustment

The effect of random noise in the weight vector, caused by gradient estimation noise, is to increase the mean square error signal. If the weight vector was noise free and converged exactly to $\mathbf{W}_{\text{opt}}$ then the mean square error in the steady state ξ would be ξ_{opt}. The increase in mean square error may be characterized by a dimensionless ratio M which Widrow [29] has denoted 'misadjustment'.

$$M = \frac{\xi - \xi_{\text{opt}}}{\xi_{\text{opt}}} \tag{3.141}$$

Now from equation 3.103, the mean square error in the steady state is given by

$$\xi = \xi_{\text{opt}} + E\{\mathbf{V}'(j)^T\mathbf{\Lambda}\mathbf{V}'(j)\} \tag{3.142}$$

therefore

$$\xi - \xi_{\text{opt}} = E\{\mathbf{V}'(j)^T\mathbf{\Lambda}\mathbf{V}'(j)\} \tag{3.143}$$

$$= \sum_{p=0}^{n-1} \lambda_p E\{\left(v'_p(j)\right)^2\} \tag{3.144}$$

In the previous section it was demonstrated that if the steady state weight vector was close to W_{opt} then $Cov.\{\mathbf{V}'(j)\} = \mu\xi_{\text{opt}}\mathbf{I}$. The above then becomes

$$\xi - \xi_{\text{opt}} = \mu\xi_{\text{opt}} \sum_{p=0}^{n-1} \lambda_p \tag{3.145}$$

$$= \mu\xi_{\text{opt}} Tr.\{\mathbf{\Phi}_{xx}\} \tag{3.146}$$

The misadjustment ratio is therefore given by

$$M = \mu Tr.\{\phi_{xx}\} = \mu n E\{x^2(j)\} \tag{3.147}$$

All adaptive systems which operate in real time experience a degradation in performance because their statistical estimates are based on a limited data sample. The faster a system adapts, in general, the poorer will be its steady state performance. The misadjustment ratio M is a direct measure of this performance degradation, and we can relate this to the adaptation rate by comparing the above with eqn 3.117 to reveal the relation

$$M = \frac{nT}{4\tau_{\text{mse}}} \tag{3.148}$$

3.5 Truncation and causality

The ideal solution to noise cancellation problems requires filters whose impulse responses, in general, extend infinitely over both positive and negative time. Realizable adaptive filters can only implement causal impulse responses of finite duration. In this section it is intended to examine the consequences of causality and truncation.

3.5.1 The transfer function

The transfer function of a linear shift invariant discrete time system is the Z transform of its impulse response. The system described by the difference equation

$$y(j) + \sum_{p=1}^{N} a_p y(j-p) = \sum_{q=1}^{M} b_q x(j-q) \tag{3.149}$$

has the corresponding transfer function

$$H(z) = \frac{\sum_{q=1}^{M} b_q z^{-q}}{1 + \sum_{p=1}^{N} a_p z^{-p}} \tag{3.150}$$

The solution $y(j)$ to this difference equation is the sum of two parts [35]:

1. The homogeneous solution, which is a characteristic solution with arbitrary coefficients, found by setting the forcing terms $x(j)$ to zero. It has terms of the form $A\alpha^j$ (A arbitrary).

2. The particular solution, which is one output sequence $y(j)$ possible given the input sequence $x(j)$.

The transfer function of a system thus defines a whole family of possible impulse responses $h(j)$. A unique response is determined either by specifying the initial conditions of the system, or equivalently, by specifying the region of convergence of the Z transform [35].

The Z transform of the infinite sequence $x(j)$ is given by

$$X(z) = \sum_{j=-\infty}^{\infty} x(j)z^{-j} \tag{3.151}$$

The region of convergence is that region of the complex plane for which this sum converges to a finite value. If we define a *right-sided* sequence as a sequence $x(j)$ which is only non-zero for values of j greater than or equal to some number j_1, then the region of convergence is the portion of the z plane lying outside a circle centred on the origin. The circle, of radius r_1, passes through the pole furthest from the origin.

For a *left-sided* sequence i.e. one that is only non-zero for values of j less than or equal to some number j_2 the region of convergence is the inside of a circle centred on the origin. The circle, of radius r_2, passes through the pole closest to the origin.

An infinite sequence can be written as the sum of a left-handed sequence and a right-handed sequence. The Z transform of the combined *two-sided* sequence is equal to the sum of the transforms of the left and right-handed sequences. The region of convergence of the total transform is then the intersection of the regions of convergence of the individual transforms.

It is evident that the transform can only converge as $z \rightarrow \infty$ if all terms involving positive powers of z are zero. The sequence $x(j)$ must therefore be zero for $j < 0$ i.e. it is causal. Similarly, in order for the transform to converge at the origin the sequence must be zero for $j > 0$. I have denoted such sequences anti-causal. On the unit z circle the transform is given by

$$X(e^{\imath\theta}) = \sum_{j=-\infty}^{\infty} x(j)e^{-\imath\omega j} \tag{3.152}$$

The series will converge if

$$\sum_{j=-\infty}^{\infty} |x(j)| < \infty \tag{3.153}$$

This relation is the condition that the sequence represents the impulse response of a stable system. The above results are summarized in the following table.

Region of Convergence	Sequence	System characteristic
$r_1 < \|z\|$	right-sided	Max $\|z_p\| = r_1$
$\|z\| < r_2$	left-sided	Min $\|z_p\| = r_2$
$r_1 < \|z\| < r_2$	two-sided	
$0 < \|z\| < \infty$	finite	FIR, stable
includes $z = \infty$	$h(j) = 0 \quad j < 0$	causal
includes $\|z\| = 1$	$\sum \|h(j)\| < \infty$	stable
includes $z = 0$	$h(j) = 0 \quad j > 0$	anti-causal

In the analysis of sampled data systems it is usual to invert Z transforms so that the corresponding sequences are causal, and some texts define the inverse transform in this way. The region of convergence of the Z transform must then be the outside of the circle $|z| = r_1$. If the transform includes any poles within the unit z circle the terms of the sequence diverge, and represents an unstable system. This constraint is, however, inappropriate when considering the Wiener transfer function. The correct solution to the Wiener filtering problem (equation 3.31) is the stable inverse.

3.5.2 The Wiener transfer function

If we consider the typical noise cancellation problem of figure 3.2 with the outside noise sources m_0 and m_1 ignored for simplicity then the ideal (Wiener) transfer function is given by

$$W^*(z) = \frac{H_0(z)}{H_1(z)} \tag{3.154}$$

The poles of $W^*(z)$ are coincident with the poles of $H_0(z)$ together with the zeros of $H_1(z)$. $H_0(z)$ and $H_1(z)$ represent real world transmission channels and are thus both causal and stable. Their poles all lie within the unit z circle. If $H_1(z)$ is a minimum phase system its zeros will also lie within the unit z circle and $W^*(z)$ will be causal. In general however this will not be so and the Wiener solution will be non-causal.

When the additional uncorrelated noise signals $m_0(j)$ and $m_1(j)$ are present

the Wiener solution is given by

$$W^*(z) = \frac{S_{nn}(z)H_0(z)H_1(\frac{1}{z})}{S_{nn}(z)H_1(z)H_1(\frac{1}{z}) + S_{m_1m_1}(z)} \tag{3.155}$$

The poles of $W^*(z)$ are thus given by the sum of the poles of $S_{nn}(z)$, $H_0(z)$ and $H_1(\frac{1}{z})$, together with the zeros of $[S_{nn}(z)H_1(z)H_1(\frac{1}{z}) + S_{m_1m_1}(z)]$.

- $S_{nn}(z)$ is the power spectral density of the noise signal $n(j)$. It is equal to the Z transform of the autocorrelation function, which is symmetric about $k = 0$. The poles of $S_{nn}(z)$ therefore occur in reciprocal pairs i.e. for every pole inside the unit z circle at $z = p_i$ there is one outside at $z = 1/p_i$.

- $H_0(z)$ is a real world transmission channel and is thus causal and stable. Its poles lie within the unit z circle.

- $H_1(z)$ is a real world transmission channel. The poles of $H_1(\frac{1}{z})$ therefore lie outside the unit z circle.

- $[S_nn(z)H_1(z)H_1(\frac{1}{z}) + S_{m_1m_1}(z)]$ is the total power spectral density of the signals at the reference input. Its zeros, like its poles, occur in reciprocal pairs.

In the presence of outside noise sources, the majority of the poles of the Wiener transfer function will occur in reciprocal pairs. The remaining poles, those due to $H_0(z)$ and $H_1(\frac{1}{z})$, are as likely to lie outside the unit Z circle as within it. The Wiener impulse response is the stable inverse of this transform; therefore in general it is non-causal and it will typically decay in positive and negative time at similar rates. Examination of equation 3.55 indicates that this conclusion is unchanged in the noise cancellation situation of figure 3.

3.5.3 Non-causal inverse

In order to invert a Z transform to create a stable inverse the poles outside the unit z circle must represent a left-sided sequence, whilst those inside must represent a right-sided sequence. This is readily achieved as follows [36]:

We expand $H(z)/z$ in the form of partial fractions to get

$$H(z) = B_0 + \sum_l \frac{B_l z}{z - p_l} + \sum_m \frac{C_m z}{z - s_m} \tag{3.156}$$

where p_l are the poles of $H(z)$ within the unit z circle, and s_m those outside it. The stable inverse to the first term is simply the sequence whose only non-zero term is $x(0) = B_0$ .We have

$$\sum_{j=0}^{\infty} a^j z^{-j} = \frac{z}{z-a} \tag{3.157}$$

thus a causal inverse to the second term is given by

$$x(j) = \sum_l B_l (p_l)^j \quad j \geq 0 \tag{3.158}$$

Similarly, since

$$\sum_{j=-\infty}^{-1} a^j z^{-j} = \sum_{n=1}^{\infty} \left(\frac{z}{a}\right)^a = \frac{-z}{z-a} \tag{3.159}$$

then a left sided inverse to the third term is given by

$$x(j) = \sum_m -C_m (s_m)^j \quad j < 0 \tag{3.160}$$

The stable inverse to the transform is therefore given by the non-causal sequence

$$\begin{aligned} x(j) &= \textstyle\sum_m -C_m (s_m)^j \quad && j < 0 \\ &= B_0 + \textstyle\sum_l B_l && j = 0 \\ &= \textstyle\sum_l B_l (p_l)^j && j > 0 \end{aligned} \tag{3.161}$$

3.5.4 The causal Wiener filter

A Wiener filter is the optimal linear estimator of $d(j)$, the desired response, from data samples $x(j)$. The optimal unconstrained Wiener filter was derived in section 3.3.2. If we constrain the filter to be causal, then the output of the filter is given by

$$q(j) = \sum_{l-0}^{\infty} w(l) x(j-l) \tag{3.162}$$

with the error signal, as before, given by

$$e(j) = d(j) - q(j) \tag{3.163}$$

The orthogonality principle, applied to the optimum causal filter, states that the error signal $e(i)$ is orthogonal to the data $x(j)$, but only for $i \geq j$. We therefore obtain

$$R_{dx}(k) - \sum_{l=0}^{\infty} w(l) R_{xx}(k-l) = 0 \quad k \geq 0 \tag{3.164}$$

In order to solve this equation, we let

$$y(k) = R_{dx}(k) - \sum_{l=0}^{\infty} w(l) R_{xx}(k-l) \tag{3.165}$$

where $y(k)$ is a sequence which is zero for $k \geq 0$. Taking Z transforms gives

$$Y(z) = S_{dx}(z) - S_{xx}(z) W(z) \tag{3.166}$$

We require a solution in which $W(z)$ is stable and causal i.e. with all poles within the unit z circle, and in which all the poles of $Y(z)$ are outside the unit z circle. The solution may be obtained by the following procedure [36].

$S_{xx}(z)$ is factored into two components $A(z)$ and $A(\frac{1}{z})$. All of the poles and zeros of $A(z)$ lie within the unit z circle, whilst all those of $A(\frac{1}{z})$ lie outside the unit z circle.

$$S_{xx}(z) = A(z) A(\frac{1}{z}) \tag{3.167}$$

The ratio $S_{dx}(z)/A(\frac{1}{z})$ is expressed as the sum of two components $B^+(z)$ and $B^-(z)$, where the poles of $B^+(z)$ are all within the unit z circle and those of $B^-(z)$ are outside.

$$\frac{S_{dx}(z)}{A(\frac{1}{z})} = B^+(z) + B^-(z) \tag{3.168}$$

The optimum causal filter transfer function is then given by

$$W(z) = \frac{B^+(z)}{A(z)} \tag{3.169}$$

It is evident that this solution of equation 3.164 satisfies the constraint on $W(z)$ above. Using equations 3.167, 3.168 and 3.169 gives

$$Y(z) = A(\frac{1}{z}) B^-(z) \tag{3.170}$$

All of the poles of $Y(z)$ therefore lie outside the unit z circle and thus $Y(z)$ also satisfies its constraint.

The optimum causal filter may be considered to consist of two filters in series as shown in figure 3.4. The first filter $1/A(z)$ is a minimum-phase filter whose output $a(j)$ is an uncorrelated signal with unity variance.

The optimum unconstrained Wiener filter to estimate $d(j)$ from $a(j)$ is given by

$$B(z) = \frac{S_{da}(z)}{S_{aa}(z)} = \frac{S_{dx}(z)}{A(z)} \cdot \frac{A(z)A(z)}{S_{xx}(z)} = \frac{S_{dx}(z)}{A(\frac{1}{z})} \tag{3.171}$$

The second filter in the solution of the causal Wiener problem is the causal part of this filter. The reasons for the causal solution having this form are

1. As the signal $a(j)$ is uncorrelated the contribution of any term in the convolution summation of the filter $B(z)$ is uncorrelated with that of any other. The optimum value of any of the filter weights is therefore independent of the values of the other weights. In this case the optimum causal Wiener filter is equal to the causal part of the unconstrained Wiener filter.

2. Provided that $S_{xx}(z)$ is a rational function of z, we can filter any signal $x(j)$ to create a signal with a white spectrum. If the filter used is causal and minimum-phase, the inverse filter is also causal and minimum phase. The two signals are then statistically equivalent for linear operations [37].

3.5.5 The finite Wiener filter

We are concerned with adaptive filters implemented as adaptive transversal filters, which are only capable of implementing finite impulse responses. In section 3.4.2 the optimum finite Wiener filter was shown to be

$$W_{\text{opt}} = \mathbf{\Phi}_{xx}^{-1}\mathbf{\Phi}_{dx} \tag{3.172}$$

If we consider the argument of the previous section then it is evident that if the reference input $x(j)$ is uncorrelated the optimum finite filter is equal to the finite portion of the unconstrained Wiener filter. This is not however true if the reference input is correlated unless the amplitude of the unconstrained impulse response outside the span of the filter is negligible.

3.5.6 Output noise signal

The effect of constraining the solution to the Wiener filtering problem is to cause an increase in the output noise signal. The error signal for the un-constrained Wiener filter is

$$e(j) = d(j) - q(j) = d(j) - \sum_{l=-\infty}^{\infty} w(l)x(j-l) \tag{3.173}$$

Squaring and taking expectation values gives

$$\begin{aligned} E\{e(j)^2\} &= E\{d(j)^2\} - 2E\left\{d(j)\sum_{l=-\infty}^{\infty} w(l)x(j-l)\right\} \\ &\quad + E\left\{\sum_{l=-\infty}^{\infty} w(l)x(j-l)\sum_{m=-\infty}^{\infty} w(m)x(j-m)\right\} \end{aligned} \tag{3.174}$$

This can be re-written as

$$E\{e(j)^2\} = E\{d(j)^2\} - 2\sum_{l=-\infty}^{\infty} w(l)R_{dx}(l) + \sum_{l=-\infty}^{\infty}\sum_{m=-\infty}^{\infty} w(l)w(m)R_{xx}(m-l) \tag{3.175}$$

For the optimum solution $w^*(l)$ we have

$$R_{dx}(k) = \sum_{l=-\infty}^{\infty} w^*(l)R_{xx}(k-l) \tag{3.176}$$

thus the mean square error for the unconstrained Wiener filter is given by

$$E\{e(j)^2\} = E\{d(j)^2\} - \sum_{l=-\infty}^{\infty} w^*(l)R_{dx}(l) \tag{3.177}$$

If we repeat the above argument, replacing the lower summation limit by zero throughout, we find that the mean square error for the causal Wiener filter is given by

$$E\{e(j)^2\} = E\{d(j)^2\} - \sum_{l=0}^{\infty} w^*(l)R_{dx}(l) \tag{3.178}$$

Similarly, for the FIR Wiener filter we obtain

$$E\{e(j)^2\} = E\{d(j)^2\} - \sum_{l=0}^{N-1} w^*(l) R_{dx}(l) \tag{3.179}$$

We cannot directly compare the error performance of these filters, however, for unless the signal $x(j)$ is uncorrelated the optimum values $w^*(l)$ are different in each case. However, we can compare the performance of the causal and non-causal filter by expressing the above results in terms of the uncorrelated signal $a(j)$. We obtain

$$E\{e(j)^2\} = E\{d(j)^2\} - \sum_{l=-\infty}^{\infty} b(l) R_{da}(l) \quad \text{unconstrained} \tag{3.180}$$

$$= E\{d(j)^2\} - \sum_{l=0}^{\infty} b(l) R_{da}(l) \quad \text{causal} \tag{3.181}$$

$$\tag{3.182}$$

$b(l)$ is the unconstrained Wiener filter for estimating $d(j)$ from the uncorrelated unity variance signal $a(j)$. It is the stable inverse of $B(z)$, given by

$$B(z) = \frac{S_{da}(z)}{S_{aa}(z)} = S_{da}(z) \tag{3.183}$$

$b(l)$ is therefore equal to $R_{da}(l)$. We can thus finally write the equations for the mean square error signal in the following form

$$E\{e(j)^2\} = E\{d(j)^2\} - \sum_{l=-\infty}^{\infty} R_{da}(l)^2 \quad \text{unconstrained} \tag{3.184}$$

$$= E\{d(j)^2\} - \sum_{l=0}^{\infty} R_{da}(l)^2 \quad \text{causal} \tag{3.185}$$

$$\tag{3.186}$$

Expressing the equations in this form enables us to determine the effect of causality on the performance of the filter.

3.5.7 Delay in primary signal path

If a delay of r samples is inserted in the primary signal path of an adaptive noise cancelling system, as in figure 3.5, a corresponding delay will occur in

the optimal unconstrained filter impulse response. By choosing a suitable value of r we can centre the ideal response on the finite weighting sequence of the realizable transversal filter. The ideal response may now be well approximated by the causal and finite adaptive filter provided that the number of taps n is large enough.

The determination of the optimum value for the primary delay r requires knowledge of $R_{da}(k)$ which will not be known *a priori*. Widrow [23] states that the value of r is not critical over a range of values around $r = \frac{n}{2}$. This is not unreasonable given that the unconstrained Wiener impulse response decays, in general, at similar rates in both positive and negative time.

3.6 Misadjustment

The steady state output signal from an adaptive noise cancelling system contains the following components

1. The wanted signal $s(j)$.
2. Noise components due to the presence of uncorrelated noise signals $m_0(j)$ and $m_1(j)$ at the primary and reference inputs respectively
3. A noise component due to noise source $n(j)$ which remains uncancelled due to the finite and causal nature of the adaptive filter.
4. A noise component due to the effect of gradient estimation noise on the steady state weight vector, and hence the output signal. I will denote this the *misadjustment noise*.

This last source of noise has been largely neglected in the literature (e.g. [23], [38], [39]), even though in some circumstances it will be the dominant noise producing process. The reason for this is that the output signal from an adaptive noise cancelling system is the error signal of the adaptive algorithm. In conventional adaptive estimation systems the error signal is small for a well adapted system and the output noise signal due to gradient estimation noise is therefore generally small. For an adaptive noise cancelling system the error signal contains the wanted signal. The power in the error signal, and hence the misadjustment noise, is therefore substantial even for a system in which perfect noise cancellation is taking place.

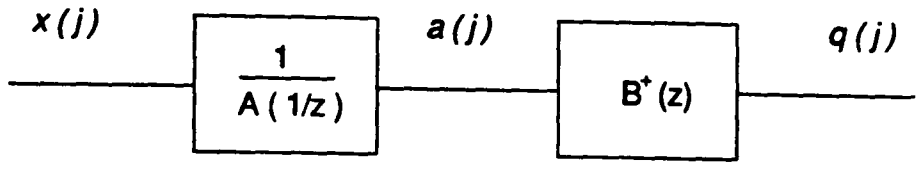

Figure 3.4: Form of the causal Wiener filter

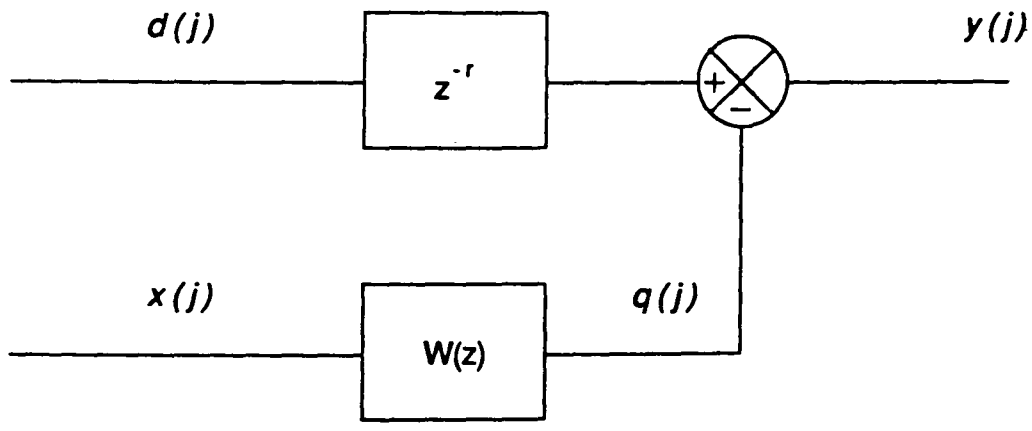

Figure 3.5: Adaptive noise cancelling system with delay in primary signal path

In section 3.4.8 it was shown that the misadjustment noise power was related to the power in the error signal when the filter weight vector was stationary at the optimum solution by the misadjustment ratio given by

$$M = \mu n E\{x(j)^2\} \tag{3.187}$$

and that if the eigenvalues of the autocorrelation matrix are sufficiently similar for the systems learning curve to be approximated by a simple exponential decay with time constant τ_{mse} then

$$M = \frac{nT}{4\tau_{\text{mse}}} \tag{3.188}$$

The effect of the misadjustment noise is to place a upper limit on the output signal to noise ratio of the adaptive noise cancellation system. If we assume that the error signal components 2 and 3 above are negligible then the misadjustment ratio is given by

$$M = \frac{\xi_{\text{m}}}{E\{s(j)^2\}} \tag{3.189}$$

where ξ_{m} is the misadjustment noise power. The signal to noise ratio of the output signal is therefore

$$\text{SNR} = \frac{1}{M} \tag{3.190}$$

In the derivation of the misadjustment ratio two assumptions were made: the independent vectors assumption (see section 3.4.4) and that the filter weight vector remained both close to the optimum weight vector W_{opt}. As a result we would expect equations 3.187 and 3.188 to be approximations accurate only for small values of misadjustment.

As the number of adaptive filter weights is increased we would expect the output noise power to decrease, since the filter is a better approximation to the optimal unconstrained Wiener filter. This conclusion ignores the effect of misadjustment noise however. As the number of weights is increased the misadjustment noise will also increase until a point is reached at which the reduction in the noise signal due to the reduction of the effect of truncation is outweighed by the increase in misadjustment noise.

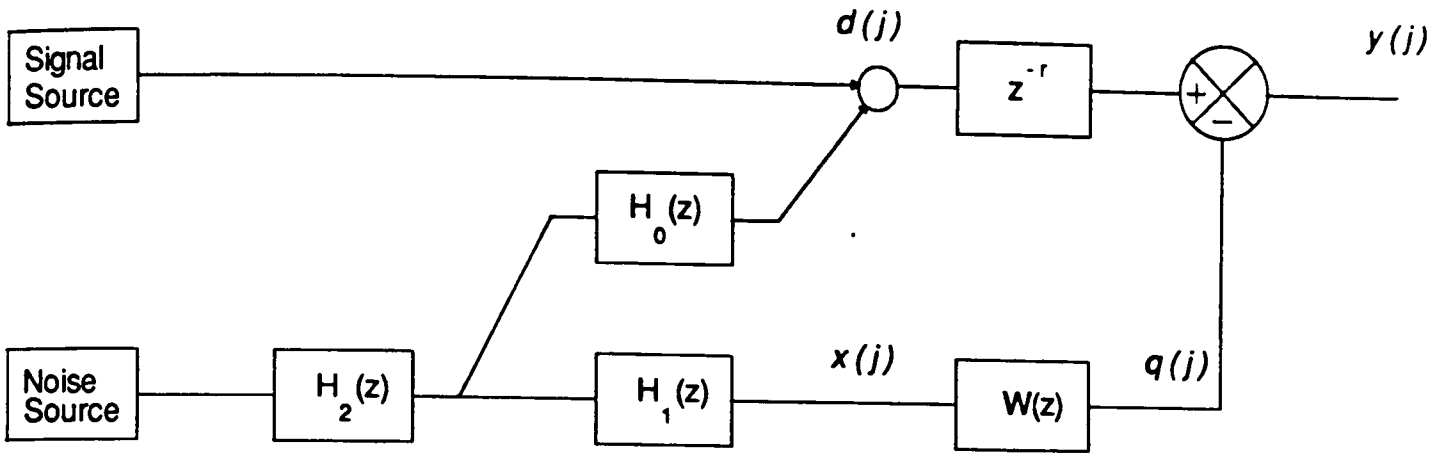

Figure 3.6: The simulated system

3.7 Simulation Results

In order to test the theoretical predictions a number of computer simulations were carried out. The system simulated is shown schematically in figure 3.6. It will be seen that this consists of an adaptive noise cancelling system, including a delay in the primary signal path, presented with the typical noise cancellation problem of figure 3.2. The additional uncorrelated noise sources m_0 and m_1 have been neglected for simplicity.

The noise source generates unity variance white Gaussian noise and the purpose of the additional filter $H_2(z)$ is to allow the power spectrum of the noise signal to be controlled.

In the simulations to be described $H_0(z)$ and $H_1(z)$ had the following forms chosen arbitrarily

$$H_0(z) = \frac{0.14 - 0.15z^{-1} + 0.41z^{-2}}{1 - 0.37z^{-1} + 0.2z^{-2}} \tag{3.191}$$

$$H_1(z) = \frac{-0.5 + z^{-1}}{1 + 0.5z^{-1}} \tag{3.192}$$

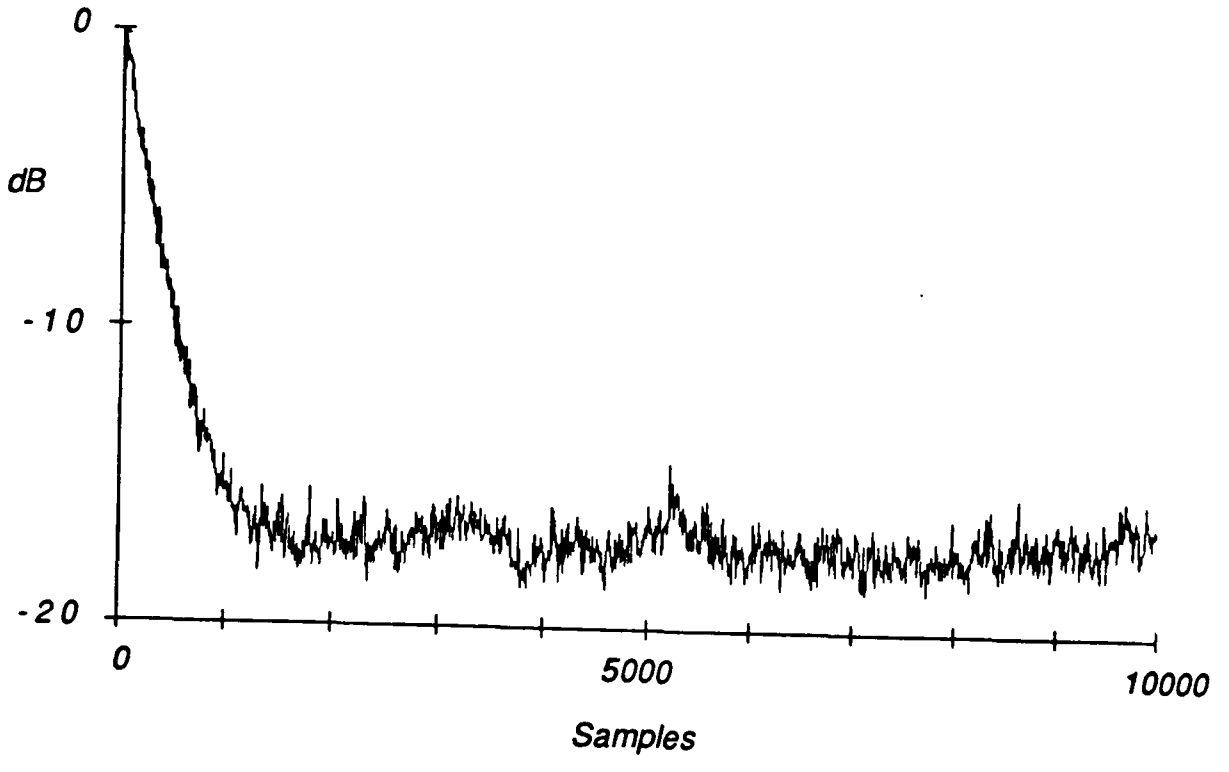

Figure 3.7: Ensemble average learning curve for an adaptive noise cancelling system with a white reference input.

3.7.1 Learning curve

Figure 3.7 shows the learning curve of an adaptive noise cancelling system when the noise source is tailored so that the reference input signal $x(j)$ is white i.e. the noise is white after it passes through filter $H_1(z)$.

The learning curve is an ensemble average estimated by averaging the results of 100 simulations. Each simulation used a different pseudo-random sequence to generate the noise source and had a randomly chosen starting phase for the wanted signal $s(j)$ which was a sinusoid at 0.1 times the Nyquist frequency.

It will be seen that the output noise power falls linearly, on a logarithmic scale, from the initial starting state and then levels out as misadjustment noise becomes the dominant noise producing process. The slope of the initial portion is approximately 10dB in 500 samples, which represents an exponential decay with a time-constant of 217 iterations. This, as expected, is slightly above the figure of 200 predicted by equation 3.117.

Figure 3.8 shows the ensemble average learning curve for a simulation in which all the parameters are identical to that of the previous figure, except that the noise source is white. After passing the filter $H_1(z)$ the reference

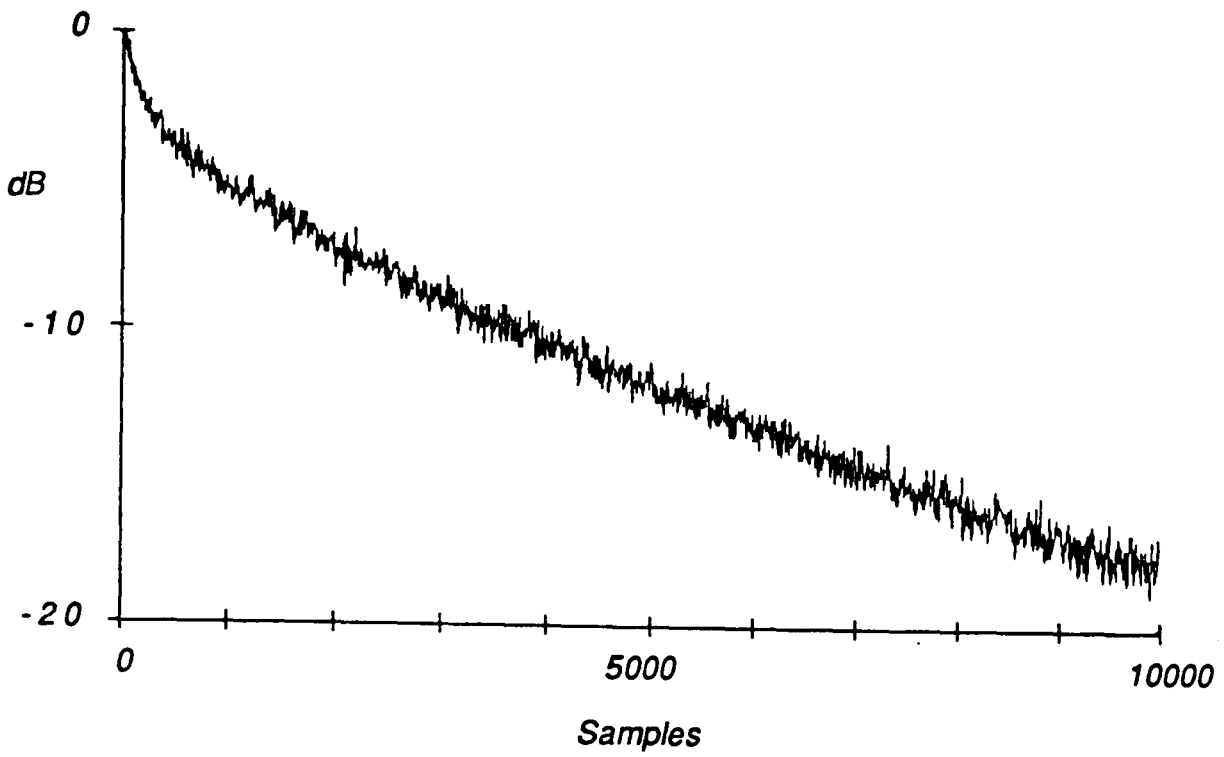

Figure 3.8: Ensemble average learning curve for an adaptive noise cancelling system with a coloured reference input.

input signal is coloured as shown in figure 3.9. In the simulated system the adaptive filter had 16 weights and the reference input was scaled to have unity variance. The eigenvalues of the input correlation matrix Φ_{zz} were calculated numerically and ranged from 0.05 to 3.63

It will be seen that, after a short period of rapid convergence, the system converges much more slowly than the system with a white reference input. The learning curve is predicted to be the sum of 16 modes with a spread of time-constants from 55 to 4000 iterations. It is clearly not exponential and no particular time-constants can be identified. The output noise power continues to decline below the level at which the previous system was limited by misadjustment noise. From figure 3.10 it will be seen that the output noise power continues to decline and reaches steady state in about 20000 iterations, when it again reaches a plateau caused by misadjustment noise.

3.7.2 Stability criteria

If the parameter μ is steadily increased the adaptation rate of the LMS algorithm will increase until a point is reached at which the algorithm becomes unstable. In section 3.4.5 several different stability criteria were discussed. The stability of the 16 tap adaptive noise cancelling system was investigated and the results are summarised in the following tables.

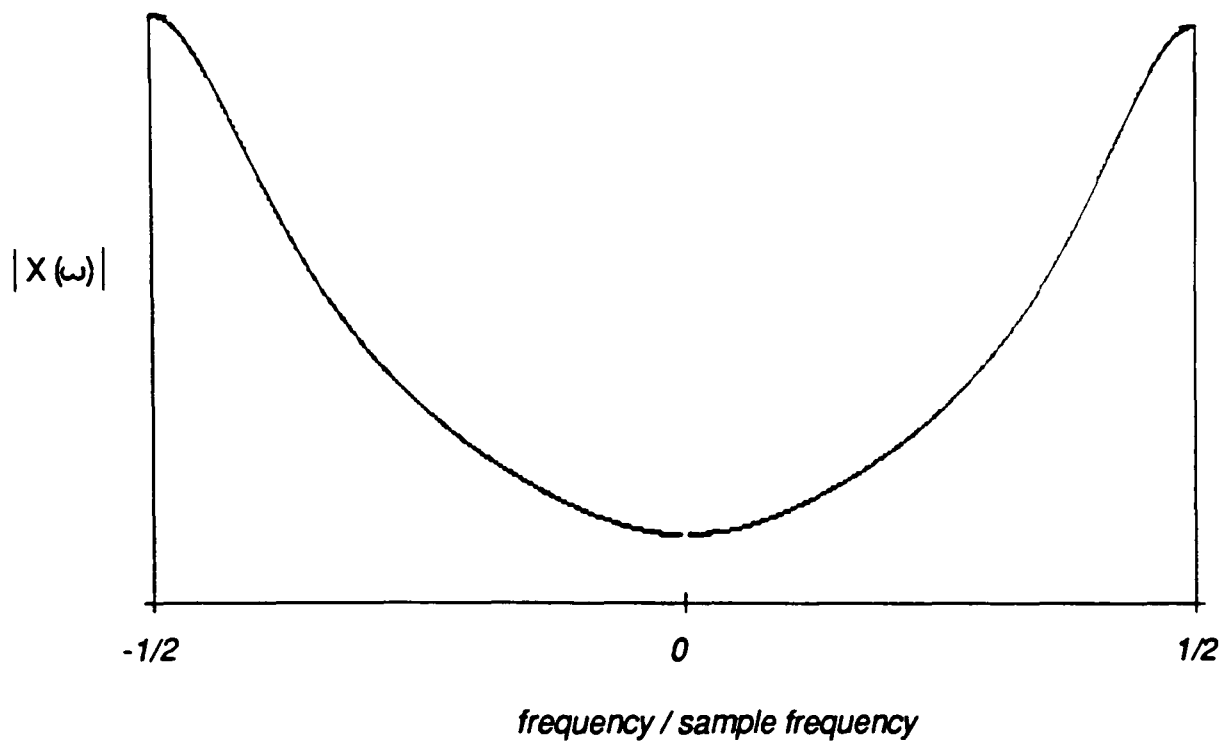

Figure 3.9: Spectrum of the reference signal $x(j)$ for those simulations in which the noise source was not tailored using filter $H_2(z)$.

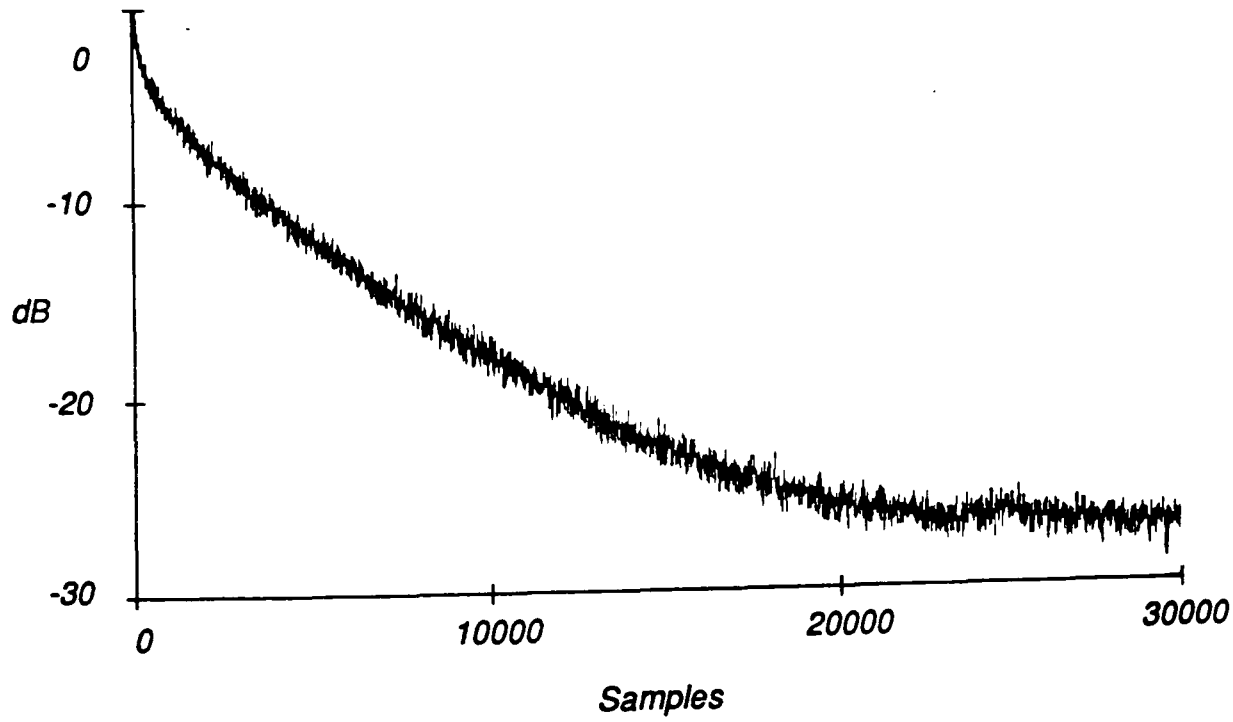

Figure 3.10: Ensemble average learning curve for an adaptive noise cancelling system with a coloured reference input.

Criterion		μ
Widrows exact	eqn 3.90	1.0
Widrows Conservative	eqn 3.93	0.0625
Feuer & Weinstein exact	eqn 3.94	0.0556
Feuer & Weinstein conservative	eqn 3.95	0.0208
Experimental value		0.0526

Table 3.1: Comparison of theoretical and experimental stability criteria for 16 tap adaptive noise cancelling system with unity variance white reference input.

Criterion		μ
Widrows exact	eqn 3.90	0.275
Widrows conservative	eqn 3.93	0.0625
Feuer & Weinstein exact	eqn 3.94	
Feuer & Weinstein conservative	eqn 3.95	0.0208
Experimental value		0.0208

Table 3.2: Comparison of theoretical and experimental stability criteria for 16 tap adaptive noise cancelling system with a coloured reference input of unity variance. The eigenvalues of the input correlation matrix were in the range 0.05 to 3.63

	Theoretical		Simulation	
	Mean	Variance	Mean	Variance
w_0	0.0019	0.00125	0.0022	0.00128
w_1	0.0038	0.00125	0.0038	0.00127
w_2	0.0076	0.00125	0.0074	0.00125
w_3	0.0151	0.00125	0.0148	0.00125
w_4	0.0303	0.00125	0.0298	0.00126
w_5	0.0605	0.00125	0.0599	0.00127
w_6	0.1210	0.00125	0.1204	0.00127
w_7	0.2420	0.00125	0.2413	0.00128
w_8	0.2041	0.00125	0.2034	0.00127
w_9	0.4646	0.00125	0.4641	0.00127
w_{10}	0.3361	0.00125	0.3357	0.00127
w_{11}	0.0314	0.00125	0.0313	0.00127
w_{12}	-0.0556	0.00125	-0.0556	0.00126
w_{13}	-0.0269	0.00125	-0.0267	0.00126
w_{14}	0.0012	0.00125	0.0015	0.00126
w_{15}	0.0058	0.00125	0.0062	0.00126

Table 3.3: Steady state weight vector behaviour for 16 tap adaptive noise cancelling system with white reference input.

The experimental values are for systems which are marginally stable. For these values of μ the output signal is dominated by a large erratically fluctuating misadjustment noise signal. With a white reference input the mean square error signal was +48 dB referred to unity variance averaged over 10^5 iterations. The performance with the coloured reference input was similar.

These results clearly indicate that Widrows stability criteria are too optimistic and confirm those of Feuer and Weinstein.

3.7.3 Weight Vector

Table 3.3 summarizes the steady state weight vector behaviour of the 16 tap adaptive noise cancelling system when the noise source is tailored so that the reference input signal $x(j)$ is white. The figures given are ensemble averages estimated by averaging 100 simulations and assuming the value of the steady state weight elements to be stationary and ergodic. Each simulation was run for 10000 iterations after convergence, which was assumed to be complete after 5000 iterations.

The theoretically expected weight vector behaviour is summarized in the first two columns. The mean weight vector figures are the values of the Wiener weight vector obtained by inverting the Z transform $H_0(z)/H_1(z)$ as described in section 3.5.3. The results are delayed by 8 samples to take the primary delay into account. The second column indicates the weight vector variance as predicted by equation 3.140. It will be seen that the weight vector behaviour is very close to theoretical expectations.

Table 3.4 summarizes the steady state weight vector behaviour of the same system when the noise source is not tailored and the reference input therefore coloured. The figures are again from 100 simulations, each run for 10000 iterations after convergence, which in this case was assumed to be complete after 20000 iterations.

As the reference input is not white it is possible that the mean weight vector may be effected by the effects of truncation. However as the ideal filter impulse response has decayed to very small values at the edges of the adaptive filter these effects are expected to be negligible. The weight vector variances are rather more varied than when the reference input was white but it will be seen that in general they are in reasonable agreement with theoretical prediction. It is interesting to note that the variance of the first and last filter weights is rather smaller than expected.

3.7.4 Misadjustment

If the filters $H_0(z)$ and $H_1(z)$ are both set to unity, the ideal filter impulse response is also unity. The adaptive transversal filter is then capable of perfectly realizing the ideal filter response for any value of n, provided that a reasonable value is chosen for the primary delay, r. The output noise signal from the adaptive noise cancelling system is then entirely due to misadjustment.

Figure 3.11 shows the results of a number of simulations carried out to investigate the manner in which misadjustment noise changes as a function of the number of filter weights, n. The filter $H_2(z)$ was also set to unity so that the reference input was uncorrelated noise with unity variance. In each simulation the primary delay was equal to $n/2$.

The upper points, indicated by circles, are the results of simulations of a system with fast adaptation ($\mu = 0.0125$). The output noise power was estimated by averaging the output noise power over 10000 iterations after convergence, which was assumed to be complete after 500 iterations.

	Theoretical		Simulation	
	Mean	Variance	Mean	Variance
w_0	0.0019	0.00125	-0.0013	0.00037
w_1	0.0038	0.00125	-0.0012	0.00108
w_2	0.0076	0.00125	0.0017	0.00131
w_3	0.0151	0.00125	0.0087	0.00130
w_4	0.0303	0.00125	0.0235	0.00123
w_5	0.0605	0.00125	0.0536	0.00118
w_6	0.1210	0.00125	0.1141	0.00120
w_7	0.2421	0.00125	0.2355	0.00128
w_8	0.2041	0.00125	0.1983	0.00139
w_9	0.4646	0.00125	0.4598	0.00149
w_{10}	0.3361	0.00125	0.3324	0.00153
w_{11}	0.0314	0.00125	0.0298	0.00151
w_{12}	-0.0556	0.00125	-0.0572	0.00140
w_{13}	-0.0269	0.00125	-0.0280	0.00123
w_{14}	0.0012	0.00125	-0.0002	0.00092
w_{15}	0.0058	0.00125	0.0036	0.00031

Table 3.4: Steady state weight vector behaviour for 16 tap adaptive noise cancelling system with coloured reference input.

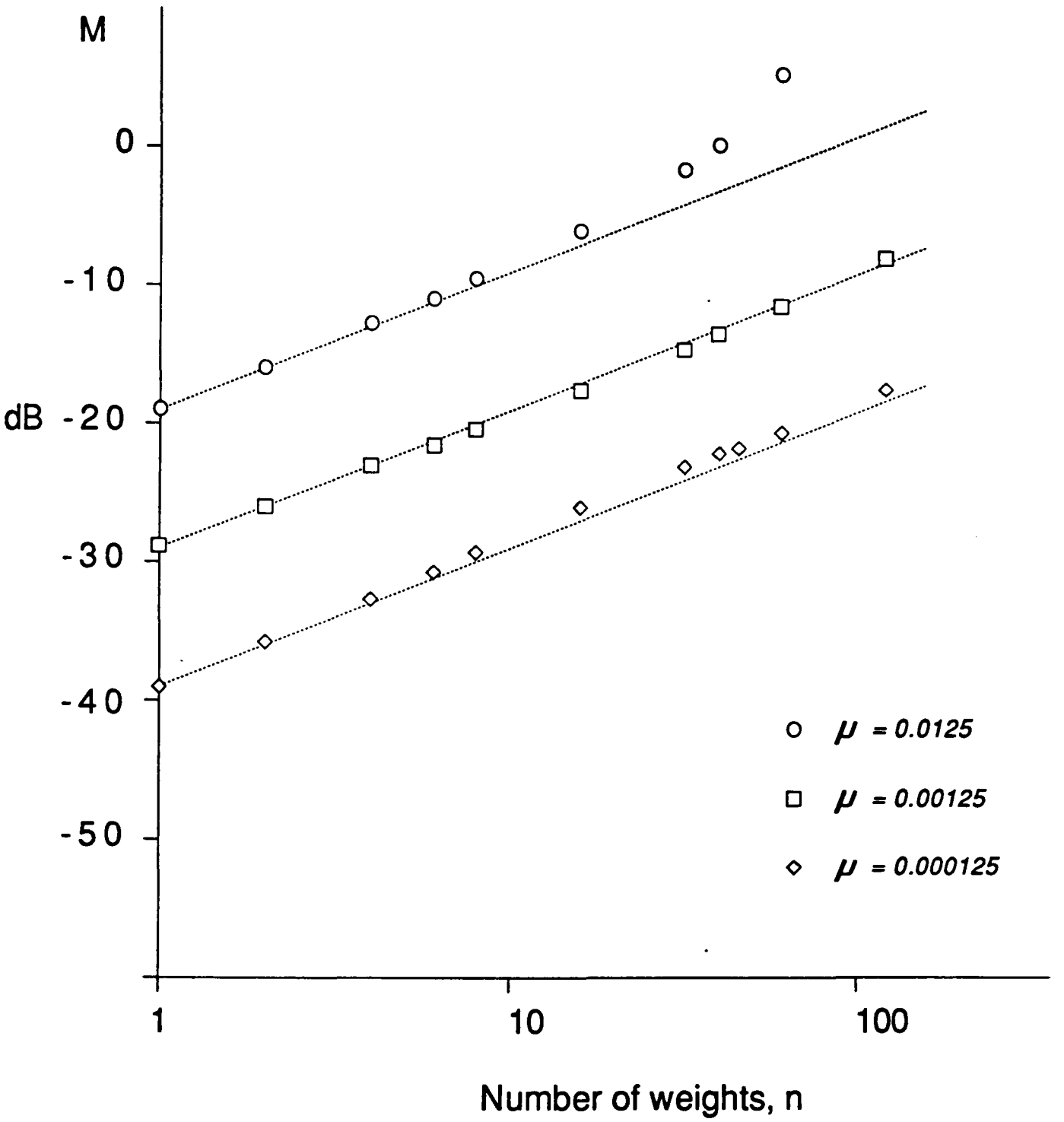

Figure 3.11: Misadjustment ratios for adaptive noise cancelling systems with an uncorrelated reference input.

Also shown are the predictions of equation 3.147. It will be seen that the agreement is very good for small values of M, but that the misadjustment increases more rapidly than predicted as M gets larger and the stability boundary is approached. This behaviour is reasonable as equation 3.147 is an approximation for small M, as discussed in section 3.4.8.

The middle points, indicated by squares, are the results of simulations of a system with moderate adaptation ($\mu = 0.00125$). The output noise power was again estimated by averaging over 10000 iterations after convergence, now assumed to be complete after 5000 iterations. The results will be seen to be in good agreement with the predictions of equation 3.147.

The lower points, indicated by rhomboids, are those due to the simulation of a system with slow adaptation ($\mu = 0.000125$). The output noise power was this time estimated by averaging over 100000 iterations after convergence, assumed to be complete after 50000 iterations. Again good agreement with equation 3.147 is found.

Figure 3.12 shows the results of a series of simulations which were similar to those of the previous graph except that the reference input was coloured. This was achieved by making $H_2(z)$ equal to the form of $H_1(z)$ used in earlier simulations.

The upper points are again those for the system with $\mu = 0.0125$. Since adaptation is slower with the coloured reference input convergence was assumed to take 2000 iterations. It will be seen that the level of misadjustment noise is substantially lower than that predicted by equation 3.147 except when the system is near the stability boundary.

The middle points are those for the system with $\mu = 0.00125$, for which convergence was assumed to take 20000 iterations. The level of misadjustment noise is consistently 9 dB below that predicted.

The lower set of points are the result of simulations of the system with $\mu = 0.000125$. Convergence was assumed to be complete after 200000 iterations and the results are the average power over 100000 iterations. Again the level of misadjustment noise is about 9 dB below that predicted.

The failure of equation 3.147 to predict the level of misadjustment noise for a non-white reference input indicates that the assumption that the data vector may be approximated as a series of uncorrelated vectors is inappropriate in this case. In the previous section it was seen that the variance of the weight vector elements was in reasonable agreement with equation 3.140. This indicates that the effect of a correlated reference input is to cause

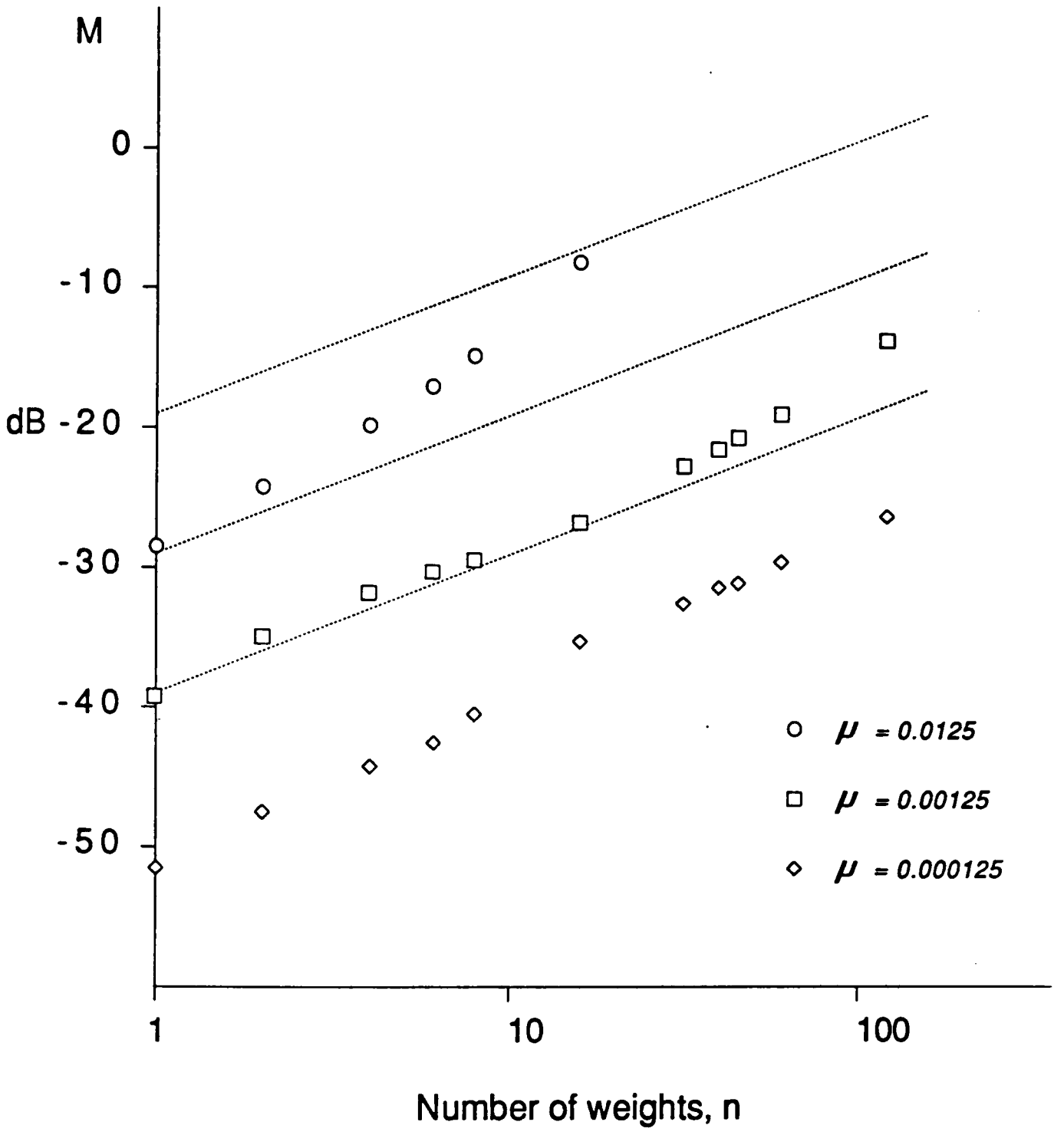

Figure 3.12: Misadjustment ratios for adaptive noise cancelling systems with a correlated reference input.

	Theoretical		Simulation	
	Mean	Variance	Mean	Variance
w_0	0.2041	0.00135	0.2032	0.00135
w_1	0.4646	0.00135	0.4634	0.00135
w_2	0.3361	0.00135	0.3351	0.00135
w_3	0.0314	0.00135	0.0303	0.00137
w_4	-0.0556	0.00135	-0.0560	0.00136
w_5	-0.0269	0.00135	-0.0273	0.00134
w_6	0.0012	0.00135	0.0011	0.00136
w_7	0.0058	0.00135	0.0053	0.00135

	Theoretical	Simulation
truncation noise	0.0781	
misadjustment noise	0.0108	
Total	0.0889	0.0885

Table 3.5: The effect of causality on an adaptive noise cancelling system with an uncorrelated reference input.

the weight vector fluctuations to become correlated, thereby reducing the misadjustment noise.

This conclusion is strengthened when it is recalled (see section 3.4.5) that a sinusoidal reference input causes highly correlated variation of the weight vector creating a notch filter with a Q determined by the value of μ [29,33].

3.7.5 Truncation and causality

A number of simulations were carried out to confirm the predictions of section 3.5 regarding the effects of causality and truncation on the output noise signal from an adaptive noise cancelling system. The filters $H_0(z)$ and $H_1(z)$ had their standard form as defined at the start of the section. The results are summarized in the following tables.

Table 3.5 summarizes the steady state performance of an 8 tap adaptive noise cancelling system with no delay in the primary signal path. The adaptive filter is then only capable of approximating the causal Wiener filter. The figures are ensemble averages estimated by averaging 1000 simulations. Each simulation was run for 10000 iterations after convergence, which was assumed to be complete after 5000 iterations.

	Theoretical		Simulation	
	Mean	Variance	Mean	Variance
w_0	0.0038	0.00173	0.0030	0.00170
w_1	0.0076	0.00173	0.0071	0.00171
w_2	0.0151	0.00173	0.0149	0.00171
w_3	0.0303	0.00173	0.0294	0.00170
w_4	0.0605	0.00173	0.0592	0.00165
w_5	0.1210	0.00173	0.1195	0.00166
w_6	0.2420	0.00173	0.2410	0.00168
w_7	0.2041	0.00173	0.2031	0.00166

	Theoretical	Simulation
truncation noise	0.3336	
misadjustment noise	0.0133	
Total	0.3469	0.3459

Table 3.6: The effect of truncation on an adaptive noise cancelling system with an uncorrelated reference input.

The noise source was tailored so that the reference input $x(j)$ was uncorrelated and of unity variance. It is then easy to apply the theory of section 3.5 since $a(j) = x(j)$. It is apparent that the optimum weight vector is equal to the causal part of the ideal filter impulse response. The output noise power due to the causality constraint is equal to the sum of the squares of the non-causal terms of the ideal filter impulse response. The measured output noise power also contains a contribution due to misadjustment, which has been estimated using equation 3.147. The weight vector variances are estimated using equation 3.140. It will be seen that there is very close correspondence between the simulation results and the theoretical predictions.

The following table summarizes the steady-state performance of the same 8 tap adaptive noise cancelling system when a delay of 7 samples is present in the primary signal path. The optimum weight vector is again given by that portion of the ideal weight vector which lies within the span of the adaptive filter. In this case the non-causal portion of the filter impulse response is well approximated and the output noise power is due to the severe truncation of the trailing portion of the impulse response. There is again very close correspondence between the simulation results and theoretical expectations.

Table 3.7 summarizes the steady state behaviour of the 8 tap adaptive noise cancelling system with no delay in the primary signal path when the reference input is coloured. The noise source was not tailored so that the

	Theoretical		Simulation	
	Mean	Variance	Mean	Variance
w_0	0.0105	0.00126	0.0130	0.00036
w_1	0.3678	0.00126	0.3699	0.00108
w_2	0.2877	0.00126	0.2894	0.00138
w_3	0.0072	0.00126	0.0083	0.00144
w_4	-0.0677	0.00126	-0.0665	0.00138
w_5	-0.0329	0.00126	-0.0325	0.00123
w_6	-0.0018	0.00126	-0.0019	0.00094
w_7	0.0043	0.00126	0.0026	0.00032

	Theoretical	Simulation
truncation noise	0.0121	
misadjustment noise	0.0010	
Total	0.0131	0.0131

Table 3.7: The effect of causality on an adaptive noise cancelling system with a correlated reference input.

reference input is no longer white after passing the filter $H_1(z)$. The figures are again ensemble averages estimated by averaging 100 simulations. Each simulation was run for 10000 iterations after convergence, which was now assumed to require 20000 iterations.

The optimum causal Wiener filter was calculated using the theory of section 3.5.4, and the output noise power calculated using equation 3.185. The measured output noise power also contained a contribution due to misadjustment which was estimated from the results of figure 3.12. It will be seen that there is close correspondence between the simulation results and theoretical expectations.

The following table summarizes the steady-state performance of the same 8 tap adaptive noise cancelling system with a correlated reference input when a delay of 7 samples is present in the primary signal path. For this case the non-causal portion of the filter impulse response can be well approximated but the causal portion of the ideal impulse response is severely truncated. It is necessary to calculate the optimum weight vector using equation 3.74 since the correlated reference input causes the optimum weight vector to differ from that portion of the ideal weight vector which lies within the filter's span. The output noise signal due to the truncation was calculated using equation 3.75. The measured output noise power also contained a contribution due to misadjustment which was estimated from the results of

	Theoretical		Simulation	
	Mean	Variance	Mean	Variance
w_1	0.0008	0.00131	-0.0007	0.00038
w_2	0.0025	0.00131	-0.0004	0.00103
w_3	0.0053	0.00131	0.0021	0.00122
w_4	0.0108	0.00131	0.0078	0.00126
w_5	0.0218	0.00131	0.0194	0.00123
w_6	0.0435	0.00131	0.0422	0.00115
w_7	0.0872	0.00131	0.0872	0.00097
w_8	-0.1056	0.00131	-0.1051	0.00035

	Theoretical	Simulation
truncation noise	0.0478	
misadjustment noise	0.0010	
Total	0.0488	0.0494

Table 3.8: The effect of truncation on an adaptive noise cancelling system with a correlated reference input.

figure 3.12. It can be seen that there is close correspondence between the simulation results and theoretical expectations.

3.8 Conclusions

Ideal solutions to typical noise cancelling problems have been derived in a treatment which is more general than that previously published [23]. This enables the potential performance of an adaptive noise cancellation system to be estimated in most situations of practical interest.

The LMS algorithm is generally used in adaptive noise cancelling systems and appears to be a good choice for this application. The stability and convergence of the algorithm were discussed and the theoretical expectations compared with results from computer simulation. The learning curves of stable systems have slightly longer time constants than predicted, but this behaviour is expected as the derivation assumes perfect gradient estimates. The conventional stability criteria for the LMS algorithm due to Widrow were found to be too optimistic whilst the results were consistent with a recent stability analysis by Feuer and Weinstein.

There is an output noise component due to the effect of gradient estimation noise on the steady state weight vector, which is denoted misadjustment

noise. This is an important noise source for adaptive noise cancelling systems since the power in the error signal driving the adaptive algorithm, and hence the misadjustment noise, is substantial even for a system in which perfect cancellation is taking place. In order to predict the output noise power due to misadjustment it is necessary to assume that the data forms a series of uncorrelated vectors in order to make the mathematics tractable. It was found that the resulting analysis predicted the misadjustment noise well when the reference input was uncorrelated. However for a correlated reference input the misadjustment noise power is well below that predicted, even though the weight vector variation is comparable with the predicted value. This indicates the uncorrelated vectors assumption is unjustified in this context and that the effect of a correlated reference input is to cause the weight vector fluctuations to become correlated.

Ideal solutions to noise cancellation problems require filters whose impulse responses, in general, extend infinitely over both positive and negative time. Adaptive transversal filters can only implement causal impulse responses of finite duration. The effects of causality and truncation on the weight vector solutions and the output noise signal have been discussed and found to be in close agreement with the results of computer simulation.

Chapter 4

Automatic classification of gramophone records

4.1 Introduction

In this chapter the last of the case studies is described. The problem addressed is the design of equipment to automatically assess the quality of gramophone records for quality control purposes.

The need for such equipment has been recognised since the early 1960's and a long research programme at THORN EMI Central research laboratories has produced several automatic classification machines using analogue signal processing. This development culminated in 1977 in a machine known as the mark V Disk Defect Detector (DDD).

The increasing use of close microphone techniques and electronically synthesized music since then have caused a gradual reduction in the accuracy of the classification made by the machine. It was recognised that the mark V DDD was at the practical limit for an analogue signal processing approach thus the investigation to be described reports on the application of digital signal processing to this problem. Results of this work have been published in a paper entitled 'A new approach to the automatic detection of pressing faults on gramophone records' by S.J.Roome and J.W.Richards which appeared in the October 1985 issue of the Journal of the Institution of Electronic and Radio Engineers.

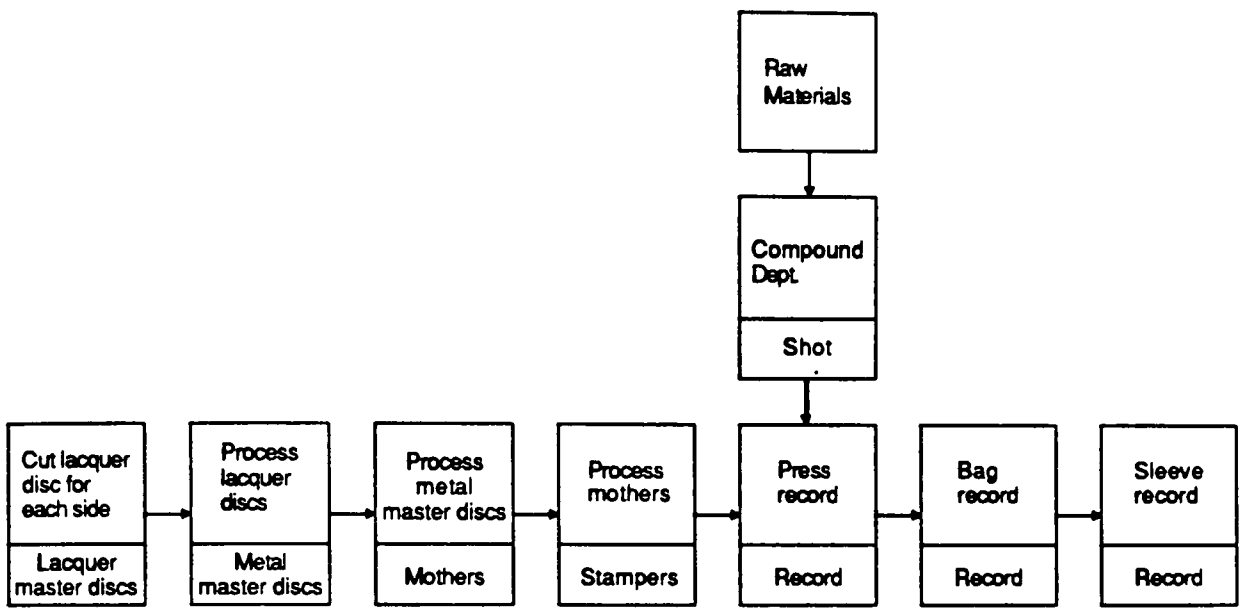

Figure 4.1: Stages in the conventional gramophone record process

4.2 Gramophone record defects

4.2.1 Manufacture of a gramophone record

The various stages in the manufacture of a gramophone record are shown in figure 4.1 which is adapted from [40]. The first stage is to cut a pair of lacquer disks from the master tape recording of the programme material. This is done on a record cutting lathe, which is rather like a record player but with the playback stylus replaced by a heated cutting stylus. This is driven to create a spiral groove, whose modulation carries the recorded signals, in the surface of the soft smooth lacquer disk.

The left (L) and right (R) channels of a stereo signal modulate the groove in orthogonal directions, as shown in figure 4.2 so that in principle there is no cross-talk between them. The depth and lateral deviation of the groove depend on the signal content of the L and R channels. In-phase components of the signals correspond to lateral modulation of the groove, and out-of-phase components to vertical modulation. Thus, for a monophonic record, where L and R channels are identical, the groove depth and width remain constant and the signal is carried entirely by the lateral deviation of the groove.

In order to space the grooves as closely together as possible without them running into each other, a look-ahead technique is used. When an analogue

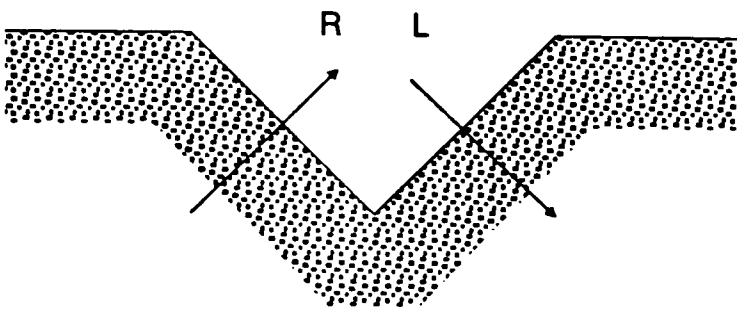

Figure 4.2: Modulated gramophone record groove

master tape is replayed a second advance head is used whose signals control the pitch of the spiral cut into the lacquer. A similar technique, employing a digital delay line, is used when the signals on the master tape are digitally encoded.

From each lacquer disc a metal negative is made. A layer of silver is deposited onto the surface of the lacquer and it is then electroplated with nickel. This process is known as matrixing.

The metal negative is then used to create a positive 'mother' by a second matrix operation. In order to make it possible to separate the mother from the negative on which it is grown, the negative is coated with an electrically conductive monomolecular layer of a colloid before electroplating takes place.

From the mother a number of stampers are created by a third matrix operation. Each stamper is then used to create a large number of gramophone records by the 'pressing' operation.

The pair of stampers representing the two sides of the record are fitted to mould blocks in the record press. During the press cycle the following operations occur:

1. a shot of vinyl mix is placed within the press with a finished label above and below it
2. the mould blocks are heated (usually by steam) and brought together to press the shot into an LP

frequency response	20Hz-20kHz
total harmonic distortion	< 0.5 % (1KHz, peak level, 280mm diameter)
rumble	> 64 dB (DIN B weighted)
signal to noise ratio	> 69 dB (1kHz-16kHz)
playing time	> 30 min per side

Table 4.1: Specifications of a DMM gramophone record

3. the blocks are then cooled with water before the record is released
4. the stampers are separated and the record removed
5. the excess flash is trimmed from the edge

This whole process takes a total of 20 to 25 seconds to create a single gramophone record. The end result is a finished record which is soft and which will take about 24 hours to cure to its normal hard state.

A recent improvement to the process of gramophone record production is the introduction of Direct Metal Mastering (DMM [1]). In DMM the production of the intermediate negative and positive is eliminated by cutting a metal master directly from a copper coated stainless steel disk. This reduces the surface noise of the resulting gramophone records because each matrix operation adds slight imperfections to the surface detail within the groove.

A modern gramophone record is made from a co-polymer of polyvinyl chloride and polyvinyl acetate, lubricant and stabilizer additives and sufficient carbon black to give the characteristic colouring. An LP is 12 inches (305 mm) in diameter and weighs approximately 120 g. Specifications of a DMM record are given in table 4.1.

4.2.2 Gramophone record defects

Defects in gramophone records may be divided into three broad categories:

Lacquer faults It is possible for defects to be introduced into the recorded programme during production of the master tape [41], or during the process of cutting the lacquer discs. These faults would then be present

[1] DMM is a trademark of TELDEC

on all gramophone records subsequently produced. In practice lacquer faults are very rare and do not represent a quality control problem since they can be isolated by auditioning a single trial pressing.

Handling damage Gramophone records are relatively fragile and may easily be damaged during handling operations. Handling damage will usually be unique to each record and is thus not controllable by batch sampling techniques. The incidence of handling damage to gramophone records has been very much reduced by the introduction of machines which automatically insert the records into inner sleeves immediately after pressing and is now also comparatively rare.

Pressing faults Once an event, such as damage to a stamper, has occurred pressing faults will be present on each subsequent record pressed during a production run. As soon as a pressing fault is detected during batch sampling, it will be examined under a microscope to determine the exact cause, corrective action taken, and the offending batch of records scrapped.

The prompt detection, assessment, and diagnosis of pressing faults is thus a central concern of a quality control programme for the manufacture of gramophone records. It is in this area that most of the work in automatic fault detection has been carried out, and to which the investigation described in this chapter was addressed.

4.2.3 Pressing faults

Pressing faults may be divided into three categories: those due to imperfections in matrix operations; those due to shortcomings in the record material; and those due to faulty processing. The most important examples of each will now be described.

Matrix faults During the electroplating operations that produce the nickel stamper it is possible for the presence of contaminants to cause pinholes in the finished stamper. When records are pressed the vinyl material will be extruded through these holes causing small spikes within the record groove. This pressing defect is known as spot damage and manifests itself as intermittent loud clicks when the record is played. This defect is difficult for automatic quality control equipment to detect because the record is played in the soft uncured state. The replay stylus deflects the spike of vinyl resulting in a click with a magnitude much reduced from that which will be experienced by the consumer. Spot damage is not visible without magnification

Material faults Rigorous precautions are taken to ensure the purity of the record vinyl. Even so a particle of a contaminant, such as a grain of sand, occasionally enters the record press. As the vinyl shot is compressed into a record this may produce a radial scratch on one stamper, which will be reproduced on all subsequent records.

If an excessive proportion of additives is present in the vinyl composition, then these will appear as a white colouration of the surface of the record known as bloom. This does not always result in an audible defect, but it is often manifested as a low-level cyclic susurration known as swish.

Processing faults The most troublesome processing faults are release damage, non-fill, and apex damage.

Pre-release damage is localised damage of the outer wall of the record groove caused by contraction of the cooling record before the stamper has completely separated from the vinyl. Post-release damage is localised damage of the groove shoulder and the land, caused by the stamper coming back into contact with the record again after the stampers have separated. Both forms of release damage are sometimes referred to as stitching because of the appearance of the patterns of reflected light on the gramophone record. Release damage causes a disturbing rasping noise called tearing since it sounds like cloth being torn.

Non-fill, also referred to as 'air marks', is an irregular distribution of cavities in the outside wall of the record groove caused by incomplete moulding. It may appear as a random pattern or irregular streaks on the surface of the record and manifests itself as irregular clicks.

Apex damage is a series of defects within the bottom of the grooves due to damage to the apex of the stampers. This is caused by the two stampers momentarily touching before the vinyl expands to fill the mould cavity. Apex damage usually causes a tearing noise similar to release damage and is not normally visible without magnification.

4.3 Quality Control

4.3.1 Problems in the quality control of gramophone records

The quality control of gramophone record production is difficult because of the large number of items to be tested, the wide variety of manufacturing defects which are possible, and the difficulty of testing completed gramophone records to the present high levels of performance.

At the EMI Manufacturing and Distribution plant at Uxbridge Road, Hayes, Middlesex 25 million 12 inch and 23 million 7 inch (173mm) records were pressed during 1984. This amounts to approximately 20 million hours of recorded material. Even with the use of batch sampling techniques and highly skilled listeners, auditioning of the material is an impracticable method of assuring the quality of the product.

It is difficult, even for trained staff, to listen critically to material for long periods. In addition it is extremely difficult, if not impossible, to maintain a consistent standard of gramophone record quality based on subjective assessment. Many factors subconsciously and significantly affect human judgement of the severity of the noises resulting from gramophone record defects. The variation due to these factors (which include state of health, emotional state, enjoyment of programme and fatigue) is large and difficult to compensate.

To assess the quality of a record requires that the defects be identified, and the severity of the resulting noises estimated. The criteria by which a listener distinguishes sounds due to gramophone record defects from those of the recorded programme are complex and not well understood. In general it appears that a listener will regard as a defect any sound that does not appear consistent with the recorded programme, based on their previous experience. It is interesting to note that the improved dynamic range of programme material due to the introduction of digital audio tape machines caused some records to be erroneously returned by consumers as defective. This was due to sounds, such as the clattering of woodwind keys, being heard that would have previously been masked by tape noise.

It may be possible to develop a machine which effectively emulates the human ability to recognise defects, but such a machine would be too complex and expensive for quality control purposes. It has been suggested that signals due to defects could be detected by comparing the replayed signal with a copy of the master tape. In practice this procedure would be very difficult to carry out, not least because of the huge repertoire and rapid turnover of a modern record manufacturing plant.

Optical inspection of gramophone records has formed an important part of quality control procedures in the past [40]. However, not all defects are visually apparent, and there is poor correlation between the appearance of a defective record and the audible severity of the defects. The large reduction in the incidence of handling damage caused by the introduction of automated bagging of gramophone records immediately after pressing has also made it apparent that visual inspection was probably responsible for creating as many defects as were detected.

It has already been noted that the assessment of the severity of gramophone record defects by a listener is affected by subjective factors. However several objective criteria which affect the consensus opinion of the severity of a defect are known. These are

- the amplitude and character of the noise due to the defect
- the nature of the programme at the time
- whether the defect is cyclic (recurring every revolution)

Defects that occur in the midst of programme are masked somewhat by that programme. The degree to which masking takes place is difficult to estimate, but it is greatest when noise and signal occupy similar frequency bands and falls off rapidly with increasing frequency separation.

Defects which are cyclic, that is which recur with a period equal to that of one record revolution are more annoying than the same defects randomly distributed. The listener becomes aware of the defect and anticipates the repetition of the noise, spoiling the enjoyment of the recorded programme.

4.3.2 Current equipment

The need for automatic equipment to detect gramophone defects has been recognised since the early 1960s. The equipment was intended specifically for the detection of pressing faults and the specification included low cost, ruggedness and the ability to give a rapid assessment of record quality.

In 1977 the mark V Disk Defect Detector was produced as the culmination of a long programme of work in this area by THORN EMI Central Research Laboratories [42]. This machine distinguishes between audio signals due to record defects and recorded programme on the basis of the signal envelope. It is assumed that recorded sounds will have a perceptible decay envelope due to room reverberations and the physics of musical instruments, whilst defects will typically have rapid rise and fall times.

Since it is easier to detect rapid rise-times than rapid fall-times with analogue circuitry the mark V DDD plays the record backwards. Impulsive noises such as clicks could therefore be distingushed from impulsive music (such as cymbal crashes) by the presence of rapid rise-times in the reversed signal. A number of analogue detectors of graded sensitivity operate in parallel to categorise defects as large clicks, scratches and 'gritty' noises. To

increase the speed of assessment a rotational speed of 78 rev/min is used, this increases the throughput of the system when testing LPs by a factor of 2.34 .

The mark V DDD has been very successful and is currently in use with record plant throughout the world. It is the only machine for the automatic testing of gramophone records to be made commercially available to the gramophone record industry.

When the equipment was designed, a discrimination criterion based on the finite decay envelope of natural sounds was reasonably effective for quality control purposes. Since then, however, the use of close microphone techniques and electronically synthesized sounds have become commonplace. The decay envelopes of these sounds can be very short eroding the validity of the design criterion as a general discrimination procedure. The result is that the Mark V DDD is susceptible to the spurious identification of certain music waveforms as defects. This effect is known as 'music breakthrough' and is most likely to occur at the high levels of sensitivity required to detect 'gritty' noises, which are often embedded in music.

In addition the results from the Mark V DDD require skilled interpretation in order to make a pass/fail judgement on the quality of the tested record. This still allows human inconsistency to affect the standard of gramophone record production.

These problems, combined with a requirement for higher standards of gramophone record quality caused by the competition from Compact Disk, led to a complete re-appraisal of strategies for the automatic identification of gramophone record defects for use in a new generation of quality control equipment. It was recognised that the Mark V DDD represented a practical limit to the complexity that could be achieved with analogue signal processing. A project to investigate the application of digital signal processing to this problem was carried out by the author under the supervision of Mr J.W.Richards and resulted in the design and construction of a prototype disk defect detector equipment. This equipment then underwent two field trials at the record factory of EMI Manufacturing and distribution.

4.4 A digital signal processing solution

4.4.1 Introduction

Gramophone record defects are capable of generating a wide range of noise signals which will be heard superimposed on the recorded programme. These noises may be informally grouped into categories based on the character of the sound.

- Clicks and their cyclic counterparts scratches, are the popular conception of gramophone record defects. In practice most clicks heard by the consumer are probably due to handling damage after the record was purchased. However several pressing faults may cause similar noises including spot damage, non-fill and stamper damage.
- Tearing noises are probably the most disturbing of all gramophone defects. These are generally caused by release damage or apex damage.
- Frying noises are periods of enhanced noise level reminiscent of the sound of frying and are often caused by matrix faults. Cyclic low-level frying is referred to as 'swish' and is generally due to material problems.
- Grit is a term used to describe frequent small clicks and is usually due to matrix problems.
- Bumps are repetitive low-level low-frequency noises, which are usually due to local deformations of the stamper.

As a result of a detailed analysis of the replay signals from a large number of defective records it was found that a large majority of noises due to record defects were composed of one or a series of impulsive waveforms. This conclusion was surprising considering the widely differing character of the noises and the wide spectrum of defects causing them. The major exception is the category of low-frequency defects known as bumps. These defects are fortunately rare and it was decided to ignore them during the development of a prototype machine.

The problem to be addressed by automatic equipment for use in the quality control of gramophone record production was approached in three parts: distinguishing impulsive signals due to defects from those of recorded programme; grouping these impulses so that they correspond to recognisable defects; and assessing the severity of the defects.

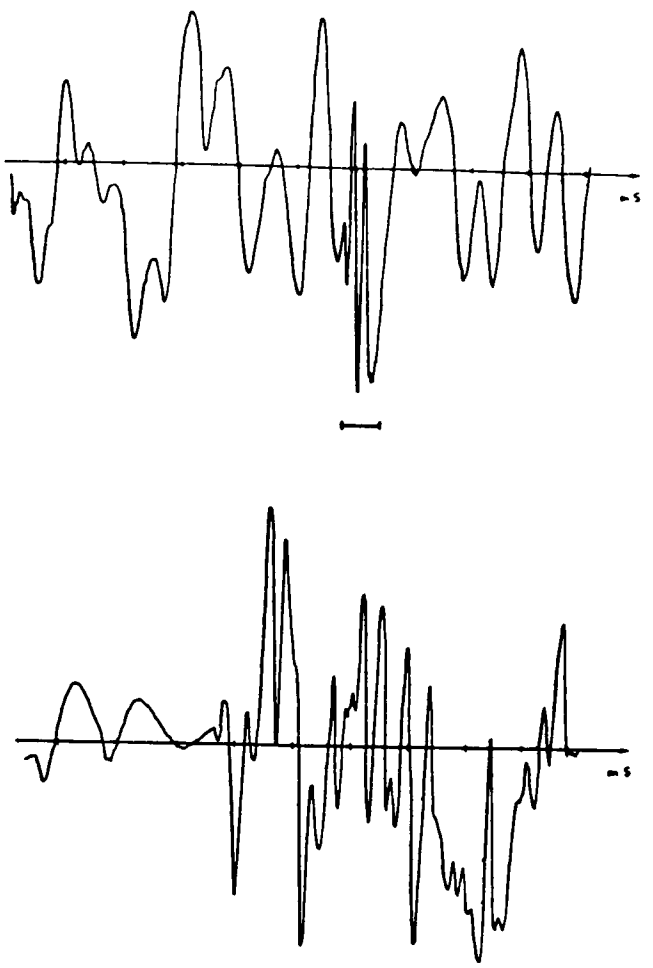

Figure 4.3: Voltage/time waveforms: (a) click embedded in music; (b) piece of synthesized music.

4.4.2 Identification of defect impulses

Various methods by which impulses due to gramophone record defects could be distinguished from recorded programme were investigated. The difficulty of this task is illustrated by figure 4.3 which shows a trace from a passage containing a click embedded in music and also a piece of synthesized music without any defects.

In principle the problem is to take each portion of the signal replayed from a gramophone record and to decide whether it is due to recorded programme or to the presence of a defect. This problem is inherently difficult as it is required to detect defects in the presence of an enormous variety of recorded programme. These include speech, classical music, popular music (typically containing many special effects and synthesized sounds), outside recordings and special effects.

There are few constraints on the characteristics of signals recorded on gramo-

phone records. The primary constraint is that the signal lies within the audio bandwidth, and this is obviously also true of the noise signals resulting from defects which cause annoyance to the consumer. The conjecture that the signals caused by gramophone record defects had a very wide bandwidth, extending beyond the limits of human hearing, has been tested in previous work at THORN EMI Central research Laboratories and did not yield a reliable detection method.

These problems could be readily overcome if redundancy were added to the signal in a controlled manner. Detecting defects on a monophonic gramophone record, for example, is greatly simplified since the L and R channels should be identical. It is straightforward to add redundancy to digital audio signal for the purpose of detecting errors and this allows the detection of manufacturing defects on CD disks to be a simple mechanistic process. Unfortunately this approach is not applicable to conventional LP records.

In the absence of any definitive criteria for distinguishing between signals due to recorded programme and those due to defects a probabilistic approach had to be adopted. It was accepted that there would be a finite probability of wrongly classifying portions of signal, and a technique was sought in order to maximise the probability of correct decisions. The assignment of objects to categories using probabilistic methods is the essence of pattern recognition.

The classic pattern recognition procedure is to develop rules to quantify characteristics of the object, and then plot the positions of the characteristics of a test set in a multi-dimensional space. If the characteristics are clustered in a manner corresponding to the desired categories. Then the chosen method of characterization may be used to categorise the objects with a high probability of success. Development of an effective method of quantifying the characteristics of an object is known as 'feature extraction' and is fundamental to the process of pattern recognition.

Several pattern recognition techniques were investigated and one, Syntactic String Analysis [43] appeared ideally suited to the characterization of impulsive signals. Syntactic string analysis consists of describing a signal by a string of symbols and classifying them according to the order in which the symbols occur i.e. according to their grammar or syntax. The symbols are assigned to segments of the signal according to the values of characteristics (features).

Unfortunately there is currently no theoretical basis for the choice of method for obtaining features from a signal. Features must be chosen on the basis of intuition and experiment. A test set of known good and defective signals was

stored in digital form on a computer and various feature extraction methods and symbol assignment rules were simulated. The features used to assign the symbols, the range of values corresponding to each particular symbol, and the syntax of a defect symbol were chosen to maximise the probability of correct identification of the test signals on an empirical basis.

The method that was evolved is based on the recognition that that the impulsive signals due to pressing faults characteristically have voltage waveforms containing a number of steep slopes and rapid changes of direction. The audio signal from the replay of the gramophone record to be tested is sampled and then classified into segments based on the values of the first and second inter-sample differences.

The value of the first inter-sample difference is the slope of the voltage waveform. If the slopes before and after a sample point have different signs then the value of the second inter-sample difference at that point is denoted the apex value at that point. The waveform was classified into a string containing 5 different symbols using the following assignment rules:

1. If the slope at a sampling instant exceeds a threshold value, the waveform at that instant is classified as a positive slope, denoted by the symbol /.

2. If the slope at a sampling instant is negative and its magnitude exceeds the slope threshold value then the waveform at that instant is classified as a negative slope, denoted by the symbol \.

3. If the apex value, as defined above, is greater than an apex threshold value the waveform is classified as a positive apex denoted by the symbol $\wedge$.

4. If the apex value, as defined above, is negative and its magnitude is greater than the apex threshold value the waveform is classified as a negative apex denoted by the symbol $\vee$.

5. If neither the slope nor apex thresholds are exceeded the waveform at the sampling instant is classified as an empty segment.

6. If a series of empty segments occurs which lasts less than a time-out value then it is not symbolised.

7. If series of empty segments occurs lasting greater than the time-out value then it is symbolised by the symbol Δ.

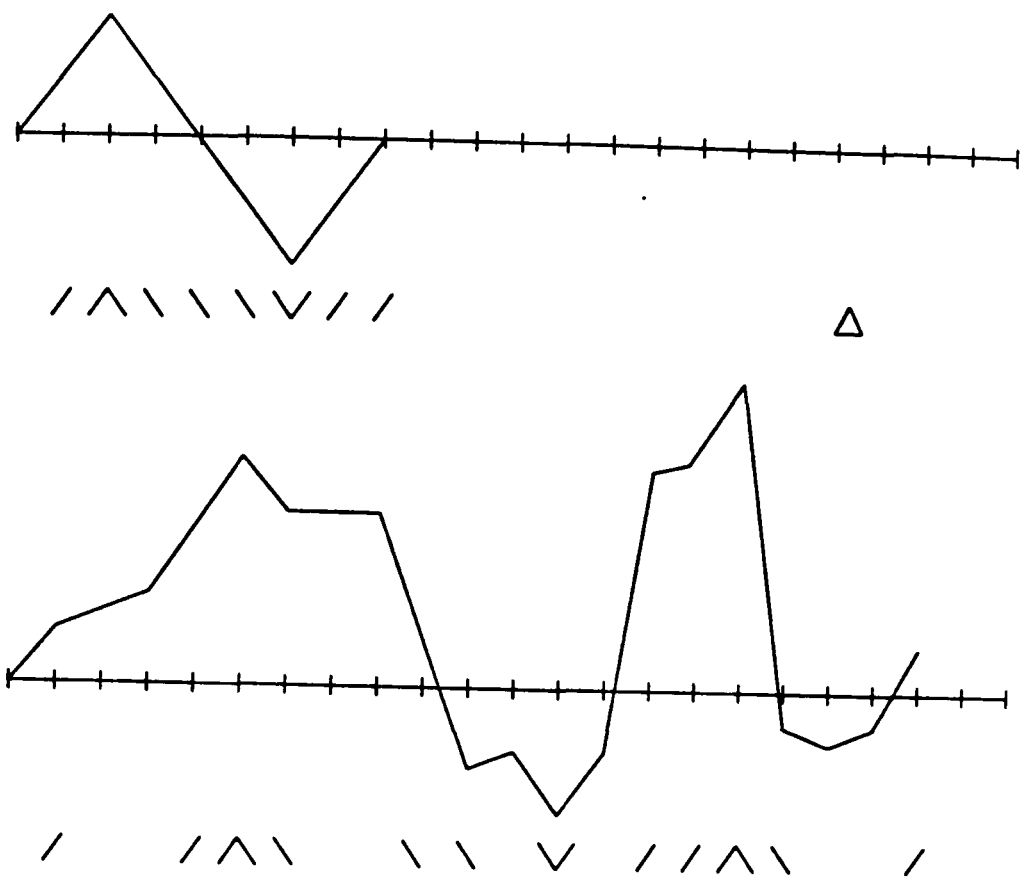

Figure 4.4: Two waveforms which conform to the defect syntax

Defect impulses are characterized by a sequence of symbols which must start with a positive slope (/) or negative slope (\). The full syntax for a defect impulse starting with a positive slope is :

$$((/)^* \wedge (\backslash)^* \vee)^*$$

whilst that for a defect impulse starting with a negative slope is :

$$((\backslash)^* \vee (/)^* \wedge)^*$$

where $(\ )^*$ indicates that the portion within parentheses may be repeated any number of times. Two examples of impulsive waveforms which conform to the syntax are shown in figure 4.4.

In order to achieve sufficient sensitivity to detect small impulsive defects audible in periods of silence or low-level programme, whilst maintaining an adequate resistance to spurious triggering during periods of high level programme it was found to be necessary to normalize the threshold values used in the classification process to the programme level.

click	Isolated impulse or group with duration less than 10 mS
tearing	mean interval between impulses less than 10mS
frying	mean interval between 10 mS and 70 mS
grit	mean interval between 70 mS and 800mS

Table 4.2: Assignment of groups of impulses to informal noise categories

The method by which the programme level was measured was empirically designed to approximate the masking effect of music programme on impulsive defects. The programme was filtered by a single-pole high-pass filter with a cut-off frequency of 1 kHz. It was then full-wave rectified and the programme level estimated by a circuit with a rise -time of 0.5 mS and a fall-time of 200 mS

4.4.3 Defect classification

In addition to identifying those impulsive signals due to gramophone record defects it is necessary to group them so that they correspond to recognisable defects and then to assess the severity of the resulting noise.

The grouping strategy it was decided to implement was as follows

1. The impulses are collected into groups called 'patches'.
2. Each patch is assigned one of the informal noise categories: click; tearing; frying; grit. The mean interval between impulses within a patch was used to make the assignment (see table 4.2) and was found to give a reliable indication of the character of the resulting noise.
3. The patches are then checked against those of the previous revolution of the disk to check whether any of them are repeated cyclically, since they are then manifestations of same defect. The most familiar example is a cyclically repeated click which is a scratch -but in fact all of the noise categories may occur cyclically.

The position of each impulse, expressed as the angular position from some arbitrary reference, and the number of revolutions from the start is stored. This enables the start and end position of each patch to be established and hence cyclicity determined. The definition of cyclicity used was as follows : two clicks are cyclic if they occur 1.8 s (one revolution) apart to within 10 mS; two patches are cyclic if they are of the same noise type and if any part of one is separated from any part of the other by 1.8 S.

4.4.4 Assessment of defect severity

The main objective of the prototype Disk Defect Detector is to obtain a consistent assessment of gramophone record quality which is in line with the consensus opinion of human listeners. The following procedure for quantitatively estimating the audible severity of the defects on a gramophone record was developed empirically.

1. Each impulse considered to be due to a defect is given a score based on the total energy in the impulse [44]. This is estimated from the syntax parameters together with additional information from the hardware including the total number of samples in the impulse and the programme level.

2. The severity of the noise due to a patch of impulses is then estimated from the severity of its constituent impulses. This was initially made equal to the sum of the severities of its constituent impulses for simplicity and this was found to correlate reasonably well with subjective assessment of the annoyance value.

3. If the defect is one which is cyclic then the severity of the defect is estimated as the severity rating of the first patch (or click) plus twice the sum of the scores for the following patches, to take into account the increased annoyance this causes.

4. The severity of all the defects on the record is then summed to give an overall quality rating for the record.

It was intended that a pass/fail judgement on the record quality should be made from the resulting quality rating, although in practice the record would probably be auditioned in borderline cases.

4.5 Experimental equipment

The feasibility of the Syntactic String Analysis technique for the discrimination of the signals due to gramophone record defects was originally explored by computer simulation. However the processing time involved, typically several minutes for a few seconds of material, severely limited the amount of material that could be used to develop the technique and refine the parameters.

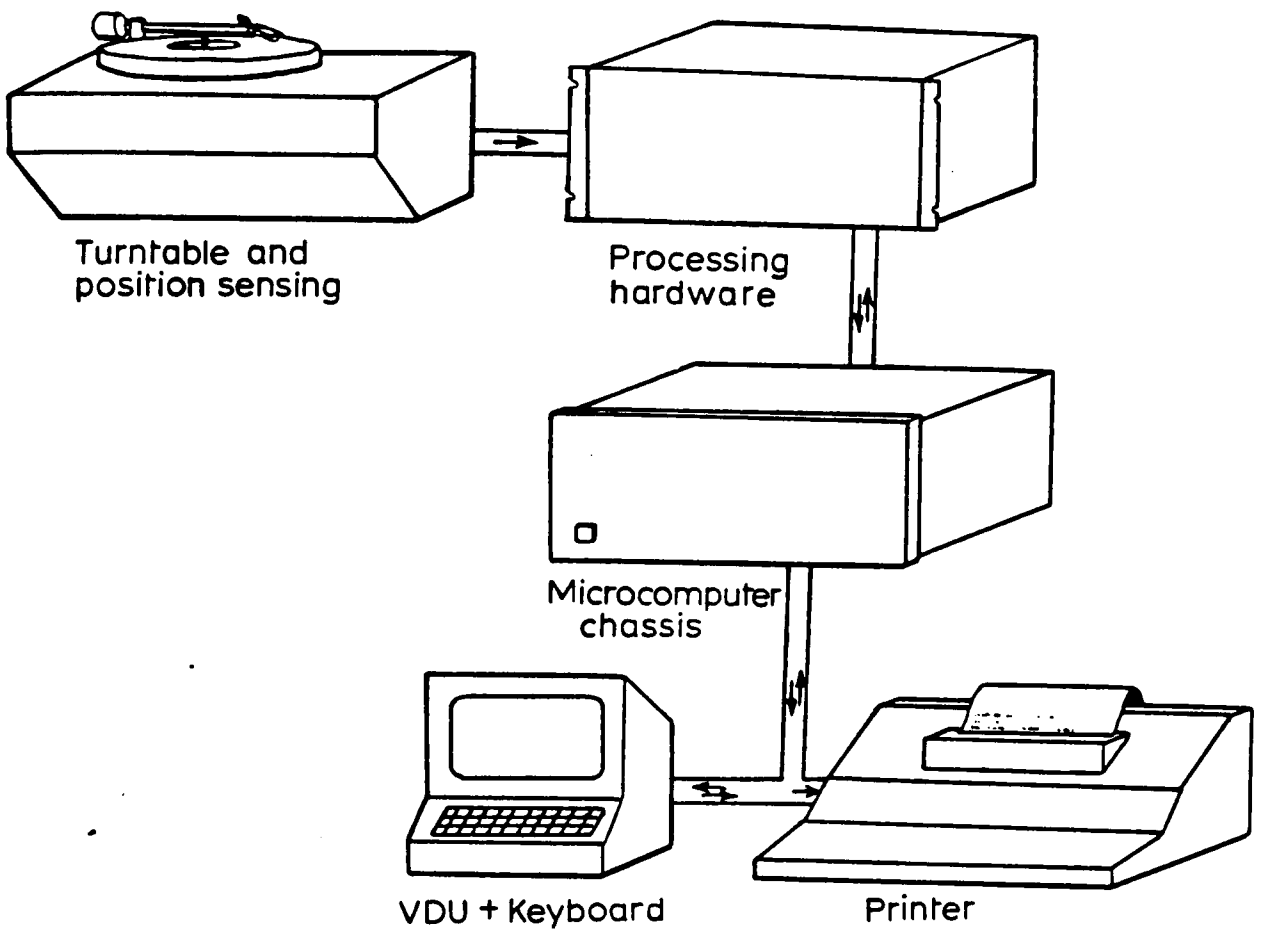

Figure 4.5: Layout of the experimental system

The investigation of the classification and assessment strategies described above clearly required the ability to use complete LP sides as source material which was far beyond the capabilities of a simulation approach. A prototype advanced disk defect detector was therefore designed and built which embodied the identification, classification and assessment techniques described above.

The prototype equipment consisted of three main parts: a turntable unit; a real time processing rack; and a microcomputer system. This is shown schematically in figure 4.5.

The turntable unit sends both audio signals and high resolution data on the turntable position to the real-time processing hardware. The processing hardware samples the incoming audio signal and continually converts it into a stream of symbols which are then examined to see whether they meet the syntax of a defect impulse. When a defect impulse has been identified data on the exact position of the defect on the record and on the severity of the impulse are latched and passed on (via an interrupt) to the microcomputer system.

The microcomputer temporarily stores this information in its memory, and as a background task (when not handling interrupts) sifts through this data attempting successive levels of classification. Initially the severity of the impulse is estimated, next any patches of impulses are identified, and finally any cyclic defects are categorised. Once classified, information about defects is displayed on the system console and also copied to a hard copy printer. When testing of the record is terminated the total severity of the defects on the record is reported.

4.5.1 Turntable unit

The turntable unit comprised a turntable with 180 strobe marks/rev, a tone arm mounted on a high resolution optical encoder, a cartridge and interface circuitry. Preliminary investigation was carried out by playing records at 33 rpm so that the record could be listened to as it was tested. The final form of the equipment however used a speed of 78 rpm in order to increase the through-put of the system. A stylus and cartridge were chosen which gave a response useful up to 48 KHz. The preamplifiers incorporated an equaliser to compensate for stylus and cartridge resonances, but no RIAA equalization was performed.

4.5.2 Processing hardware

The processing hardware consisted of four main parts:

- A/D converter
- threshold normalization circuitry
- segment identification hardware
- syntax analyser

In addition interfaces to both the microcomputer system and the turntable unit, and timing generation circuits, were contained within the hardware rack. An overall schematic of the signal processing hardware is shown in figure 4.6.

The segment identification hardware consists of two successive differencing circuits. The outputs from these are compared with the relevant normalized

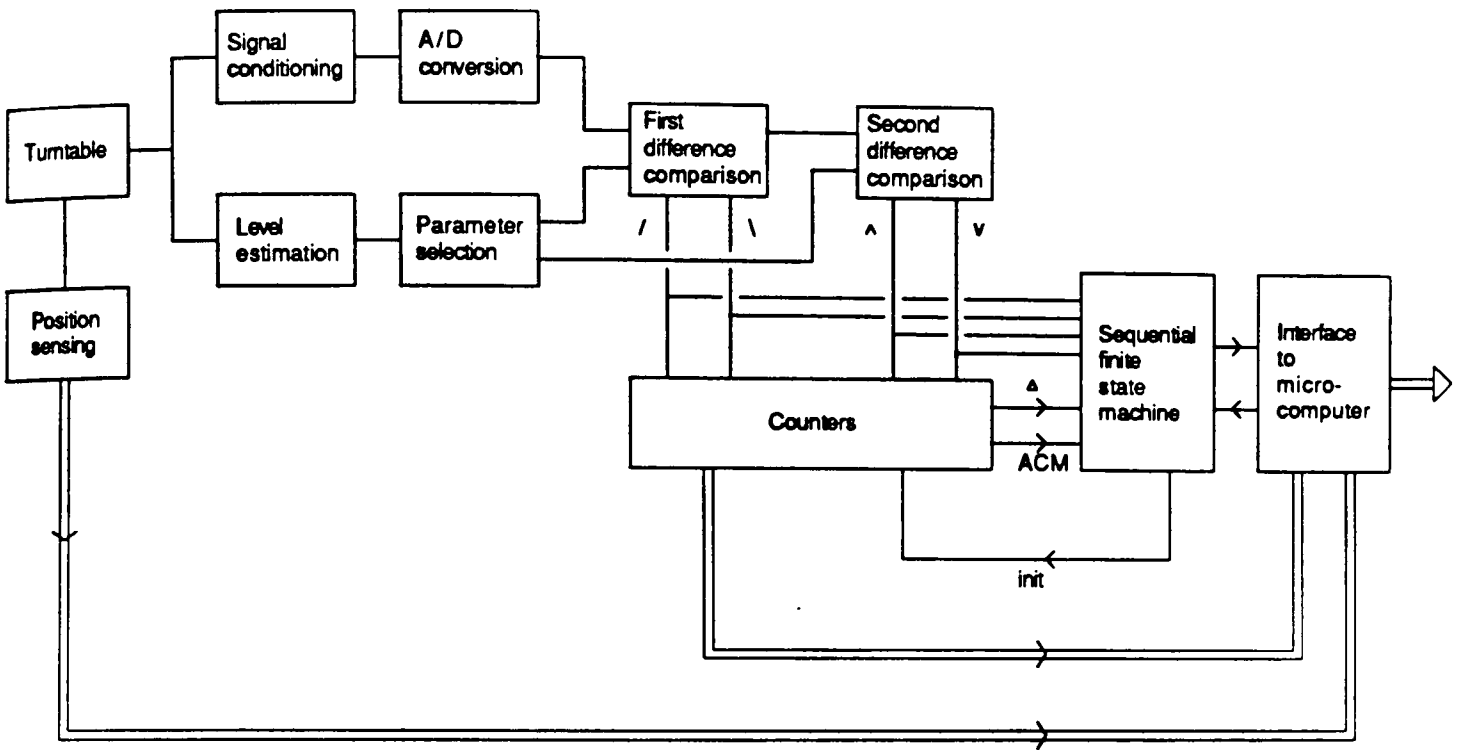

Figure 4.6: Overall schematic of processing hardware

slope and apex threshold values on a sample by sample basis. Flags showing the detection of positive or negative slopes and positive and negative apexes are then input to the syntax analyser. In addition a counter circuit generates time-out flag if only empty segments have occurred for the time-out period. A count of the total number of samples within a defect impulse is also made.

The threshold values were stored as tables in EPROM accessed according to the estimate of the programme level. A digital delay in the programme path was used so that advance information of the programme level could used in this process.

The syntax analyser was a sequential finite state machine [45] realized using programmable logic which implemented the defect syntax described in section 4.4.2. When a defect impulse was detected a signal was normally generated which interrupted the microcomputer system. However the number of apexes within defect impulses was monitored and once this exceeded a preset maximum the ACM flag was set. Since an impulse with a very large number of apexes is most probably due to spurious triggering on music or other programme, the ACM flag caused the syntax analyser to light an error indicator rather than interrupt the microcomputer.

4.5.3 Microcomputer system

The microcomputer system was an INTEL single board microcomputer based on the 8085 microprocessor, together with additional Random Access Memory, a VDU and a hard copy printer. The microcomputer system was responsible for controlling the signal processing hardware, classifying and assessing the severity of the defects and generating the output displays.

The software consisted of six tasks running under the INTEL RMX80 multi-tasking executive. Each task was a self contained software module written in a combination of PLM/80 [46] and assembler. The tasks ran independently, but communicated by exchanging messages and sharing tables of data. Each task was assigned a priority and the multi-tasking executive runs the highest priority task that has work to do. The tasks, in descending order of priority, were

Supervisor The supervisor task is responsible for overall control of the defect processing.

Impulse Interrupt This task responds to the interrupt from the hardware when a defect impulse has been detected. It stores the data provided by the hardware and calculates an estimate of the impulse severity.

Terminal Handler This task controls the keyboard, VDU and printer.

Patch The patch processing task reads the table of impulse data created by the impulse interrupt task and groups impulses into patches.

Defect This task reads the table of patch data, grouping together patches that are cyclic.

Output This generates the output display for each complete defect.

A typical output from the testing of a defective record is shown in figure 4.7. The following points may be noted:

- A range of sensitivities are available, this allows the level of quality control to be altered if desired. A more sensitive setting may be used for top range classical material than for pop records, where a certain number of minor faults may be deemed commercially acceptable.
- The rows in the printout list the defects found. The first column gives the type of defect, the second the severity estimate and the last four the start and end positions of the defect.

- At the end of the analysis, the final score for the record is printed. The final line gives the reason for halting the processing of the record. Normally this would be because all of the record had been tested, however, this can also be caused prematurely, for example by the operator or if the stylus gets locked in one groove.

4.6 Experimental Results

After a period of refinement the equipment was taken to EMI Records gramophone record pressing plant in order to undergo field trials. This enabled the detection, classification and assessment techniques to be further refined and tested on many hours of very varied programme from uncured pressings.

In the first phase of testing the prototype equipment was used at a speed of 33 rpm and a visual indicator was connected to the impulse detection flag. This enabled simultaneous comparison of the performance of the prototype with the sound of the record to be carried out. The records were then also tested on the mark V analogue equipment in order to provide a standard of comparison. The results showed that the prototype was superior to the mark V equipment in the detection of certain types of defect when testing classical repertoire, but that it was susceptible to the erroneous identification of some POP and MOR music as due to gramophone record defects.

An investigation into the cause of the music break-through problems lead to a redesign of the analogue circuitry responsible for estimating the programme level in order to improve its linearity, dynamic range and bandwidth. An extensive second phase of field trials was then carried out in which the performance of the prototype was again compared with that of the Mark V equipment. Each record was also listened to very carefully by the author and, in most cases, the quality control manager.

The results showed that the experimental equipment was capable of accurately identifying a wide variety of pressing defects and that it was also extremely resistant to spurious triggering by music programme. A comprehensive search for difficult programme material revealed only one type of programme for which spurious triggering was a serious problem : the Koto ensemble. The Koto is a traditional Japanese musical instrument.

A detailed comparison of the performance of the mark V analogue equipment and the prototype was carried out. This indicated that for classical

```
DISK DEFECT DETECTOR PROGRAM REV 3.0

RECORD ID    :KATE BUSH - THE KICK INSIDE - (EMC3223) SIDE1
SENSITIVITY :4

PLEASE START TURNTABLE

  DEFECT  TYPE  SEVERITY          START              END
                                RADIUS TACHO     RADIUS TACHO
       GRIT            66          0   138          0      5
       CLICK           15          1    17          1     17
       GRIT            99          1   164          0     98
       CLICK           28          1    11          1     11
       GRIT           175          1   109          1    107
       CLICK           28          1    37          1     37
       CLICK           20          1    19          1     19
       GRIT           102          2   113          2    152
       FRYING         167          5    24          5     87
       CLICK           54          7    56          7     56
CYCLIC FRYING         268         13    29         13     96
       CLICK           50         18   157         13    157
       SCRATCH        164         20   157         20    157
       CLICK           23         22    76         22     76
CYCLIC TEARING        321         54   145         54    169
       CLICK           67         62    40         62     40
       CLICK           17         87   175         87    175
       TEARING        198         92    63         92     95
       CLICK           28        102   125        102    125
       CLICK           53        126    58        126     58

       RECORD SCORE WAS ***  1893 ***


PROCESSING TERMINATED - END OF RECORD

RECORD ID:
```

Figure 4.7: Typical output display

music programme the prototype now had approximately the same sensitivity to defects as the Mark V but was less susceptible to spurious triggering on music. On pop repertoire it was found, as expected, that the mark V equipment was prone to spurious triggering and was rather insensitive to defects.

The overall performance of the prototype system was good and was clearly better than the mark V equipment. In order to increase the throughput of the prototype it was modified to operate at a rotational speed of 78 rpm. This was first attempted using the conventional pick-up cartridge (Stanton 500A) used in the previous tests. The poor high frequency performance of the cartridge was however found to result in a deterioration in sensitivity and defect classification and an increase in spurious output.

After contacting several different manufacturers a cartridge (Glanz MFG31E) was discovered which had a response useful up to 40KHz. The frequency response of the cartridge was measured and a filter to equalise this incorporated into the equipment. The performance of the equipment was then tested on a representative selection of pressings and found to be similar to that which had been obtained at 33 rpm.

A final extended field trial of the prototype was then carried out by quality assurance staff at the Uxbridge road record factory. Pressings were again tested by both the prototype and mark V machines and compared with an aural assessment. The following conclusions were drawn:

- The prototype equipment was capable of rapidly and accurately detecting a wide range of pressing defects and was highly immune to spurious triggering by music programme.
- The only statistically significant type of defect that it was unable to detect are those consisting of low frequency sounds.
- The equipment was not capable of detecting every defect that is detectable by a trained listener under good conditions.
- The main short-coming was the detection of certain types of defect in the presence of music programme. Further refinement of the parameter normalisation process might be able to improve performance in this area.
- The equipment represented a considerable improvement in performance over that offered by the Mark V.

- The method of assigning a total severity score to the defects on the record was not optimal, but it gave a consistent assessment of record quality and thus represented a considerable improvement in the methods currently used.

4.7 Conclusions

The application of digital signal processing to the identification, classification and assessment of the signals due to pressing faults on gramophone records has been investigated. A system using syntactic string analysis for identification of impulsive signals and hierarchical schemes for defect classification and assessment has been developed and a prototype equipment designed and built.

The equipment was extensively tested in field trials at a record manufacturing plant and compared with both the current generation of analogue equipment and aural assessment by trained listeners. It was found to be capable of reliably and accurately detecting a wide range of pressing faults, and represented an advance over the current analogue equipment.

The equipment is not capable of detecting all of the faults which can be heard by a trained listener and this objective is probably not realizable. However, unlike a human listener the assessment of record quality offered by the equipment was consistent, and offers a considerable improvement over the methods currently used in gramophone record production.

Chapter 5

Conclusions

5.1 The industrial application of DSP

This thesis considered the application of digital signal processing to industrial signal processing problems. Three case studies were undertaken: computer simulation of a microwave communications link; adaptive cancellation of noise or interference superimposed on a wanted signal and the design of equipment for the automatic detection and assessment of pressing faults on gramophone records.

5.1.1 First case study

A computer simulation of an analogue signal processing system is essentially a digital signal processing system implemented using a general purpose computer and obtaining its input signals from mathematical models rather than sensors. In order that the behaviour of the simulation reliably models that of the real-world system it is necessary to apply appropriate theoretical, software engineering, testing and validation techniques, as described in chapter 2. Very similar considerations are necessary during the implementation of a digital signal processing system using programmable DSP hardware which has recently become available.

5.1.2 Second case study

The traditional method of removing noise or interference from a corrupted signal is to filter it, retaining frequency components dominated by the

wanted signal and discarding those dominated by the interference. Adaptive noise cancelling is a powerful alternative technique, in which the signal from a second sensor is adaptively filtered and subtracted from the corrupted signal. A comprehensive theoretical study supported by computer simulation has demonstrated the potential effectiveness of the technique. Stability and convergence of the adaptive algorithm; misadjustment noise and the effects of realizability constraints are all important in practical applications.

5.1.3 Third case study

In the final investigation digital signal processing techniques were applied to the design of equipment to automatically assess the quality of gramophone records for quality control purposes. A prototype equipment was designed and built and extensive field testing showed that it was capable of rapidly and accurately finding a wide variety of pressing faults in the presence of a wide range of recorded programme.

5.1.4 General

Each of these investigations considered the solution of a real industrial signal processing problem using digital signal processing techniques. In the first two cases solution of these problems using conventional analogue techniques is impractical and in the final study a DSP solution was compared with a state-of-the-art analogue solution (obtained after many years of effort) and shown to be superior. These studies therefore clearly illustrate the potential of DSP for the solution of industrial signal processing problems and their variety is indicative of the wide range of possible applications.

5.2 The solution of industrial DSP problems

A signal processing problem may be solved in one of three ways: theoretically; by experiment or by simulation. The case studies that have been reported illustrate the characteristics of these three modes of investigation.

5.2.1 Theoretical investigation

Theoretical investigation of a signal processing problem is very powerful and can lead to a deep understanding of the problem and its solutions. How-

ever the use of theoretical methods generally requires approximation and idealization in order to become mathematically tractable. The validity of these assumptions can then only be checked by some other method of investigation. This was illustrated in the second case study by comparison of theoretical predictions of the level of output misadjustment noise with the results of computer simulation. The uncorrelated vectors assumption, necessary to make the mathematical treatment of the LMS algorithm tractable, was revealed to be inappropriate when the reference input was uncorrelated.

Industrial signal processing problems are concerned with a wide variety of environments, which are often poorly characterized. Theoretical investigation then becomes difficult or impossible and more empirical methods of solution must be found. In order to pursue a theoretical investigation of the detection of gramophone record defects, for example, would require some form of statistical model for both music, or other recorded programme, and for the signals from gramophone record defects. In order to extend the analysis to include the automatic assessment of record quality a further model would also be required which would quantify the disturbance caused by defect signals in programme. In practice none of these models were available.

5.2.2 Experimental investigation

Experimental investigation tackles the signal processing problem directly and thus problems of approximation and idealization can be avoided. However the design and construction of hardware can be expensive and time consuming. The understanding of a problem that is achieved by empirical investigation is not as deep as that obtained from theoretical study. For example, the understanding of the nature of the signals from gramophone record defects achieved as a result of the second case study is trivial compared to that which would have been obtained had the theoretical investigation outlined above been possible.

5.2.3 Computer simulation

Given the expense and time often involved in the experimental investigation of industrial signal processing problems a third alternative, simulation on a general purpose digital computer, is an increasingly attractive option. Computer simulation is similar in many respects to experimental investigation but is usually cheaper, often quicker, repeatable and allows real-world constraints to be avoided. The primary weakness of this approach is the

difficulty of ensuring that an assumption in the system model, or an undiscovered software error, does not render the simulation outputs invalid. A methodology for tackling this problem, based on a systems approach, was outlined in chapter 2.

Bibliography

[1] Lender, A. (1981), 'Correlative (Partial Response) Techniques and Applications to Digital Radio Systems', *in* Feher, K. (1981), 'Digital Communications: Microwave Applications', (Prentice-Hall).

[2] Lender, A. (1963), 'The Duobinary Technique for High Speed Data Transmission', IEEE Trans. Communications and Electronics 82, May 1963, p214-218.

[3] Lender, A. (1964), 'Correlative Digital Communication Techniques', IEEE Trans. Communications Technology, December 1964, p128-135.

[4] Wolfram, S. (1984), 'Computer Software in Science and Mathematics', Scientific American, 251, 3, 188-203.

[5] Ziemer, R.E. and Peterson, R.L. (1985), 'Digital Communications and Spread Spectrum Systems', (MacMillan)

[6] Ingram, D.G.W. (1979), 'Analysis and Design of Digital Transmission Systems', Computers and Digital Techniques, 2, 3, 121-133.

[7] Fashano, M. and Strodtbeck, A.L. (1984), 'Communication System Simulation and Analysis with SYSTID', IEEE J. SAC 2,1, 8-29.

[8] Potter D. (1977), 'Computational Physics', (Wiley)

[9] Leigh, J.R. (1983), 'Modelling and Simulation', (Peter Peregrinus).

[10] Ahmed, N. and Rao, K.R. (1975), 'Orthogonal transforms for Digital Signal Processing', (Springer-Verlag:Berlin).

[11] Rabiner, L.R. and Gold, B. (1975), 'Theory and application of Digital Signal Processing', (Pretice-Hall).

[12] Bracewell, R. (1965), 'The Fourier Transform and its Applications', (Wiley)

[13] Brooks, F.P. (1987), 'No Silver Bullet: Essence and Accidents of Software Engineering', Computer, April 1987, p10-19

[14] Whitty, R.W., Fenton, N.E. and Kaposi, A.A. (1984), 'Structured Programming. A Tutorial guide.', Software and Microsystems, 2,3,54-65.

[15] Chantler, A. (1981), 'Programming Techniques and Practice', (NCC)

[16] EDN (1986), 'Defensive Programming simplifies program maintenance', Electronic Design News, August 7 1986, p157-160.

[17] McCracken, D.D. (1984), 'Computing for Engineers and Scientists with FORTRAN 77', (Wiley)

[18] Holtzman, J.C. and Shanmugan, K. (1984), 'Digital Simulation of Communications Channels: and overview', AGARD Conf. Proc. 363, 21-1,8

[19] Jeruchim, M.C. (1984),'Techniques for estimating the bit error rate in the simulation of digital communication systems', IEEE J. SAC 2,1 153-170.

[20] Marsan, M.A. *et al* (1984), 'Digital Simulation of Communications Systems with TOPSIM III', IEEE J. SAC 2,1, 29-42

[21] Modestino, J.W. and Matis, K.R. (1984), 'Interactive Simulation of Digital Communication Systems', IEEE J. SAC 2,1, 51-76

[22] Kailath, T. (1974),'A View of Three Decades of Linear Filtering Theory', IEEE Trans. IT, 20, 2, 146-181.

[23] Widrow, B. *et al* (1975) 'Adaptive Noise Cancelling: Principles and Applications', Proc. IEEE, 63,12,1692-1716.

[24] Wiener, N.(1949),'The interpolation,Extrapolation and Smoothing of Stationary Time Series',(Wiley).

[25] Papoulis, A. (1965), 'Probability, Random Variables and Stochastic Processes', (McGraw-Hill: New York).

[26] Cowan,C.F.N. (1987),'Performance Comparisons of Finite Linear Adaptive Filters', IEE Proc F, 3, 211-216.

[27] Widrow,B. and Hoff,M.(1960),'Adaptive Switching Circuits', *in*IRE WESCON Conv. Rec. 4, 96-104.

[28] Widrow B., McCool,J.M.,Larimore,M.G. and Johnson,C.R. (1976),'Stationary and non-stationary learning characteristics of the LMS adaptive filter', Proc. IEEE, 1976,64,1151-1161.

[29] Widrow,B. and Stearns,S.D.(1985) 'Adaptive Signal Processing', (Prentice-Hall).

[30] Derusso, P.M., Roy,R.J. and Close, C.M. (1967) ,'State Variables for Engineers', (Wiley).

[31] Gardner, W.A. (1984), 'Learning characteristics of stochastic- gradient-descent algorithms: A general study, analysis and critique', Signal Processing, 6, 113-133 (North-Holland).

[32] Feuer, A. and Weinstein, E. 'Convergence Analysis of LMS Filters with Uncorrelated Gaussian Data', IEEE Trans. ASSP-33, 1, 222- 230.

[33] Glover, J.R. (1977), 'Adaptive Noise Cancelling applied to Sinusoidal Interferences', IEEE Trans. ASSP-25, 484-491, Dec 1977.

[34] Shensa, M.J. (1980), 'Non-Wiener Solutions of the Adaptive Noise Canceller with a Noisy Reference', IEEE Trans. ASSP-28,4,468 -473.

[35] Oppenheim,A.V. and Schafer, R.W. Schafer (1975), 'Digital Signal Processing', (Prentice-Hall).

[36] Papoulis, A. (1977), 'Signal Analysis' (1977), (McGraw-Hill).

[37] Kaliath, T. (1968), 'An innovations approach to least- squares estimation – part 1: linear filtering in additive white noise', IEEE AC-13, 6, 646-654.

[38] Paul, J.E. (1978), 'Adaptive digital techniques for audio noise cancellation', Proc. IEEE Int. Symp. Cct. & Sys., May 1978.

[39] Pulsipher, D., Boll,S.F., Rushforth, C., and Timothy, L. (1979), 'Reduction of non-stationary acoustic noise in speech using LMS adaptive noise cancelling', Proc IEEE Int. Conf. Acoust.,Speech & Signal Processing, April 1979.

[40] Uecke, E.H. (1956) , 'The control of quality in gramophone records',J. Audio Engng Soc. 4, no. 4, pp159-162, October 1956.

[41] Richards, J.W. (1983), 'Digital audio mixing', The Radio and Electronic Engineer', 53, no. 7/8, pp257-264, July/August 1983.

[42] Batchelor, M. (1967), 'Improvements in or relating to apparatus for monitoring grooved sound records', British Patent 1177934, filed february 1967.

[43] Gonzalez, R.C. and Thomason, M.G. (1978), 'Syntactic Pattern Recognition' (Addison-Wesley, New York, 1978).

[44] Broch, J.T. (1975), 'Acoustic Noise Measurements', (Bruel and Kjäer, Copenhagen 1975)

[45] Aleksander, I. and Hanna, F.K. (1976), 'Automata theory: An Engineering Approach', (Crane Russak, New York, 1976).

[46] McCracken, D.D. (1977), 'A guide to PL/M programming for microcomputer applications', (Addison-Wesley, 1977).